

Acousto-optic interaction in biconical tapered fibers: shaping of the stopbands

Gustavo Ramírez-Meléndez,^a Miguel Ángel Bello-Jiménez,^{a,*} Christian Cuadrado-Laborde,^{b,c} Antonio Díez,^c José Luis Cruz,^c Amparo Rodríguez-Cobos,^a Raúl Balderas-Navarro,^a and Miguel Vicente Andrés Bou^c

^aUniversidad Autónoma de San Luis Potosí, Instituto de Investigación en Comunicación Óptica, Av. Karakorum 1470 Lomas 4a Secc., 78210 San Luis Potosí, S.L.P., México

^bInstituto de Física Rosario (CONICET-UNR), Optical Metrology Lab, Ocampo y Esmeralda, S2000EYP Rosario, Argentina

^cUniversidad de Valencia, Departamento de Física Aplicada y Electromagnetismo, ICMUV, C/Dr. Moliner 50, Burjassot, 46100 Valencia, Spain

Abstract. The effect of a gradual reduction of the fiber diameter on the acousto-optic (AO) interaction is reported. The experimental and theoretical study of the intermodal coupling induced by a flexural acoustic wave in a biconical tapered fiber shows that it is possible to shape the transmission spectrum, for example, substantially broadening the bandwidth of the resonant couplings. The geometry of the taper transitions can be regarded as an extra degree of freedom to design the AO devices. Optical bandwidths above 45 nm are reported in a tapered fiber with a gradual reduction of the fiber down to 70 μm diameter. The effect of including long taper transition is also reported in a double-tapered structure. A flat attenuation response is reported with 3-dB stopband bandwidth of 34 nm. © 2016 Society of Photo-Optical Instrumentation Engineers (SPIE) [DOI: 10.1117/1.OE.55.3.036105]

Keywords: acousto-optic interaction; biconical tapered fiber; acousto-optic filter.

Paper 151598 received Nov. 13, 2015; accepted for publication Feb. 16, 2016; published online Mar. 8, 2016.

1 Introduction

In-fiber acousto-optic (AO) devices based on flexural acoustic waves have been investigated for years because of their applications as frequency shifters,¹ tunable filters,² and modulators.³ Recently, the AO has been investigated as a powerful tool for measuring axial inhomogeneities along optical fibers.⁴ When the fundamental flexural acoustic mode propagates along an uncoated single-mode optical fiber (SMF), the acoustic fields produce a periodical perturbation of the fiber, both refractive index changes and geometrical effects, which leads to an intermodal resonant coupling between the fundamental core mode and some specific cladding modes of the SMF.¹⁻³ This AO interaction can be seen as the dynamic counterpart of a conventional asymmetric long period fiber grating (LPG), whose transmission characteristics can be controlled dynamically by the amplitude and frequency of the acoustic wave. At the output fiber, only the light that remains guided by the core is transmitted, showing a transmittance spectrum with one or several attenuation notches at the wavelengths of the resonant couplings.

The effect of including tapered fibers to improve the AO response has been reported in previous works.³⁻⁸ However, these works paid attention first to the enhancement of the acoustic intensity by reducing the cross section of the fiber and second to the shift of the resonant wavelength in uniform tapered fibers. Thus, the use of a thin optical fiber produces a more efficient intermodal coupling that enables shorter and faster devices, as well as a reduction of the required acoustic power. This fiber tapering can be carried out either by chemical etching or by a fusion and pulling technique.

It is possible to adjust the wavelength of the resonant coupling between two specific modes by changing the frequency of the acoustic wave. However, the spectral bandwidth of a

given resonance is determined by the dispersion curves of the involved modes and it is not straightforward how to develop techniques to control such a bandwidth. Kim et al.⁹ explored the simultaneous excitation of the acoustic wave generator with two frequencies, while Jung et al.¹⁰ concatenated different fibers. Feced et al.⁶ concatenated three fibers with different sections to demonstrate a gain flattening filter and pointed out the interest of exploiting the taper radius as a new degree of freedom in the design of AO filters. Jin et al.¹¹ demonstrated an enhancement of the bandwidth of the AO notches by using uniform fibers with a reduced diameter prepared with chemical etching. Complimentarily, Li et al.¹² investigated fibers with different dispersion curves in order to narrow the optical notches.

Here, we investigate how tapering can be exploited to control the spectral bandwidth of the transmission notches. It is known that the dispersion curves of both the acoustic and optical modes change with the radius of the fiber.³ Thus, smooth and long tapered fibers can effectively control the bandwidth of a given coupling by slightly shifting the resonance wavelength, enabling a geometrical design technique, since the shape of fiber tapers can be controlled accurately using a fusion and pulling technique.¹³ In Sec. 2, we start with the numerical modeling of acoustically induced LPG formed in a tapered structure. Then, in Sec. 3, we describe the experimental results and the comparison with the theory, in order to demonstrate the effects of the taper transitions on the spectral response of the AO device. Finally, our conclusions are summarized in Sec. 4.

2 Numerical Modeling of the Acousto-Optic Interaction in a Tapered Fiber

In this section, we present the numerical technique that we have implemented to simulate the spectral response of the

*Address all correspondence to: Miguel Ángel Bello-Jiménez, E-mail: m.bello@cactus.iico.uaslp.mx

Experimental Investigation of Fused Biconical Fiber Couplers for Measuring Refractive Index Changes in Aqueous Solutions

Marco V. Hernández-Arriaga, Miguel A. Bello-Jiménez, A. Rodríguez-Cobos,
and Miguel V. Andrés, *Member, IEEE*

Abstract—A detailed experimental study of a simple and compact fiber optic sensor based on a fused biconical fiber coupler is presented, in which the sensitivity is improved by operating the coupler beyond the first coupling cycle. The sensor is demonstrated to perform high sensitivity measurements of refractive index changes by means of variation of sugar concentration in water. The device is operated to achieve a linear transmission response, allowing a linear relation between the sugar concentration and the output signal. The initial sensitivity was measured as 0.03 units of normalized transmission per unit of sugar concentration (g/100 mL), with a noise detection limit of a sugar concentration of 0.06 wt% of sugar concentration. Improvements in sensitivity were studied by operating the coupler beyond their first coupling cycles; achieving an improved sensitivity of 0.15 units of normalized transmission per unit of sugar concentration, and a minimum detection limit of 0.012 wt% of sugar concentration. From this result, the minimum detectable refractive index change is estimated as 2×10^{-5} refractive index unit.

Index Terms—Fiber optic sensor, fused biconical fiber coupler, refractive index sensor.

I. INTRODUCTION

FIBER-OPTIC couplers have attracted considerable attention in recent years for their ability to detect small changes in the refractive index (RI) of liquid solutions. A fiber coupler is a four-port device with a transmission spectrum that is strongly affected by the refractive index of the surrounding medium due to the evanescent field that is generated along the coupling region [1]. This effect has proven to be useful for sensing applications [2]. Recent approaches of fiber-coupler based RI sensors include fused biconical fiber couplers [3]–[7], optical microfibers [8]–[12], photonic crystal fibers [13], [14], and specially designed

two-core optical fibers [15], [16], all of them offering the advantages of high sensitivity, *in situ* measurements, compact size, and immunity to external electromagnetic interference. Most of these sensors are codified in wavelength and the achieved sensitivities are in the range of 1,125 to 30,100 nanometer (nm) per refractive index unit (RIU), with a minimum detection limit of 4×10^{-4} to 4×10^{-7} RIU, respectively.

From the point of view of implementation, the necessity of expensive equipment, such as optical spectrum analyzers, for measuring the shift in wavelength heavily affects the use of fiber-coupler based RI sensors. Thus, it is worthwhile to consider an alternative scheme based on the dependence of the power coupling on the surrounding medium. The two complementary outputs of a fiber coupler enable a straightforward normalization, i.e. the ratio between the difference and the addition, which automatically compensates for power fluctuations. In earlier works the dependence of the power coupling of traditional fused biconical tapered couplers on the external RI has been presented and it has been proposed that it is possible to use such a structure to develop a fiber based refractometer [1], [17]. Tazawa et al. [2] have implemented this power measurement approach to demonstrate a biosensor with estimated 4×10^{-6} RIU detection limit. Recently, it has been demonstrated that modal interferometers based on integrated waveguides provide one of the best resolutions ever reported (2.5×10^{-7} RIU) [18]. A fused biconical couplers is, in fact, a modal interferometer in which the phase difference between the symmetric and antisymmetric supermodes determine the power distribution at the output fibers. Small changes of the external RI do not modify substantially the coupling coefficient, but they generate a significant phase difference between supermodes. In terms of fiber-coupler based RI sensors, this last point deserves particular attention for the detection of slight changes in the refractive index of aqueous solutions. Although several schemes have reported this effect [1], [2], [17], they did not study the conditions for an optimal performance of the reported device. Here our purpose is the experimental analysis of a fused biconical fiber coupler, operated beyond the first coupling cycle, with a power transmission that depends on the surrounding medium.

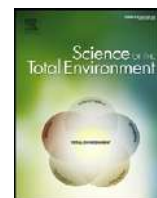
The objective is not only to gain insights into the dynamics of this kind of device, but also looking forwards an improvement of its performance. Based on this motivation, the

Manuscript received July 10, 2015; revised August 26, 2015; accepted August 27, 2015. Date of publication September 16, 2015; date of current version December 10, 2015. This work was supported in part by Promep under Grant DSA/103.5/14/10476 and in part by the Consejo Nacional de Ciencia y Tecnología under Grant 206425 and Grant 222476. The associate editor coordinating the review of this paper and approving it for publication was Dr. Anna G. Mignani.

M. V. Hernández-Arriaga, M. A. Bello-Jiménez, and A. Rodríguez-Cobos are with the Instituto de Investigación en Comunicación Óptica, Universidad Autónoma de San Luis Potosí, San Luis Potosí 78210, Mexico (e-mail: dmxsol@hotmail.com; m.bello@cactus.iico.uaslp.mx; roca@cactus.iico.uaslp.mx).

M. V. Andrés is with the Departamento de Física Aplicada y Electromagnetismo, Institute of Materials Science, Universidad de Valencia, Valencia 46100, Spain (e-mail: miguel.andres@uv.es).

Digital Object Identifier 10.1109/JSEN.2015.2475320



Chemical and surface analysis during evolution of arsenopyrite oxidation by *Acidithiobacillus thiooxidans* in the presence and absence of supplementary arsenic



Hugo Ramírez-Aldaba^a, O. Paola Valles^{a,b}, Jorge Vazquez-Arenas^{c,1}, J. Antonio Rojas-Contreras^b, Donato Valdez-Pérez^d, Estela Ruiz-Baca^a, Mónica Meraz-Rodríguez^e, Fabiola S. Sosa-Rodríguez^f, Ángel G. Rodríguez^g, René H. Lara^{a,*}

^a Facultad de Ciencias Químicas, Departamento de Ciencia de Materiales, Universidad Juárez del Estado de Durango (UJED), Av. Veterinaria S/N, Circuito Universitario, Col. Valle del Sur, 34120 Durango, Dgo, Mexico

^b Instituto Tecnológico de Durango, UPIDET, Av. Felipe Pescador 1830 Ote. Col. Nueva Vizcaya, 34080 Durango, Dgo, Mexico

^c Departamento de Química, Universidad Autónoma Metropolitana-Iztapalapa, Av. San Rafael Atlixco 186, Col. Vicentina, Iztapalapa, México DF 09340, Mexico

^d Instituto Politécnico Nacional, UPALM, Edif. Z-4 3er Piso, CP 07738 México D.F, Mexico

^e Departamento de Biotecnología, Universidad Autónoma Metropolitana-Iztapalapa, Av. San Rafael Atlixco 186, Col. Vicentina, Iztapalapa, México DF 09340, Mexico

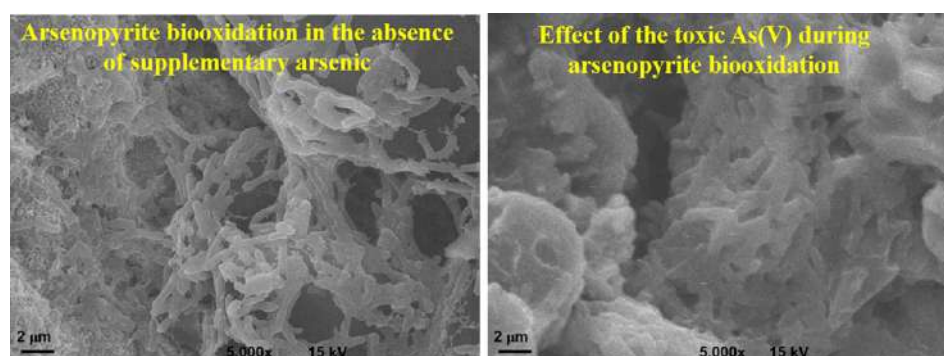
^f Universidad Autónoma Metropolitana-Azcapotzalco, Área de Crecimiento Económico y Medio Ambiente, Departamento de Economía, Av. San Pablo 180, Azcapotzalco, México DF 02200, Mexico

^g CIACyT, Universidad Autónoma de San Luis Potosí, Av. Sierra Leona 550, Lomas 2da sección, 78230 San Luis Potosí, SLP, Mexico

HIGHLIGHTS

- Biofilm structures occur as compact micro-colonies.
- Surface transformation reactions control arsenopyrite and cell interactions.
- Toxic arsenic does not limit biofilm formation but damage its evolution.
- Biofilm adhesion forces are lowered in the presence of supplementary arsenic.
- Synthesis of protein is mitigated in the presence of supplementary arsenic.

GRAPHICAL ABSTRACT



ARTICLE INFO

Article history:

Received 10 February 2016

Received in revised form 18 May 2016

Accepted 19 May 2016

Available online 14 June 2016

Editor: D. Barcelo

Keywords:

Arsenopyrite biooxidation

ABSTRACT

Bioleaching of arsenopyrite presents a great interest due to recovery of valuable metals and environmental issues. The current study aims to evaluate the arsenopyrite oxidation by *Acidithiobacillus thiooxidans* during 240 h at different time intervals, in the presence and absence of supplementary arsenic. Chemical and electrochemical characterizations are carried out using Raman, AFM, SEM-EDS, Cyclic Voltammetry, EIS, electrophoretic and adhesion forces to comprehensively assess the surface behavior and biooxidation mechanism of this mineral. These analyses evidence the formation of pyrite-like secondary phase on abiotic control surfaces, which contrast with the formation of pyrite (FeS₂)-like, orpiment (As₂S₃)-like and elementary sulfur and polysulfide (S_n²⁻/S⁰) phases found on biooxidized surfaces. Voltammetric results indicate a significant alteration of arsenopyrite due to (bio)oxidation. Resistive processes determined with EIS are associated with chemical and electrochemical

* Corresponding author.

E-mail addresses: lcrh75@ujed.mx, lcrh75@hotmail.com (R.H. Lara).

¹ CONACYT research fellow.

Research Article

Evolutionary Algorithm Geometry Optimization of Optical Antennas

Ramón Díaz de León-Zapata,^{1,2} Gabriel González,² Efrén Flores-García,¹ Ángel Gabriel Rodríguez,² and Francisco Javier González²

¹*Instituto Tecnológico de San Luis Potosí, Avenida Tecnológico s/n, 78376 Soledad de Graciano Sánchez, SLP, Mexico*

²*Universidad Autónoma de San Luis Potosí, Álvaro Obregón 64, 78000 San Luis Potosí, SLP, Mexico*

Correspondence should be addressed to Ramón Díaz de León-Zapata; ramondz@hotmail.com

Received 7 April 2016; Revised 25 May 2016; Accepted 2 June 2016

Academic Editor: Sotirios K. Goudos

Copyright © 2016 Ramón Díaz de León-Zapata et al. This is an open access article distributed under the Creative Commons Attribution License, which permits unrestricted use, distribution, and reproduction in any medium, provided the original work is properly cited.

Printed circuit antennas have been used for the detection of electromagnetic radiation at a wide range of frequencies that go from radio frequencies (RF) up to optical frequencies. The design of printed antennas at optical frequencies has been done by using design rules derived from the radio frequency domain which do not take into account the dispersion of material parameters at optical frequencies. This can make traditional RF antenna design not suitable for optical antenna design. This work presents the results of using a genetic algorithm (GA) for obtaining an optimized geometry (unconventional geometries) that may be used as optical regime antennas to capture electromagnetic waves. The radiation patterns and optical properties of the GA generated geometries were compared with the conventional dipole geometry. The characterizations were conducted via finite element method (FEM) computational simulations.

1. Introduction

Printed circuit antennas which have been extensively used in the radio frequency (RF) spectrum have also been used to detect electromagnetic radiation at optical and infrared frequencies. The use of these types of antennas at optical frequencies provides several advantages over traditional optical and infrared detectors; among these advantages are low profile, low cost, faster response times, compatibility with integrated circuit technology, and wavelength and polarization selectivity [1, 2].

Even though several RF antenna designs have been successfully used at optical and infrared frequencies [3], the design of antennas at optical frequencies by using traditional RF antenna design rules can result in nonoptimized antennas due to the dispersion of material properties that can be neglected at lower frequencies [4, 5].

Evolutionary algorithms imitate nature, where all living organisms possess specific genetic material which contains information about each organism that can be transferred

to new generations via reproduction. The other organism involved in reproduction also transfers some of its characteristics [6]. These characteristics are encoded in genes stored in chromosomes, which together constitute the genetic material known as a genotype [7]. Genes are modified during the characteristic transfer process as a consequence of the crossover between maternal and paternal chromosomes. Mutation may also occur, altering the information contained within the genes of a given chromosome. Although the newly created individual possesses the information of its parents, the combination of two different organisms makes the individual unique. This organism begins life in an environment that is not significantly different from that of its parents. The new organism develops in a manner that allows it to survive and transfer its genome, permitting the species to persist in a given environment. An individual that cannot adapt to its environment will struggle to survive and transfer its genes to new generations.

These evolutionary processes can be used to optimize the solution of nonanalytical problems assuming that the

Structural characterization of AlGaAs:Si/GaAs (631) heterostructures as a function of As pressure

Leticia Ithsmel Espinosa-Vega, Miguel Ángel Vidal-Borbolla, Ángel Gabriel Rodríguez-Vázquez, Irving Eduardo Cortes-Mestizo, Esteban Cruz-Hernández, and Víctor Hugo Méndez-García^{a)}

Center for the Innovation and Application of Science and Technology, Universidad Autónoma de San Luis Potosí, Sierra Leona 550, Lomas 2a Secc., San Luis Potosí, 78210 SLP, Mexico

Satoshi Shimomura and David Vázquez-Cortés

Graduate School of Science and Engineering, Ehime University, 3 Bukyo-cho, Matsuyama, Ehime 790-8577, Japan

(Received 22 November 2015; accepted 7 March 2016; published 21 March 2016)

AlGaAs:Si/GaAs heterostructures were grown on (631) and (100) GaAs substrates and studied as a function of the As cell beam equivalent pressure. High-resolution x-ray diffraction patterns showed that the highest quality AlGaAs epitaxial layers were grown at $P_{As} = 1.9 \times 10^{-5}$ for (100)- and $P_{As} = 4 \times 10^{-5}$ mbar for (631)-oriented substrates. Raman spectroscopy revealed higher crystalline quality for films grown on (631) oriented substrates. The GaAs- and AlAs-like modes of the AlGaAs(631) films exhibited increased intensity ratios between the transverse optical phonons and longitudinal optical phonons with increasing P_{As} , whereas the ratios were decreased for the (100) plane. This is in agreement with the selection rules for (631) and high-resolution x-ray diffraction observations. Anisotropy and surface corrugation of the AlGaAs(631) films also were characterized using atomic force microscopy and Raman spectroscopy. © 2016 American Vacuum Society.

[<http://dx.doi.org/10.1116/1.4944452>]

I. INTRODUCTION

The III–V compound semiconductors are very important in electronics and optoelectronics applications. For example, AlGaAs/GaAs heterostructures have been widely used in the fabrication of visible light-emitting diodes,¹ laser diodes, and solar cells.² Additionally, a great deal of research is focused on low-dimensional systems such as quantum wires (QWRs) because they are essential for enhancing the properties of such optoelectronic devices. Self-assembly on high-index (HI) substrates is a promising technique that has been used in the last few decades for achieving QWRs with high density and high optical quality. In this technique, the planes that are energetically unstable tend to break up into low-index facets to minimize their surface energies.³ The most investigated HI planes that partially sustain favorable QWR characteristics include the (311)A, (331), (775)B, and (631) surfaces.^{4–9} Recently, we have demonstrated that under appropriate growth conditions, uniform nanoscale step arrays can be synthesized in the homoepitaxial growth of GaAs(631)A.⁹ The large-order-correlated nanoscale facets of GaAs(631)A further can be used as nanotemplates for the self-assembly of QWRs. In this direction, the homoepitaxial growth is not enough to produce QWRs because no electron confinement is achieved. Thus, more research is needed on heteroepitaxial growth.

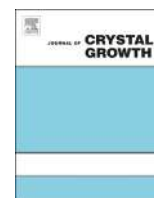
In the present work, we studied the synthesis and characteristics of corrugated AlGaAs/GaAs(631) heterostructures as a function of the As-cell beam equivalent pressure. Growth was conducted simultaneously on the GaAs(100)

plane for comparison. The results showed improved crystalline quality and surface corrugation order of the AlGaAs(631) film as the arsenic pressure, P_{As} , increased. However, for (100)-oriented surfaces, no surface corrugation was observed within the explored P_{As} range.

II. EXPERIMENTAL METHODS

Prior to loading into the molecular beam epitaxy (MBE) system, semi-insulating GaAs(631)A substrates were etched in a “Semico Clean” (Furuuchi Chemical Corp., Japan) solution and then predegassed at 380 °C under ultrahigh vacuum for 20 min. Oxide desorption was then conducted in the growth chamber at 640 °C for 15 min under As_4 flow. A 100-nm-thick GaAs layer was grown as a buffer layer at a temperature of 660 °C and growth rate of 0.3 $\mu\text{m}/\text{h}$. Following deposition of the GaAs layer, the substrate temperature was set to 700 °C to deposit a 1- μm -thick Si-doped AlGaAs layer at a growth rate of 0.3 $\mu\text{m}/\text{h}$. The nominal Al concentration of the ternary alloy was 30%. The Si-effusion cell temperature was set to obtain a doped Si carrier concentration of $1 \times 10^{18} \text{ cm}^{-3}$ in the GaAs(100)-oriented samples. Finally, a 25-nm-thick undoped GaAs layer was grown at 700 °C to avoid oxidation of the samples. Samples were prepared with the As_4 beam equivalent pressure P_{As} varying in the range of $0.5\text{--}4 \times 10^{-5}$ mbar. The morphology of the nanostructures was studied using atomic force microscopy (AFM) operated in the contact mode. The crystalline quality and structural properties were analyzed by high-resolution x-ray diffraction (HRXRD) and Raman scattering (RS) measurements with a 532-nm photomodulation source.

^{a)}Electronic mail: victor.mendez@uaslp.mx



Tuning emission in violet, blue, green and red in cubic GaN/InGaN/GaN quantum wells



I.E. Orozco Hinostroza^a, M. Avalos-Borja^{a,b}, V.D. Compeán García^c, C. Cuellar Zamora^c,
A.G. Rodríguez^c, E. López Luna^c, M.A. Vidal^{c,*}

^a Instituto Potosino de Investigación Científica y Tecnológica, Camino a la Presa San José 2055, Col. Lomas 4a Sección, 78216 San Luis Potosí, México

^b Centro de Nanociencias y Nanotecnología, Universidad Nacional Autónoma de México, A. Postal 2681, Ensenada, Baja California, México

^c Coordinación para la Innovación y Aplicación de la Ciencia y Tecnología (CIACyT), Universidad Autónoma de San Luis Potosí (UASLP), Álvaro Obregón 64, 78000 San Luis Potosí, México

ARTICLE INFO

Article history:

Received 9 October 2015

Received in revised form

18 November 2015

Accepted 25 November 2015

Communicated by H. Asahi

Available online 2 December 2015

Keywords:

A3. Quantum wells

A3. Molecular beam epitaxy

B2. Semiconducting III–V materials

B3. Heterojunction semiconductor devices

ABSTRACT

Light emission in the three primary colors was achieved in cubic GaN/InGaN/GaN heterostructures grown by molecular beam epitaxy on MgO substrates in a single growth process. A heterostructure with four quantum wells with a width of 10 nm was grown; this quantum wells width decrease the segregation effect of In. Photoluminescence emission produced four different emission signals: violet, blue, green-yellow and red. Thus, we were able to tune energy transitions in the visible spectrum modifying the In concentration in cubic $\text{In}_x\text{Ga}_{1-x}\text{N}$ ternary alloy.

© 2015 Elsevier B.V. All rights reserved.

1. Introduction

In the past decades, nitride semiconductors have been used to fabricate electronic and optoelectronic devices [1–17]. Among the most important applications is solid-state lighting. Using α -GaN and α -InGaN it was possible to build a blue light-emitting diode (LED) [1]. Since this major breakthrough, the development of methods to improve growing conditions has brought remarkable results in light emitting devices [2–6]. Theoretically, due to band gap energy values of α -GaN (3.4 eV) and α -InN (0.7 eV), the ternary InGaN alloy can be used to cover the electromagnetic spectrum from UV to near infrared. Growing conditions that result in more than a 30% concentration of In may lead to high defect density because of the large lattice mismatch between GaN and InN (11%). Furthermore, high indium content leads to a strong quantum confinement stark effect, which reduces the radiative recombination efficiency of carriers and hinders the long wavelength range transitions. Recent reports have studied the optimization of green-yellow emission in hexagonal InGaN-based devices [3–5]. Nonetheless, red wavelength transitions with planar

InGaN heterostructures remain difficult to obtain. Thus, to produce white light emitting diodes, a blue or UV LED is covered with a phosphor, which absorbs the light and reemits it with a longer wavelength. However, using phosphors such as $\text{Ce}^{3+}:\text{Y}_3\text{Al}_5\text{O}_{12}$ (one of the most common phosphors) reduces the long-term reliability and lifetime of the device [6]. Different approaches have been made to overcome this issue. One of them is to synthesize quantum wells by varying the In mole fraction in the active layer to obtain the long wavelength emission without phosphors [7]. Another approach to produce white light is to use the structures such as quantum dots in wells [8], dots in wires [9], nanorods [10], nanopillars [11] and other nanostructures [12]. Typically, these nitride semiconductors crystallize into a hexagonal phase. Therefore, most of the previous work is based on the InGaN wurtzite phase. Nevertheless, the cubic phase has some advantages over the hexagonal phase, such as the lack of spontaneous and piezoelectric polarization [9]. Moreover, β -GaN has a lower band gap energy (3.28 eV) than α -GaN. Thus, low energy emissions in the ternary β -InGaN alloy can be obtained with a smaller In concentration than in α -InGaN.

Although it is more difficult to synthesize InGaN and GaN cubic films, it has been possible to grow them using the Metal-Organic Chemical Vapor Deposition (MOCVD), Metal-Organic Vapor Phase Epitaxy and Molecular Beam Epitaxy (MBE) techniques on the 3C-

* Corresponding author.

E-mail addresses: ignacio.orozco@ipicyt.edu.mx (I.E. Orozco Hinostroza), mavidalborbolla@yahoo.com.mx (M.A. Vidal).

Selection for distinct gene expression properties favours the evolution of mutational robustness in gene regulatory networks

C. ESPINOSA-SOTO

Instituto de Física, Universidad Autónoma de San Luis Potosí, San Luis Potosí, Mexico

Keywords:

gene regulatory networks;
mutational robustness;
stabilizing selection.

Abstract

Mutational robustness is a genotype's tendency to keep a phenotypic trait with little and few changes in the face of mutations. Mutational robustness is both ubiquitous and evolutionarily important as it affects in different ways the probability that new phenotypic variation arises. Understanding the origins of robustness is specially relevant for systems of development that are phylogenetically widespread and that construct phenotypic traits with a strong impact on fitness. Gene regulatory networks are examples of this class of systems. They comprise sets of genes that, through cross-regulation, build the gene activity patterns that define cellular responses, different tissues or distinct cell types. Several empirical observations, such as a greater robustness of wild-type phenotypes, suggest that stabilizing selection underlies the evolution of mutational robustness. However, the role of selection in the evolution of robustness is still under debate. Computer simulations of the dynamics and evolution of gene regulatory networks have shown that selection for any gene activity pattern that is steady and self-sustaining is sufficient to promote the evolution of mutational robustness. Here, I generalize this scenario using a computational model to show that selection for different aspects of a gene activity phenotype increases mutational robustness. Mutational robustness evolves even when selection favours properties that conflict with the stationarity of a gene activity pattern. The results that I present support an important role for stabilizing selection in the evolution of robustness in gene regulatory networks.

Introduction

Across the evolutionary tree, many phenotypic traits have a tendency to change little or remain unaltered after new random mutations (de Visser *et al.*, 2003; Kitano, 2004; Wagner, 2005; Whitacre, 2012; Félix & Barkoulas, 2015). Such mutational robustness occurs in many scales of biological organization, from the folding of macromolecules such as RNA and proteins (Ancel & Fontana, 2000; Xia & Levitt, 2002; Ferrada & Wagner, 2008) to the behaviour of molecular networks (von Dassow *et al.*, 2000; Eldar *et al.*, 2002; Meir *et al.*, 2002; Espinosa-Soto *et al.*, 2004; Manu *et al.*, 2009; Noman

et al., 2015) to cell lineages (Yang *et al.*, 2014), morphological traits (Braendle & Félix, 2009) or even fitness (Kitano, 2004; Eyre-Walker & Keightley, 2007).

Mutational robustness has important effects on a system's *variability* (Wagner & Altenberg, 1996; Pigliucci, 2008), and hence in its potential to evolve. When we consider a single organism, a first glance suggests that mutational robustness obstructs evolutionary change because it decreases the probability of producing new phenotypic variation. Nonetheless, when we consider evolving populations, we find that robustness may increase evolvability. The reason is that mutational robustness favours that a population accumulates 'cryptic' genetic variation that lacks phenotypic effects (Rutherford & Lindquist, 1998; Gibson & Dworkin, 2004; Dworkin, 2005; Schlichting, 2008; Paaby & Rockman, 2014). Then, distinct organisms in the population may have access to very different phenotypic variants after new perturbations (Flatt, 2005; Masel & Trotter,

Correspondence: Carlos Espinosa-Soto, Instituto de Física, Universidad Autónoma de San Luis Potosí, Manuel Nava 6, Zona Universitaria, CP 78290, San Luis Potosí, Mexico.
Tel.: +52 (444) 8262363; 133; fax: +52 (444) 8133874
e-mail: c.espinosa@ifisica.uaslp.mx

Dynamical and Tuneable Modulation of the Tamm Plasmon/Exciton–Polariton Hybrid States Using Surface Acoustic Waves

J.V.T. BULLER^{a,*}, E.A. CERDA-MÉNDEZ^a, R.E. BALDERAS-NAVARRO^b AND P.V. SANTOS^a

^aPaul-Drude-Institut für Festkörperelektronik, 10117 Berlin, Germany

^bInstituto de Investigación en Comunicación Óptica-UASLP, 78000 San Luis, Mexico

In this work, we discuss theoretically the formation of the Tamm plasmon/exciton–polariton hybrid states in an (Al,Ga)As microcavity and their modulation by surface acoustic waves. The modulation of the Tamm plasmon/exciton–polariton states origins in the change of the excitonic band gap energy and the thickness change of the sample structure layers due to the induced strain fields by surface acoustic waves. The frequency f_{SAW} of the acoustic modulation of the Tamm plasmon/exciton–polariton states is limited by the thickness of the upper distributed Bragg reflector. For the Tamm plasmon/exciton–polariton states in $\text{Al}_x\text{Ga}_{1-x}\text{As}/\text{GaAs}$ structures f_{SAW} is in the range of 370 MHz while f_{SAW} in GHz range is possible for the parametric Tamm plasmon/exciton–polariton states. In both cases, the acoustic modulation is several meV for typical acoustic power levels.

DOI: [10.12693/APhysPolA.129.A-26](https://doi.org/10.12693/APhysPolA.129.A-26)

PACS: 71.36.+c, 42.55.Sa, 85.50.-n

1. Introduction

The development of new optoelectronic devices operating at low threshold powers and at high switching frequencies is a complex and challenging task, which can only be overcome by exploiting new physical phenomena [1–4] and applying them to device implementations [5, 6]. One of such new promising physical phenomenon are exciton–polaritons in semiconductor microcavities (MCs). Exciton–polaritons are unique bosonic half-light half-matter quasiparticles that result from the strong coupling between the photonic mode of a MC and quantum well (QW) excitons embedded in the active MC region (*cf.* Fig. 1a, [7]). The inter-excitonic interactions between polaritons give rise to optical nonlinearities several orders of magnitude higher than in purely photonic systems. Due to the photonic component polaritons have a very low effective mass (10^{-5} – 10^{-4} mass of a free electron) leading to a de Broglie wavelength λ_{dB} of a few μm and thus to the possibility to form macroscopic coherent quantum phases at low densities and at elevated temperatures (on the order of a few K) as well as to be manipulated by micro-scale potentials [8, 9]. Various polariton-based device concepts, like polariton-based transistors and logic gates, as well as their implementation in quantum information processing have been proposed [10, 11].

The fabrication of polaritonic devices requires reliable and practical potentials for controlling, confining and guiding exciton–polaritons in MC structure. One interesting option is provided by dynamic strain

potentials [12] induced by a surface acoustic wave (SAW) [13, 14]. SAWs are mechanical vibrations propagating along a surface (*cf.* Fig. 1c): the strain field of a SAW with wavelength λ_{SAW} smaller than λ_{dB} creates a tuneable acoustic lattice for the control of the polariton properties. Since the SAW penetration depth is comparable to λ_{SAW} , an efficient acoustic modulation requires that λ_{SAW} is larger than the thickness of the upper MC distributed Bragg reflector (DBR). In this contribution, we demonstrate that this limitation can be overcome by exploiting plasmonic resonances induced by thin metallic stripes deposited on the top of the MC structure. In this case, new quasiparticles called the Tamm plasmon/exciton–polaritons (TPEP) form by the superposition of the Tamm plasmons (TPs) at the metal–semiconductor interface and the exciton–polaritons in the MC [10]. The aim of this work is to explore the dynamical and tuneable modulation of TPEP modes by SAW at frequencies close to and in the gigahertz range.

2. Sample design

The proposed sample structure supporting TPEP states consists of a gold layer on top of a DBR consisting of $\text{Al}_x\text{Ga}_{1-x}\text{As}$ layers with a thickness $\lambda/(4n_i)$ ($i = \text{Al}_{15}\text{Ga}_{85}\text{As}$, $\text{Al}_{80}\text{Ga}_{20}\text{As}$), where n_i is the refractive index and λ the MC resonance wavelength (*cf.* Fig. 1a). The structure supports TP modes at the metal–semiconductor interface only when the DBR layer adjacent to the metal has a higher refractive index than its following DBR layer [16]. The energy E_{T} of the TP mode can be tuned by changing the thickness of the metal and/or of the adjacent DBR layer. When E_{T} is in resonance with the MC mode and the QW exciton energy, the resulting coupled system can be described using the three level coupled oscillator model given by

*corresponding author; e-mail: buller@pdi-berlin.de

Exciton-polariton gap soliton dynamics in moving acoustic square latticesJ. V. T. Buller,^{1,*} R. E. Balderas-Navarro,^{1,2} K. Biermann,¹ E. A. Cerda-Méndez,^{1,2,3} and P. V. Santos¹¹*Paul-Drude-Institut für Festkörperelektronik, 10117 Berlin, Germany*²*Instituto de Investigación en Comunicación Óptica, Universidad Autónoma de San Luis Potosí, Avenida Karakorum 1470, Lomas 4^a Secc, 78216, San Luis Potosí, México*³*Instituto de Física Universidad Autónoma de San Luis Potosí, Avenida Manuel Nava #6, Zona Universitaria, Código Postal 78290 San Luis Potosí, México*

(Received 18 May 2016; revised manuscript received 22 August 2016; published 22 September 2016)

The modulation by a surface acoustic wave (SAW) provides a powerful tool for the formation of tunable lattices of exciton-polariton macroscopic quantum states (MQSs) in semiconductor microcavities. The MQSs were resonantly excited in an optical parametric oscillator configuration. We investigate the temporal dynamics of these lattices using time and spatially resolved photoluminescence (PL). Photoluminescence images of the MQSs clearly show the motion of the lattice at the acoustic velocity. Interestingly, the PL intensity emitted by the MQSs as well as their coherence length oscillate with the position of the lattice sites relative to the exciting laser beam. The coherence length and the PL intensity are correlated. The PL oscillation amplitude depends on both the intensity and the size of the exciting laser spot and increases considerably for excitation intensities close to the optical threshold power for the formation of the MQS. The oscillations are explained by a model that takes into account the combined effects of SAW reflections, which dynamically distort the amplitude of the potential, and the spatial phase of the acoustic lattice within the exciting laser spot. This paper could pave the way to tailor polariton-based light-emitting sources with intensity variations controlled by the SAWs.

DOI: [10.1103/PhysRevB.94.125432](https://doi.org/10.1103/PhysRevB.94.125432)**I. INTRODUCTION**

Exciton-polaritons result from the strong coupling between photons confined in a microcavity (MC) and excitons in quantum wells (QWs) inserted in it. They are half-light, half-matter quasiparticles with bosonic character. The excitonic component gives rise to strong nonlinear interactions between exciton-polaritons, while the photonic component leads to a very low effective mass m_{eff} (10^{-4} – 10^{-5} mass of the electron) and, consequently, de Broglie wavelengths λ_{dB} of a few microns [1,2]. The latter enables the formation of macroscopic quantum states (MQSs) of exciton-polaritons at particle densities considerably lower and at temperatures considerably higher than in atomic systems [3,4]. These remarkable properties of exciton-polaritons in semiconductor optical MCs have opened the way for several device functionalities such as polariton-based lasers [5,6], transistors [7,8], and logic gates [9,10].

In analogy to optical lattices of cold atoms [11], tunable lattices for exciton-polariton MQSs can be formed via the periodic spatial modulation introduced by a surface acoustic wave (SAW). Surface acoustic waves are mechanical vibrations that can be electrically excited using interdigital transducers (IDTs) deposited on the MC surface [12] [cf. Fig. 1(a)]. The moving strain field of the SAW creates regions of tension and compression in the MC, thus spatially modulating the MC optical resonance energy as well as the band gap energy of the embedded QWs [13]. By superimposing two orthogonal SAW beams, one can create the two-dimensional square lattice potential illustrated in Fig. 1(a). For small SAW amplitudes Φ_{SAW} , λ_{dB} can become comparable to or even longer than the SAW wavelength λ_{SAW} . Under this condition, the acoustic

modulation creates a folded band structure for exciton-polariton MQSs with dispersion and energy gaps controlled by Φ_{SAW} . The mini-Brillouin zones (MBZs) formed by the lattice, which are illustrated in the inset of Fig. 1(b), have dimensions $k_{\text{SAW}} = 2\pi/\lambda_{\text{SAW}}$ determined by the SAW periodicity.

As for the polariton dispersion, the symmetry and spatial coherence of MQSs in an acoustic lattice also depend on the lattice amplitude Φ_{SAW} . Large Φ_{SAW} flattens the lowest dispersion branch and inhibits the tunneling of exciton-polaritons between lattice sites, thus fragmenting the extended phase via the formation of independent MQSs localized at the minima of the SAW potential [14]. Phases with extended coherence appear, in contrast, for moderate Φ_{SAW} , where the lowest dispersion branch exhibits considerable energy dispersion [15]. Interestingly, the most robust MQS under a moderate Φ_{SAW} does not form at the Γ point of the lowest dispersion branch but rather at the M points, where the effective mass of exciton-polaritons is negative [cf. Fig. 1(b)]. Recently, we have demonstrated that these phases are gap-soliton-like condensates (GSs) [16]. Gap-soliton-like condensates are metastable self-localized excitations originating from the compensation of the repulsive interparticle interactions by their negative kinetic energy. Gap-soliton-like condensates have also been observed in other physical systems [17] and may prove to be of relevance for quantum information processing [18,19].

Previous investigations on exciton-polaritons and GSs in acoustic lattices have been carried out using optical spectroscopy in the continuous wave (cw) domain and were, therefore, unable to capture the GS temporal dynamics in the moving acoustic lattice. In this paper, we address this issue via photoluminescence (PL) studies carried out with time and spatial resolutions which are much shorter than the temporal and spatial SAW periods, respectively. We start by describing the experimental techniques employed to prepare the MC sample and to map the time-dependent GS wave

*buller@pdi-berlin.de



PAPER

Spatial self-organization of macroscopic quantum states of exciton-polaritons in acoustic lattices

OPEN ACCESS

RECEIVED

8 December 2015

REVISED

27 May 2016

ACCEPTED FOR PUBLICATION

6 June 2016

PUBLISHED

1 July 2016

Original content from this work may be used under the terms of the [Creative Commons Attribution 3.0 licence](#).

Any further distribution of this work must maintain attribution to the author(s) and the title of the work, journal citation and DOI.

J V T Buller¹, E A Cerda-Méndez^{2,4}, R E Balderas-Navarro², K Biermann¹ and P V Santos¹¹ Paul-Drude-Institut für Festkörperelektronik, Hausvogteiplatz 05-7, D-10117 Berlin, Germany² Instituto de Investigación en Comunicación Óptica, Universidad Autónoma de San Luis Potosí, Av. Karakorum 1470, Lomas 4ª Secc, 78210, San Luis Potosí, México³ Instituto de Física Universidad Autónoma de San Luis Potosí, Av. Manuel Nava #6, Zona Universitaria, C.P. 78290 San Luis Potosí, México⁴ Author to whom any correspondence should be addressed.E-mail: ecerda@cactus.iico.uaslp.mx**Keywords:** semiconductor microcavities, surface acoustic waves, exciton-polaritons, solitonsSupplementary material for this article is available [online](#)**Abstract**

Exciton-polariton systems can sustain macroscopic quantum states (MQSs) under a periodic potential modulation. In this paper, we investigate the structure of these states in acoustic square lattices by probing their wave functions in real and momentum spaces using spectral tomography. We show that the polariton MQSs, when excited by a Gaussian laser beam, self-organize in a concentric structure, consisting of a single, two-dimensional gap-soliton (GS) state surrounded by one dimensional (1D) MQSs with lower energy. The latter form at hyperbolic points of the modulated polariton dispersion. While the size of the GS tends to saturate with increasing particle density, the emission region of the surrounding 1D states increases. The existence of these MQSs in acoustic lattices is quantitatively supported by a theoretical model based on the variational solution of the Gross–Pitaevskii equation. The formation of the 1D states in a ring around the central GS is attributed to the energy gradient in this region, which reduces the overall symmetry of the lattice. The results broaden the experimental understanding of self-localized polariton states, which may prove relevant for functionalities exploiting solitonic objects.

1. Introduction

The manipulation of macroscopic quantum states (MQS), systems where a collection of particles share a single macroscopic wave function, is a fascinating topic that has been investigated in diverse research fields [1, 2]. The possibility to engineer artificial periodic potentials to shape the properties of a MQS has allowed the simulation of solid-state quantum phase-transitions [3], the implementation of quantum computation protocols [4] and the exploration of the cross-over of MQS physics with nonlinear optics concepts [5]. Notable examples of MQS systems are atomic Bose–Einstein condensates (BECs) in optical and/or magnetic traps and supercurrents in superconducting circuits. Another type of MQS exists in semiconductor planar microcavities (MC) [6, 7], where, in contrast to atoms in BECs or Cooper pairs in superconductors, the components are photonic states dressed by excitons called exciton-polaritons. Exciton-polaritons are bosonic light–matter quasi-particles that form when photons couple strongly with quantum-well (QW) excitons in a semiconductor MC. While the inter-excitonic interactions provide an optical nonlinearity which is several orders of magnitude stronger than in purely photonic systems, the small mass arising from the photonic component gives polaritons a de Broglie wavelength of a few micrometres. The latter enables them to generate MQSs at lower densities and higher temperatures (on the order of a few kelvin) than in atomic systems as well as to be coherently manipulated by micrometric potentials [8–15]. Of particular interest are tuneable modulation schemes, which can produce potentials for polaritons analogue to optical lattices for cold atoms. Such potentials may be provided by the



Cubic GaN films grown below the congruent sublimation temperature of (0 0 1) GaAs substrates by plasma-assisted molecular beam epitaxy

Arturo Alanís, Heber Vilchis^{a)}, Edgar López, and Miguel A. Vidal

View Affiliations

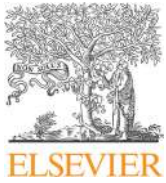
Journal of Vacuum Science & Technology B, Nanotechnology and Microelectronics: Materials, Processing, Measurement, and Phenomena **34**, 02L115 (2016); doi: <http://dx.doi.org/10.1116/1.4943661>

PDF ABSTRACT FULL TEXT FIGURES TOOLS SHARE METRICS

III-V semiconductors Reflection high energy electron diffraction Thin film growth Plasma temperature Crystal structure

ABSTRACT

Gallium nitride films were synthesized on GaAs (0 0 1) substrates at temperatures lower than the congruent sublimation temperature of GaAs. By controlling isothermal desorption of the substrate and setting experimental parameters in the early growth stage, the authors obtained cubic GaN films. No nitridation process or growth of a buffer layer was necessary prior to GaN growth of GaN. *In situ* reflection high-energy electron diffraction (RHEED) and *ex situ* high-resolution x-ray diffraction were used to study the crystalline qualities of the films. The measured pole diagram of cubic GaN at $2\theta = 34.5^\circ$ was consistent with RHEED results and confirmed the crystalline structure. Photoluminescence measurements showed a strong emission only at 3.21 eV.



Structural and Raman studies of Ga₂O₃ obtained on GaAs substrate



C. Galván^a, M. Galván^b, J.S. Arias-Cerón^{b,*}, E. López-Luna^a, H. Vilchis^a, V.M. Sánchez-R^b

^a Coordination for the Innovation and Application of Science and Technology-UASLP, Sierra Leona # 550 Lomas 2da Sección, Cp. 78120 San Luis Potosí, Mexico

^b Solid State Electronics Section, Department of Electrical Engineering – CINVESTAV-I.P.N. Av. Instituto Politécnico Nacional, 2508, San Pedro Zacatenco, C.P. 07360 México D.F., Mexico

ARTICLE INFO

Article history:

Received 9 February 2015

Received in revised form

27 October 2015

Accepted 27 October 2015

Keywords:

Gallium oxide

Nanostructures

Raman scattering

Thermal oxidation

ABSTRACT

Ga₂O₃ were synthesized by controlled thermal oxidation of GaAs substrates at atmospheric pressure. The crystalline structure and vibrational modes were studied as a function of growth temperature within a range of 750–950 °C. Samples grown in the range of 750–850 °C present nanostructured surface and the samples obtained at higher temperature are oriented to the (004) β-phase. Crystalline structure was confirmed by X-ray diffraction, and Raman scattering studies. The evolution of the surface morphology was analyzed by atomic force microscopy, and scanning electron microscopy.

© 2015 Elsevier Ltd. All rights reserved.

1. Introduction

In recent years, wide band gap oxide semiconductors such as CuAlO₂ (3.2 eV), In₂O₃ (3.6 eV), ZnO (3.3 eV), SnO (3.6 eV) and Ga₂O₃ (4.9 eV) have attracted considerable attention due to their great potential in technological applications. For example, these materials are used in spin-transport electronic devices, metal-oxide-semiconductor field effect transistors and short wavelength optoelectronic devices [1–5]. Among them, Ga₂O₃ has received considerable attention because of its thermal stability, as well as its optical and electrical properties. These properties make Ga₂O₃ a desirable material for the development of high temperature gas sensors [6], efficient transparent conducting layers [7] and short-wavelength light-emitting devices [5].

The five modifications of Ga₂O₃ are known as α, β, γ, δ, and ε phases [8]. Among these modifications, β-Ga₂O₃ is the most stable modification with a melting point of 1780 °C. It has a base-centered monoclinic crystal structure, where the oxygen ions are in a distorted cubic packing arrangement and the gallium ions are in distorted tetrahedral and octahedral sites [9]. Various synthesis techniques have been employed to grow β-Ga₂O₃ films and nanostructures, using either a physical or a chemical deposition technique. The characteristics of the deposited films will vary

depending on the experimental conditions such as pressure, growth temperature, deposition rate, annealing conditions, and reactants [10–19]. They will also depend on the deposition method employed, whether it is sputtering [11,12], thermal evaporation [13,14], pulsed laser deposition [15], molecular beam epitaxy [16,17], metal-organic chemical vapor deposition [18], ultrasonic spray pyrolysis [19], or atmospheric pressure chemical vapor deposition [20]. These works also reported the structural and optical properties of β-Ga₂O₃ thin films. However, the results indicate poor crystalline quality, and high costs.

In this work, we report the synthesis and characterization of Ga₂O₃ samples, grown by Controlled Thermal Oxidation of GaAs substrates in dry oxygen environment. In contrast with other methods reported, this technique does not use an external gallium source. Controlled thermal desorption of the GaAs substrates were realized in order to obtain a gallium rich surface, which was used as native source of gallium. The studied samples were grown at different temperatures, in order to study the crystal structure, surface morphology, vibrational modes, compositional analysis and ultra-violet emission. The results obtained are analyzed and discussed here.

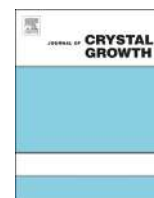
2. Experimental procedure

Ga₂O₃ samples were synthesized in a CVD reactor at atmospheric pressure. The CVD equipment features a custom-built horizontal system with two gas inlet lines. Pure N₂ is introduced through one of the inlet lines, to maintain a controlled environment in the growth chamber. Through the other inlet, at 80/20%

* Corresponding author.

E-mail addresses: galvan.constantini@gmail.com (C. Galván), miguel_galvan_a@yahoo.com.mx (M. Galván), jarias@sees.cinvestav.mx (J.S. Arias-Cerón), edgar.luna@uaslp.mx (E. López-Luna), heber.vilchis@uaslp.mx (H. Vilchis), victors@sees.cinvestav.mx (V.M. Sánchez-R).

¹ CONACYT Research Fellow.



Tuning emission in violet, blue, green and red in cubic GaN/InGaN/GaN quantum wells



I.E. Orozco Hinostroza^a, M. Avalos-Borja^{a,b}, V.D. Compeán García^c, C. Cuellar Zamora^c,
A.G. Rodríguez^c, E. López Luna^c, M.A. Vidal^{c,*}

^a Instituto Potosino de Investigación Científica y Tecnológica, Camino a la Presa San José 2055, Col. Lomas 4a Sección, 78216 San Luis Potosí, México

^b Centro de Nanociencias y Nanotecnología, Universidad Nacional Autónoma de México, A. Postal 2681, Ensenada, Baja California, México

^c Coordinación para la Innovación y Aplicación de la Ciencia y Tecnología (CIACyT), Universidad Autónoma de San Luis Potosí (UASLP), Álvaro Obregón 64, 78000 San Luis Potosí, México

ARTICLE INFO

Article history:

Received 9 October 2015

Received in revised form

18 November 2015

Accepted 25 November 2015

Communicated by H. Asahi

Available online 2 December 2015

Keywords:

A3. Quantum wells

A3. Molecular beam epitaxy

B2. Semiconducting III–V materials

B3. Heterojunction semiconductor devices

ABSTRACT

Light emission in the three primary colors was achieved in cubic GaN/InGaN/GaN heterostructures grown by molecular beam epitaxy on MgO substrates in a single growth process. A heterostructure with four quantum wells with a width of 10 nm was grown; this quantum wells width decrease the segregation effect of In. Photoluminescence emission produced four different emission signals: violet, blue, green-yellow and red. Thus, we were able to tune energy transitions in the visible spectrum modifying the In concentration in cubic $\text{In}_x\text{Ga}_{1-x}\text{N}$ ternary alloy.

© 2015 Elsevier B.V. All rights reserved.

1. Introduction

In the past decades, nitride semiconductors have been used to fabricate electronic and optoelectronic devices [1–17]. Among the most important applications is solid-state lighting. Using α -GaN and α -InGaN it was possible to build a blue light-emitting diode (LED) [1]. Since this major breakthrough, the development of methods to improve growing conditions has brought remarkable results in light emitting devices [2–6]. Theoretically, due to band gap energy values of α -GaN (3.4 eV) and α -InN (0.7 eV), the ternary InGaN alloy can be used to cover the electromagnetic spectrum from UV to near infrared. Growing conditions that result in more than a 30% concentration of In may lead to high defect density because of the large lattice mismatch between GaN and InN (11%). Furthermore, high indium content leads to a strong quantum confinement stark effect, which reduces the radiative recombination efficiency of carriers and hinders the long wavelength range transitions. Recent reports have studied the optimization of green-yellow emission in hexagonal InGaN-based devices [3–5]. Nonetheless, red wavelength transitions with planar

InGaN heterostructures remain difficult to obtain. Thus, to produce white light emitting diodes, a blue or UV LED is covered with a phosphor, which absorbs the light and reemits it with a longer wavelength. However, using phosphors such as $\text{Ce}^{3+}:\text{Y}_3\text{Al}_5\text{O}_{12}$ (one of the most common phosphors) reduces the long-term reliability and lifetime of the device [6]. Different approaches have been made to overcome this issue. One of them is to synthesize quantum wells by varying the In mole fraction in the active layer to obtain the long wavelength emission without phosphors [7]. Another approach to produce white light is to use the structures such as quantum dots in wells [8], dots in wires [9], nanorods [10], nanopillars [11] and other nanostructures [12]. Typically, these nitride semiconductors crystallize into a hexagonal phase. Therefore, most of the previous work is based on the InGaN wurtzite phase. Nevertheless, the cubic phase has some advantages over the hexagonal phase, such as the lack of spontaneous and piezoelectric polarization [9]. Moreover, β -GaN has a lower band gap energy (3.28 eV) than α -GaN. Thus, low energy emissions in the ternary β -InGaN alloy can be obtained with a smaller In concentration than in α -InGaN.

Although it is more difficult to synthesize InGaN and GaN cubic films, it has been possible to grow them using the Metal-Organic Chemical Vapor Deposition (MOCVD), Metal-Organic Vapor Phase Epitaxy and Molecular Beam Epitaxy (MBE) techniques on the 3C-

* Corresponding author.

E-mail addresses: ignacio.orozco@ipicyt.edu.mx (I.E. Orozco Hinostroza), mavidalborbolla@yahoo.com.mx (M.A. Vidal).

Symbolic complexity for nucleotide sequences: a sign of the genome structure

R Salgado-García¹ and E Ugalde²

¹Centro de Investigación en Ciencias-IICBA, Universidad Autónoma del Estado de Morelos, Avenida Universidad 1001, Cuernavaca Morelos, C.P. 62209, Mexico

²Instituto de Física, Universidad Autónoma de San Luis Potosí, Avenida Manuel Nava 6, Zona Universitaria, 78290 San Luis Potosí, Mexico

E-mail: raulsg@uaem.mx

Received 18 January 2016, revised 28 August 2016

Accepted for publication 5 September 2016

Published 10 October 2016



CrossMark

Abstract

We introduce a method for estimating the complexity function (which counts the number of observable words of a given length) of a finite symbolic sequence, which we use to estimate the complexity function of coding DNA sequences for several species of the *Hominidae* family. In all cases, the obtained symbolic complexities show the same characteristic behavior: exponential growth for small word lengths, followed by linear growth for larger word lengths. The symbolic complexities of the species we consider exhibit a systematic trend in correspondence with the phylogenetic tree. Using our method, we estimate the complexity function of sequences obtained by some known evolution models, and in some cases we observe the characteristic exponential-linear growth of the *Hominidae* coding DNA complexity. Analysis of the symbolic complexity of sequences obtained from a specific evolution model points to the following conclusion: linear growth arises from the random duplication of large segments during the evolution of the genome, while the decrease in the overall complexity from one species to another is due to a difference in the speed of accumulation of point mutations.

Keywords: symbolic complexity, symbolic dynamics, genome structure

(Some figures may appear in colour only in the online journal)

1. Introduction

Nucleotide sequences carry information about an individual's life as well as their evolutionary history. A lasting problem in modern genomics is how this information is organized in the genome or, in other words, what the structure of the genome is from an information theory



Effects of growth temperature on the incorporation of nitrogen in GaNAs layers

José Ángel Espinoza-Figueroa, Víctor Hugo Méndez-García, Miguel Ángel Vidal, and Esteban Cruz-Hernández^{a)} more...

View Affiliations

Journal of Vacuum Science & Technology B, Nanotechnology and Microelectronics: Materials, Processing, Measurement, and Phenomena **34**, 02L111 (2016); doi: <http://dx.doi.org/10.1116/1.4942900>

PDF ABSTRACT FULL TEXT FIGURES TOOLS SHARE METRICS

Secondary ion mass spectroscopy X-ray diffraction Semiconductor growth III-V semiconductors Interstitial defects

ABSTRACT

Ternary III-N-V semiconductor alloys are interesting and complex materials. GaNAs is one such material that has been studied extensively; however, the accurate determination of the N content within this material in which the growth conditions significantly increases the amount of interstitial N has not yet been reported. To address this problem, GaNAs layers (100 nm) were prepared using molecular beam epitaxy at temperatures between 400 and 600 °C with a high nominal N concentration (3%). The N content was determined using high resolution x-ray diffraction (HRXRD), secondary ion mass spectrometry (SIMS), and low-temperature photoluminescence (PL). The N concentration determined using these techniques was compared. Additionally, the relationship between the growth temperature and N concentration is discussed. The incorporation of N into interstitial sites resulted in significant variations in the N content as estimated by SIMS, HRXRD,

New orientations in the stereographic triangle for self-assembled faceting

R. Méndez-Camacho,¹ V. H. Méndez-García,¹ M. López-López,²
and E. Cruz-Hernández^{1,a}

¹*Coordination for the Innovation and Application of Science and Technology, Universidad Autónoma de San Luis Potosí, S.L.P. 78210, México*

²*Physics Department, CINVESTAV-IPN, Apartado Postal 14-740, México D.F. 07000, México*

(Received 11 March 2016; accepted 17 June 2016; published online 24 June 2016)

Energetically unstable crystalline surfaces, among their uses, can be templates for the growth of periodic arrays of one-dimensional (1D) nanoscale structures. However, few studies have explored self-assembled faceting on high-index (HI) planes inside the stereographic triangle, and extant studies have not produced any criteria for encouraging the formation of one-dimensional periodic arrays. In this Letter, by analyzing the MBE growth of homoepitaxial facets on (631)A GaAs, a HI plane inside the triangle, we present a criteria to produce highly uniform 1D periodic arrays on unexplored surfaces. These families of planes are those belonging to the lines connecting the energetically stable HI GaAs (11 5 2) plane with any of the (100), (110), and (111) planes at the corners of the stereographic triangle. This novel strategy can lead to new possibilities in self-assembling 1D structures and manipulating physical properties, which in turn may result in new HI- and 1D-based experiments and devices. © 2016 Author(s). All article content, except where otherwise noted, is licensed under a Creative Commons Attribution (CC BY) license (<http://creativecommons.org/licenses/by/4.0/>). [<http://dx.doi.org/10.1063/1.4954998>]

INTRODUCTION

Energetically unstable crystalline surfaces, which tend to break up into facets of low free energy, can be used as templates for growing nanoscale one-dimensional periodic arrays (1DPAs) such as quantum wires.¹⁻⁴ Ultra-high-vacuum techniques such as molecular beam epitaxy (MBE) and metalorganic vapor phase epitaxy have been used to grow periodic corrugated structures with remarkable uniformity on surfaces with an unstable high Miller index (HI) or vicinal GaAs substrates (VSs).⁵⁻⁸ In addition to its potential for promoting self-assembled structures, epitaxial growth on HI substrates has exhibited many interesting features. For example, HI planes have many characteristics that make them important in basic and applied research, such as the amphoteric nature of Si impurities,^{9,10} atypical piezoelectric effects,¹¹ high degree of light polarization in arrays of quantum wires,⁴ observation of anisotropic topological surface states,^{12,13} and the enhancement of (In,Ga,Al)P-GaP light-emitting diodes.¹⁴

By convention, the HI and VSs are chosen to be oriented along the edges of the stereographic triangle (ST), whose corners are the (100), (110), and (111) low-index (LI) planes (which are energetically stable), as shown in Fig. 1. Such surfaces on the sides of the ST are chosen because only the LI corners can form low-energy reconstructions, and because any given HI or VS on it should decay into facets composed of combinations of two of the corner planes. By contrast, the HI planes in the ST likely have a very complex structure because it should comprise combinations of the three LI planes. For these reasons, there have been very few studies on HI planes inside the ST, and they are chosen without following specific criteria for 1DPA formation.

^aElectronic mail: esteban.cruz@uaslp.mx



Structural characterization of AlGaAs:Si/GaAs (631) heterostructures as a function of As pressure

Leticia Ithsmel Espinosa-Vega, Miguel Ángel Vidal-Borbolla, Ángel Gabriel Rodríguez-Vázquez, Irving Eduardo Cortes-Mestizo, Esteban Cruz-Hernández more...

View Affiliations

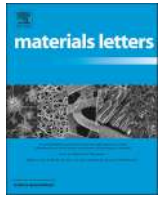
Journal of Vacuum Science & Technology B, Nanotechnology and Microelectronics: Materials, Processing, Measurement, and Phenomena **34**, 02L119 (2016); doi: <http://dx.doi.org/10.1116/1.4944452>

PDF ABSTRACT FULL TEXT FIGURES CITED BY TOOLS SHARE METRICS

III-V semiconductors Thin film growth Epitaxy Semiconductor growth Phonons

ABSTRACT

AlGaAs:Si/GaAs heterostructures were grown on (631) and (100) GaAs substrates and studied as a function of the As cell beam equivalent pressure. High-resolution x-ray diffraction patterns showed that the highest quality AlGaAs epitaxial layers were grown at $P_{As} = 1.9 \times 10^{-5}$ for (100)- and $P_{As} = 4 \times 10^{-5}$ mbar for (631)-oriented substrates. Raman spectroscopy revealed higher crystalline quality for films grown on (631) oriented substrates. The GaAs- and AlAs-like modes of the AlGaAs(631) films exhibited increased intensity ratios between the transverse optical phonons and longitudinal optical phonons with increasing P_{As} , whereas the ratios were decreased for the (100) plane. This is in agreement with the selection rules for (631) and high-resolution x-ray diffraction observations. Anisotropy and surface corrugation of the AlGaAs(631) films also were characterized using atomic force microscopy and Raman spectroscopy.



Characterization of $\text{Al}_{0.047}\text{Ga}_{0.953}\text{Sb}$ layers grown on GaSb using reciprocal space maps



Primavera López-Salazar^a, Javier Martínez-Juárez^a, Gabriel Juárez-Díaz^{b,*}, Francisco De Anda-Salazar^c, Ramon Peña-Sierra^d, Arturo García Borquez^e, Alvaro David Hernández-De la Luz^a

^a Centro de Investigaciones en Dispositivos Semiconductores, BUAP, C. U., 14 Sur y Av. San Claudio, Puebla, Pue. 72570, México

^b Facultad de Ciencias de la Computación, BUAP, C. U., 14 Sur y Av. San Claudio, Puebla, Pue. 72570, México

^c Instituto de Investigación en Comunicaciones Ópticas, Universidad Autónoma de San Luis Potosí, Av. Karakorum, Lomas Cuarta Sección, San Luis Potosí, S.L. P. 78210, México

^d Sección de Electrónica del Estado Sólido, CINVESTAV-IPN, Av. IPN No. 2405 Col Zacatenco, México D. F., México

^e Ciencia de Materiales, Escuela Superior de Física y Matemáticas del Instituto Politécnico Nacional, Unid. Prof. Adolfo López Mateos, México D.F. 07738, México

ARTICLE INFO

Article history:

Received 24 October 2015

Received in revised form

17 December 2015

Accepted 21 December 2015

Available online 24 December 2015

Keywords:

Epitaxial growth

Reciprocal space mapping

Lattice relaxation

Layer tilt

III–V compounds

GaSb based alloys

ABSTRACT

Structures of $\text{Al}_{0.047}\text{Ga}_{0.953}\text{Sb}$ layers on GaSb (100) substrates were studied by high resolution X-ray diffraction (HRXRD) using reciprocal space maps (RSM) and rocking curves around the (004) and (115) reflections. The layers were grown at 450 °C with a supersaturation of 10 °C in a conventional Liquid Phase Epitaxy (LPE) system varying the growth time from 1 to 4 min resulting in an increment of thickness. It was found that tilt, relaxation and dislocation density of the layers can be calculated using its rocking curves and reciprocal space mapping and it is found that these characteristics are influenced by the thickness of layer.

© 2015 Elsevier B.V. All rights reserved.

1. Introduction

The $\text{Al}_x\text{Ga}_{1-x}\text{Sb}$ alloy is an attractive material because of its optoelectronic properties with potential applications in devices operating in the infrared region, such as photodetectors, lasers and light emitters [1–3]. The direct bandgap of this alloy can be tuned between 0.72 and 0.93 eV by changing its composition from $x=0$ to $x=0.4$. With $x=0.047$ the alloy can operate around the wavelength of less attenuation in optical fibers at 1.55 μm [4]. However, in order to fabricate efficient optoelectronic devices is essential to have a material with high crystalline quality with a low point defects concentration and that absorbs or emits light efficiently [5]. Unfortunately, in many cases the AlGaSb layers grown on GaSb are strained owing to their mismatch, showing structural defects.

By controlling the growth conditions one may grow epitaxially a pseudomorphic AlGaSb layer on a GaSb substrate until the thickness of the layer reaches a critical value, h_c , which depends

upon both the aluminum content, x , and the growth temperature, T_c [6,7]. If this critical thickness is exceeded, it becomes energetically favorable for the stress in the epilayer to be relieved through the formation of $60^\circ a/2$ misfit dislocations at the AlGaSb/GaSb interface.

Reciprocal space mapping is often used to investigate the structural properties of epitaxial thin films (layer tilt, lattice relaxation, composition and quality of structures) [8], and the transition from the fully strained to the relaxed state can also be investigated with the help of reciprocal space maps (RSMs) [9,10]. However, to our knowledge this technique has not been applied to the characterization of AlGaSb layers on GaSb.

Based on the theory developed by Kaganer et al. [11] and geometrical calculations of Chauveau et al. [12] it is possible to find, quantitatively parameters such as layer tilt, from high resolution RSMs. In this paper we analyze by means of HRXRD, the microstructure of partially relaxed $\text{Al}_{0.047}\text{Ga}_{0.953}\text{Sb}$ epilayers on GaSb (100) substrates. Four epitaxial samples of the same composition and different thickness were investigated to analyze the structural parameters such as the relaxation, tilt and composition.

* Corresponding author.

E-mail address: j.gabriel@rocketmail.com (G. Juárez-Díaz).



Regular article

High and abrupt breakdown voltage $\text{In}_{0.15}\text{Ga}_{0.85}\text{As}_{0.14}\text{Sb}_{0.86}/\text{GaSb}$ junctions grown by LPEV.H. Compeán-Jasso^{a,*}, F. de Anda-Salazar^b, F. Sánchez-Niño^b, V.A. Mishurnyi^b, J. Martínez-Juarez^c^a CONACYT Research Fellow – Instituto de Investigación en Comunicación Óptica, Av. Karakorum 1470, Col. Lomas 4a Sec., San Luis Potosí, SLP CP 78210, Mexico^b Universidad Autónoma de San Luis Potosí, Instituto de Investigación en Comunicación Óptica, Av. Karakorum 1470, Col. Lomas 4a Sec., San Luis Potosí, SLP CP 78210, Mexico^c Centro de Investigaciones en Dispositivos Semiconductores, BUAP, C. U., 14 Sur y Av. San Claudio, Puebla, Pue. 72570, Mexico

H I G H L I G H T S

- GaInAsSb PN junctions with high and abrupt breakdown voltages by LPE.
- The structures have been submitted to annealing processes just after epitaxial growth.
- The diffusion of Te from GaSb towards the epi-layer produces this behavior.

A R T I C L E I N F O

Article history:

Received 18 June 2016

Revised 14 September 2016

Accepted 14 September 2016

Available online 14 September 2016

A B S T R A C T

p-GaInAsSb/n-GaSb junction with breakdown voltages as high as 38 V and abrupt breakdown characteristic have been fabricated by Liquid Phase Epitaxy. To obtain these characteristics the structures have been submitted to annealing processes just after epitaxial growth. The diffusion of dopant from the n-GaSb substrate towards the epitaxial layer separates the electrical junction from the epitaxial interface and produces junctions with better inverse polarization behavior.

© 2016 Elsevier B.V. All rights reserved.

1. Introduction

GaInAsSb is a very interesting material for the development of near and mid infrared devices such as LED's, laser, photodetectors and thermophotovoltaic devices that could be suitable for applications like air pollution measurement and gas monitoring, night vision, and energy conversion [1–10]. The bandgap of $\text{In}_{0.15}\text{Ga}_{0.85}\text{As}_{0.14}\text{Sb}_{0.86}$ is well suited for detection at 2.2 μm , also GaInAsSb alloys are interesting for avalanche photodetectors because their electron and hole impact ionization properties [6].

However, the lack of good GaInAsSb PN junctions hinders the marketing of competitive devices for application in the real world. A quick review [6–18] of the Current-Voltage (I-V) characteristics of GaSb and/or GaInAsSb diodes reported show that reverse current has no saturation value, it always increases smoothly as the reverse applied voltage increases and there is not an abrupt breakdown voltage, these behavior could be attributed to tunnel currents via deep levels ([13] and references therein). In all these reports the electrical PN junction coincides with a metallurgical interface between epitaxial layers.

It has been shown [19] that GaAsSb PN junctions fabricated from epitaxial structures subjected to baking at 380 °C during different times show an improvement of the inverse I-V characteristics. The growth technique used was Liquid Phase Epitaxy (LPE) and the improvement was attributed to a spatial separation between the electrical and metallurgical junctions due to the diffusion of Te during the baking time.

In this work GaInAsSb/GaSb PN junctions showing low saturation currents and abrupt breakdown voltages as high as 38 V have been fabricated by Liquid Phase Epitaxy. The grown structures were baked during 1–3 h at 500 °C just after the growth process. We describe here the growth process of the epitaxial layers, their characterization by High Resolution X-ray Diffraction (HRXD) and Photoluminescence as well as the measured I-V properties.

LPE is a very old technology, not used anymore for the commercial production of optoelectronic devices and confined only to research laboratories for basic studies; it was used in this work because it allows the growth of very pure materials and layers several microns thick in a few minutes. Thick layers are needed in some devices where the light has to be almost completely absorbed such as solar cells, PIN and avalanche photodetectors or if the device has to support high breakdown voltages.

* Corresponding author.

E-mail address: vhcompeanja@conacyt.mx (V.H. Compeán-Jasso).



Original

Hydrogen gas detector card

Francisco Sánchez Niño*, Francisco Javier De Anda Salazar

Instituto de Investigación en Comunicación Óptica IICO-UASLP, San Luis Potosí, Mexico

Received 3 December 2015; accepted 17 March 2016

Available online 28 April 2016

Abstract

A small card used for detecting hydrogen gas in a crystal growth system by the liquid phase epitaxy technique was designed and built. The small size of the card enables its portability to other laboratories where leakage detection of hydrogen or other flammable gas is required. Card dimensions are approximately 10 cm long and 5 cm wide enabling easy transportation. The design is based on a microcontroller which reads the signal from the hydrogen sensor and internally compares the read value with preset values. Depending on the signal voltage a red, yellow or green LED will light to indicate the levels of concentration of the flammable gas. The card is powered by a 9 V battery. All Rights Reserved © 2016 Universidad Nacional Autónoma de México, Centro de Ciencias Aplicadas y Desarrollo Tecnológico. This is an open access item distributed under the Creative Commons CC License BY-NC-ND 4.0.

Keywords: Hydrogen; Microcontrollers; Sensors; LPE; USB

1. Introduction

The liquid phase epitaxy technique used to fabricate optoelectronic devices is performed under a hydrogen atmosphere. This is done to prevent oxidation of the substrates and the liquid solutions; otherwise, the quality and characteristics of the components would be affected.

Once the materials have been introduced to the growth system, it is evacuated to remove gaseous pollutants. After evacuation, a flow of hydrogen is used to drag the remaining gases and thus purify the system. Furthermore, when the system is heated, oxygen reacts with the hydrogen and prevents the oxidation problems mentioned earlier.

The problem with using hydrogen is that it is highly flammable and, at concentrations in the atmosphere above 4%, it becomes dangerous because it can cause explosions of different magnitudes. Thus it is necessary to monitor the levels of hydrogen concentration in the liquid phase epitaxy laboratory. When a hydrogen concentration higher than normal is detected, it is necessary to find the source that gives rise to such concentration (Mishournyi, Hernández del Castillo, Gorvatchev, & Lastras Martínez, 2002).

The system reported here allows the detection of abnormal concentrations of hydrogen in the laboratory and locating the sources or points where the hydrogen is leaking (Sánchez-Niño & De Anda Salazar, 2015).

2. Portable card design

The design of this card is based on a PIC12F1572 microcontroller whose main features are:

- A 49-instruction set and a 16 levels stack.
- Internal clock speed of 31 kHz to 32 MHz.
- Three pulse-width-modulation (PWM) modules 16-bit, complementary waveform generator (CWG) and four internal 10-bit analog–digital converter (ADC) modules.
- One digital–analog converter (DAC) of 5 bits and one comparator.
- Two 8-bit timers, timer 0 (TMR0), timer 2 (TMR2) and one 16-bit timer, timer 1 (TMR1).

It is a new generation 8-pin plastic dual in-line package (PDIP) encapsulated microcontroller used in a variety of applications such as light emitting diodes (LED) lighting systems, control stepper motors, direct current (DC) motors, power supplies, and general purpose applications. In Figure 1, the pinout and the encapsulation of the PIC are shown (Microchip, 2004).

* Corresponding author.

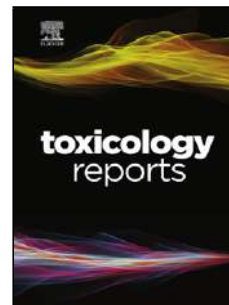
E-mail address: ninof_sanf@yahoo.com.mx (F. Sánchez Niño).

Peer Review under the responsibility of Universidad Nacional Autónoma de México.

Accepted Manuscript

Title: Effect of graphene oxide on bacteria and peripheral blood mononuclear cells

Author: J. Campos-Delgado K.L.S. Castro J.G.
Munguia-Lopez A.K. González M.E. Mendoza B. Fragneaud
R. Verdan J.R. Araujo F.J. González H. Navarro-Contreras
I.N. Pérez-Maldonado A. de León-Rodríguez C.A. Achete



PII: S2214-7500(16)30004-X
DOI: <http://dx.doi.org/doi:10.1016/j.toxrep.2016.01.004>
Reference: TOXREP 325

To appear in:

Received date: 3-12-2015
Revised date: 6-1-2016
Accepted date: 6-1-2016

Please cite this article as: J.Campos-Delgado, K.L.S.Castro, J.G.Munguia-Lopez, A.K.González, M.E.Mendoza, B.Fragneaud, R.Verdan, J.R.Araujo, F.J.González, H.Navarro-Contreras, I.N.Pérez-Maldonado, A.de León-Rodríguez, C.A.Achete, Effect of graphene oxide on bacteria and peripheral blood mononuclear cells, Toxicology Reports <http://dx.doi.org/10.1016/j.toxrep.2016.01.004>

This is a PDF file of an unedited manuscript that has been accepted for publication. As a service to our customers we are providing this early version of the manuscript. The manuscript will undergo copyediting, typesetting, and review of the resulting proof before it is published in its final form. Please note that during the production process errors may be discovered which could affect the content, and all legal disclaimers that apply to the journal pertain.

Research Article

Evolutionary Algorithm Geometry Optimization of Optical Antennas

**Ramón Díaz de León-Zapata,^{1,2} Gabriel González,² Efrén Flores-García,¹
Ángel Gabriel Rodríguez,² and Francisco Javier González²**

¹*Instituto Tecnológico de San Luis Potosí, Avenida Tecnológico s/n, 78376 Soledad de Graciano Sánchez, SLP, Mexico*

²*Universidad Autónoma de San Luis Potosí, Álvaro Obregón 64, 78000 San Luis Potosí, SLP, Mexico*

Correspondence should be addressed to Ramón Díaz de León-Zapata; ramondz@hotmail.com

Received 7 April 2016; Revised 25 May 2016; Accepted 2 June 2016

Academic Editor: Sotirios K. Goudos

Copyright © 2016 Ramón Díaz de León-Zapata et al. This is an open access article distributed under the Creative Commons Attribution License, which permits unrestricted use, distribution, and reproduction in any medium, provided the original work is properly cited.

Printed circuit antennas have been used for the detection of electromagnetic radiation at a wide range of frequencies that go from radio frequencies (RF) up to optical frequencies. The design of printed antennas at optical frequencies has been done by using design rules derived from the radio frequency domain which do not take into account the dispersion of material parameters at optical frequencies. This can make traditional RF antenna design not suitable for optical antenna design. This work presents the results of using a genetic algorithm (GA) for obtaining an optimized geometry (unconventional geometries) that may be used as optical regime antennas to capture electromagnetic waves. The radiation patterns and optical properties of the GA generated geometries were compared with the conventional dipole geometry. The characterizations were conducted via finite element method (FEM) computational simulations.

1. Introduction

Printed circuit antennas which have been extensively used in the radio frequency (RF) spectrum have also been used to detect electromagnetic radiation at optical and infrared frequencies. The use of these types of antennas at optical frequencies provides several advantages over traditional optical and infrared detectors; among these advantages are low profile, low cost, faster response times, compatibility with integrated circuit technology, and wavelength and polarization selectivity [1, 2].

Even though several RF antenna designs have been successfully used at optical and infrared frequencies [3], the design of antennas at optical frequencies by using traditional RF antenna design rules can result in nonoptimized antennas due to the dispersion of material properties that can be neglected at lower frequencies [4, 5].

Evolutionary algorithms imitate nature, where all living organisms possess specific genetic material which contains information about each organism that can be transferred

to new generations via reproduction. The other organism involved in reproduction also transfers some of its characteristics [6]. These characteristics are encoded in genes stored in chromosomes, which together constitute the genetic material known as a genotype [7]. Genes are modified during the characteristic transfer process as a consequence of the crossover between maternal and paternal chromosomes. Mutation may also occur, altering the information contained within the genes of a given chromosome. Although the newly created individual possesses the information of its parents, the combination of two different organisms makes the individual unique. This organism begins life in an environment that is not significantly different from that of its parents. The new organism develops in a manner that allows it to survive and transfer its genome, permitting the species to persist in a given environment. An individual that cannot adapt to its environment will struggle to survive and transfer its genes to new generations.

These evolutionary processes can be used to optimize the solution of nonanalytical problems assuming that the

Optical Tuning of Nanospheres Through Phase Transition: An Optical Nanocircuit Analysis

Alexander Cuadrado, Johann Toudert, Braulio García-Cámara, Ricardo Vergaz,
Francisco J. González, Javier Alda, and Rosalía Serna

Abstract—Plasmonic nanostructures can be described by equivalent impedance, allowing the analysis of their properties and performance by an RLC circuit equivalent model. In this letter, the equivalent impedance has been obtained from a power budget calculation that considers the dielectric functions of the matrix and the nanostructured material, the nanostructure geometry (in this case, spheres), the light wavelength, and its polarization. When Bi or Ga nanospheres are considered, the equivalent circuit undergoes a switching from a capacitive to and inductive response when the materials change their phase from solid to liquid. Finally, this approach is applied to the design of reconfigurable metamaterials.

Index Terms—Plasmonics, nanophotonics.

I. INTRODUCTION

NANOPARTICLES and nanostructures are at the core of nanophotonic devices due to their unique properties to focus light on subwavelength dimensions, and to selectively scatter optical radiation at different frequencies. These properties have been used to propose devices with applications in telecommunications and sensing [1], [2]. In addition, it has been shown that engineered materials, or metamaterials, built with nanoparticles show a great potential to manipulate the light response, paving the way for the development of nanoscale optical circuits for on-chip signal processing [1], [3], [4]. In this context it is necessary to develop strategies to design the basic units of such devices. The analogy between optical and electric circuits makes possible to define

Manuscript received September 6, 2016; revised October 7, 2016; accepted October 27, 2016. Date of publication November 7, 2016; date of current version November 23, 2016. This work was supported by the Ministerio de Economía y Competitividad of Spain, project 32 of CEMIE-Solar from Secretara de Energía-Sustentabilidad Energética and the Terahertz Science and Technology National Lab from CONACYT (México) under Grant TEC2012-38901-C02-01, Grant TEC2015-69916-C2-1-R, Explora Grant TEC2013-50138-EXP, Grant TEC2013-40442, and Grant PR2015-00063. (Corresponding author: Alexander Cuadrado.)

A. Cuadrado is with the Laser Processing Group, Insituto de Óptica, CSIC, 28006 Madrid, Spain, and also with the Universidad Autónoma de San Luis Potosí, Coordinación para la Innovación y Aplicación de la Ciencia y la Tecnología, Sierra Leona, 78210 San Luis Potosí, México.

J. Toudert and R. Serna are with the Laser Processing Group, Insituto de Óptica, CSIC, 28006 Madrid, Spain.

B. García-Cámara and R. Vergaz are with GDAF, Displays and Photonic Applications Group, Electronic Technology Departament, Carlos III University of Madrid, E-28911 Leganés, Madrid.

F. J. González is with the Universidad Autónoma de San Luis Potosí, Coordinación para la Innovación y Aplicación de la Ciencia y la Tecnología, Sierra Leona, 78210 San Luis Potosí, México (e-mail: a.cuadrado@csic.esb).

J. Alda is with the Applied Optics Complutense Group, University Complutense of Madrid, 28037 Madrid, Spain.

Color versions of one or more of the figures in this letter are available online at <http://ieeexplore.ieee.org>.

Digital Object Identifier 10.1109/LPT.2016.2626140

nanoresitors, nanoinductors, and nanocapacitors [5]–[8]. Through these principles, some works have experimentally studied the optical response of metamaterials and antenna coupled devices [9]–[12]. Also, by using an analytical model that considers the voltage and current values inside these structures, it is possible to obtain the impedance of metal nanoparticles [6], [13]. Accordingly, the impedance of the nanoparticles is related to the dielectric functions of their constituent material. This contribution analyzes this issue, and studies how the impedance of the system can be tuned by the geometry of nanoparticles, and by varying the dielectric permittivity function of the system by an external excitation that produces a solid-liquid phase transition.

Typically, the variation of the optical response of metal nanoparticles embedded in a medium (i.e. a plasmonic structure) has been demonstrated by modifying the dielectric function of the medium. For example, this can be done by exploiting the non-linear properties of Lithium Niobate [14], or the solid-solid phase transition of Vanadium Oxides, V_2O_5 and V_2O [15]. Another interesting option is to modify the dielectric response of the nanoparticles by inducing a phase transition in the material [16], [17], that also changes its impedance. Phase transition triggered by temperature has been used to modify the electromagnetic response of superconductor materials including plasmonic structures in nanostructured metamaterials [18], [19]. In this letter, we show that the optical impedance of Bismuth (Bi) or Gallium (Ga) nanoparticles can be tuned thanks to the solid-liquid transition. The low temperature phase transition of Bi and Ga facilitates the embedding of these nanoparticles within a dielectric matrix that remains solid across the phase transition [20], [21]. Using this, we evaluate the response of a simple metasurface built from nanospheres.

II. IMPEDANCE CALCULATION

The impedance of the spheres has been calculated using a power budget model [8] by means of a Finite Element Method tool (Comsol Multiphysics). The study is made for Bi and Ga nanospheres with two different diameters (30 and 300 nm), both in solid and liquid phase. The resonant wavelength and the reactive and resistive power distributions have been evaluated spectrally in the visible and near infrared. In order to fit with common experimental cases, these nanospheres have been immersed in Aluminum Oxide, Al_2O_3 , as surrounding medium. This is a highly transparent media in the UV-VIS-NIR range of this study (0.3–1.65 μm).

Clinical Study

Pain Measurement through Temperature Changes in Children Undergoing Dental Extractions

Eleazar S. Kolosovas-Machuca,¹ Mario A. Martínez-Jiménez,²
José L. Ramírez-GarcíaLuna,² Francisco J. González,¹ Amaury J. Pozos-Guillen,³
Nadia P. Campos-Lara,³ and Mauricio Pierdant-Perez²

¹Coordinación para la Innovación y Aplicación de la Ciencia y la Tecnología, Universidad Autónoma de San Luis Potosí, Avenida Sierra Leona 550, 78210 San Luis Potosí, SLP, Mexico

²Departamento de Epidemiología Clínica, Facultad de Medicina, Universidad Autónoma de San Luis Potosí, Avenida Venustiano Carranza 2405, 78210 San Luis Potosí, SLP, Mexico

³Posgrado de Estomatología Pediátrica, Facultad de Estomatología, Universidad Autónoma de San Luis Potosí, Avenida Manuel Nava 4, 78290 San Luis Potosí, SLP, Mexico

Correspondence should be addressed to Mauricio Pierdant-Perez; mauricio.pierdant@uaslp.mx

Received 7 September 2015; Accepted 29 December 2015

Copyright © 2016 Eleazar S. Kolosovas-Machuca et al. This is an open access article distributed under the Creative Commons Attribution License, which permits unrestricted use, distribution, and reproduction in any medium, provided the original work is properly cited.

Background and Objective. Pain evaluation in children can be a difficult task, since it possesses sensory and affective components that are often hard to discriminate. Infrared thermography has previously been used as a diagnostic tool for pain detection in animals; therefore, the aim of this study was to assess the presence of temperature changes during dental extractions and to evaluate its correlation with heart rate changes as markers of pain and discomfort. **Methods.** Thermographic changes in the lacrimal caruncle and heart rate measurements were recorded in healthy children scheduled for dental extraction before and during the procedure and compared. Afterwards, correlation between temperature and heart rate was assessed. **Results.** We found significant differences in temperature and heart rate before the procedure and during the dental extraction (mean difference 4.07°C, $p < 0.001$, and 18.11 beats per minute, $p < 0.001$) and no evidence of correlation between both measurements. **Conclusion.** Thermographic changes in the lacrimal caruncle can be detected in patients who undergo dental extractions. These changes appear to be stable throughout time and to possess very little intersubject variation, thus making them a candidate for a surrogate marker of pain and discomfort. Future studies should be performed to confirm this claim.

1. Introduction

Pain evaluation in small children can be a difficult task, since it is a multidimensional experience that possesses sensory and affective components that are often hard to discriminate by the existing scores [1, 2]. Previous experiences, fear, anxiety, and discomfort may alter pain perception; thus, poor agreement between different instruments and different raters is often the norm [3, 4]. It has been suggested that, in children younger than 7 years of age and in cognitively impaired children, evaluation of pain intensity through self-report instruments can be inaccurate due to poor understanding of the instrument and poor capacity to translate the painful experience into verbal language; therefore, complementary observational pain measurements should be used to assess

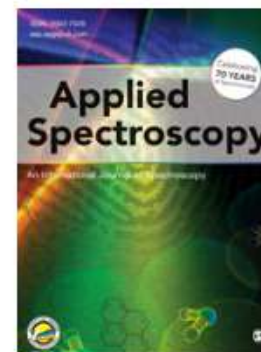
pain intensity [4]. Observational pain measurements focus on behavioral clues, such as facial expressions, movement, cry, and sleeping cycles, that allow identification of the presence of pain and its quantification in a qualitative basis [2, 4, 5]. These measurements have been shown to possess higher degrees of agreement between raters and among different instruments [4] and can be complimented with surrogate markers based on physiological changes that occur in response to pain, like heart rate changes and cortisol serum levels [6, 7]. Although these markers have high degree of intra- and intersubject variability, they have been included in some observational pain measurements scores [4, 8].

Infrared thermography has been used for the evaluation of temperature distribution in different anatomical locations [9], as well as a diagnostic and therapeutic tool to guide

Raman Spectroscopy an Option for the Early Detection of Citrus Huanglongbing

Moisés Roberto Vallejo Pérez, María Guadalupe Galindo Mendoza, Miguel Ghebre Ramírez Elías, Francisco Javier González, Hugo Ricardo Navarro Contreras, and Carlos Contreras Servín

Author Information ▾  Find other works by these authors ▾



Applied Spectroscopy Vol. 70, Issue 5, pp. 829-839 (2016)

Not Accessible

Your account may give you access

[Back to Abstract](#)

Access

To view this article you will need to login or make a payment.

If you have arrived on this page from an external web site and wish to view the article abstract first, click on the link below.

Citation

Moisés Roberto Vallejo Pérez, María Guadalupe Galindo Mendoza, Miguel Ghebre Ramírez Elías,

 Email  Share ▾

 Get Citation ▾

 [Get PDF \(686 KB\)](#)

 Save article to My Favorites

Raman spectroscopy analysis of the skin of patients with melasma before standard treatment with topical corticosteroids, retinoic acid, and hydroquinone mixture

B. Moncada¹, C. Castillo-Martínez¹, E. Arenas¹, F. León-Bejarano², M. G. Ramírez-Elías³ and F. J. González⁴

¹Dermatology Department, Hospital Central 'Dr. Ignacio Morones Prieto', Autonomous University of San Luis Potosí, San Luis Potosí, México,

²Engineering Division, University of Guanajuato, Guanajuato, México,

³School of Sciences, Autonomous University of San Luis Potosí, San Luis Potosí, México and ⁴Coordination for the Innovation and the Application of Science and Technology, Autonomous University of San Luis Potosí, San Luis Potosí, México

Background: Melasma is an abnormal acquired hyperpigmentation of the face of unknown origin, it is considered a single disease and very little has been found regarding its pathogenesis. It is usually assumed that melasma is due to excessive melanin production, but previous work using Raman spectroscopy showed degraded molecules of melanin in some melasma subjects, which may help to explain the success or failure of the standard therapy.

Methods: We perform Raman spectroscopy measurements on *in vivo* skin from melasma patients before treatment to identify the molecular structure of melanin within every melasma lesion. The Raman spectra were grouped according to the treatment response from patient, and the Raman spectra were analyzed.

Results: Raman spectroscopy measurements showed a different molecular structure of the patients who did not respond to

treatment, those patients shows atypical Raman skin spectrum with peaks associated with melanin not well defined, which is consistent with molecular degradation and protein breakdown.

Conclusion: Our results are consistent with our previous work in the sense that melasma patients who do not respond to treatment have an abnormal melanin. We believe it will eventually help to decide the treatment of melasma in clinical dermatology.

Key words: melasma – Raman spectroscopy – solar elastosis – melanin

© 2015 John Wiley & Sons A/S. Published by John Wiley & Sons Ltd
Accepted for publication 17 May 2015

MELASMA IS an abnormal acquired hyperpigmentation of the face of unknown origin. In some patients, it has been associated with pregnancy and with estrogen administration (1). Melasma rather than being a cosmetic nuisance (2) can be considered as a disorder of the normal pigmentation mechanisms and can be used to study the biological process of skin pigmentation.

Recently, new developments have arisen that shed light in the pathogenesis of melasma, among others solar elastoses, basal membrane damage as well as increased presence of mast cells and stem cell factor in biopsies of melasma (3–5).

The application of Raman spectroscopy in the field of dermatology dates back to 1992, when the first Raman spectrum of human skin was

published (6). Since then, the use of Raman spectroscopy in the skin has been diversified from characterization of skin components (7) to many other uses such as percutaneous skin absorption of drugs and metabolism of active ingredients (8, 9) interaction of water with other skin cell compounds (10, 11) and medical diagnosis (12, 13).

Raman spectroscopy has demonstrated to be a useful tool in the diagnosis of skin diseases (14). The potential use of Raman spectroscopy in medical diagnosis prompted many researchers to focus their attention on major skin conditions, one of them compared Psoriatic skin (15, 16) and healthy skin using Raman spectroscopy *in vitro* and *ex vivo*. Other studies involving the use of Raman spectroscopy were performed in the early diagnosis of skin cancer on biopsies

Responsivity and resonant properties of dipole, bowtie, and spiral Seebeck nanoantennas

Brhayllan Mora-Ventura,^a Ramón Díaz de León,^b Guillermo García-Torales,^a Jorge L. Flores,^a Javier Alda,^c and Francisco J. González^{b,*}

^aUniversidad de Guadalajara, Av. Revolución No. 1500, Guadalajara, Jal. 44430, México

^bUniversidad Autónoma de San Luis Potosí, Sierra Leona 550, Lomas 2da Sección, San Luis Potosí 78210, México

^cUniversity Complutense of Madrid, School of Optics, Arcos de Jalón 118, Madrid 28037, Spain

Abstract. Seebeck nanoantennas, which are based on the thermoelectric effect, have been proposed for electromagnetic energy harvesting and infrared detection. The responsivity and frequency dependence of three types of Seebeck nanoantennas is obtained by electromagnetic simulation for different materials. Results show that the square spiral antenna has the widest bandwidth and the highest induced current of the three analyzed geometries. However, the geometry that presented the highest temperature gradient was the bowtie antenna, which favors the thermoelectric effect in a Seebeck nanoantenna. The results also show that these types of devices can present a voltage responsivity as high as $36 \mu\text{V}/\text{W}$ for titanium–nickel dipoles resonant at far-infrared wavelengths. © The Authors. Published by SPIE under a Creative Commons Attribution 3.0 Unported License. Distribution or reproduction of this work in whole or in part requires full attribution of the original publication, including its DOI. [DOI: [10.1117/1.JPE.6.024501](https://doi.org/10.1117/1.JPE.6.024501)]

Keywords: Seebeck nanoantennas; thermoelectric nanoantennas; solar energy harvesting.

Paper 16008P received Jan. 24, 2016; accepted for publication Apr. 12, 2016; published online May 2, 2016.

1 Introduction

Optical antennas and resonant structures provide electrical field enhancement that can be used in several nanophotonic applications.^{1,2} These types of devices have been used in several fields of science and technology due to their advantages in terms of polarization sensitivity, tunability, directionality, and small footprint.³

In the last decade, thermoelectric or Seebeck nanoantennas have been proposed as potential solar energy harvesters due to their tunability and the possibility of harvesting the electromagnetic portion of the solar spectrum, which cannot be converted into electrical energy through current photovoltaic technology.^{4,5} The theory of operation of Seebeck nanoantennas consists of converting thermal energy induced by Joule heating in the nanoantenna into electrical energy by generating a voltage proportional to the difference in temperature between hot and cold bimetallic junctions.⁴ Numerical simulation predicts that this technology can harvest solar energy with a higher efficiency than direct rectifiers coupled to optical antennas.⁶ Also single-metal Seebeck nanoantennas have been proposed, which would simplify the fabrication process and allow the large-scale production of these devices using fabrication technologies such as nanoimprint lithography.^{5,7}

Even though there have been numerous reports on the design and characterization of thermoelectric nanoantennas by several groups, a key figure of merit for these types of devices, the responsivity, has not been reported yet. In this work, a numerical evaluation and comparison of the responsivity for three types of Seebeck nanoantennas using different materials and geometries is presented.

*Address all correspondence to: Francisco J. González, E-mail: javier.gonzalez@uaslp.mx

Structural analysis of the epitaxial interface Ag/ZnO in hierarchical nanoantennas

John Eder Sanchez,¹ Ulises Santiago,¹ Alfredo Benitez,¹ Miguel José Yacamán,¹ Francisco Javier González,² and Arturo Ponce^{1,a)}

¹Department of Physics and Astronomy, University of Texas at San Antonio, One UTSA Circle, San Antonio, Texas 78249, USA

²Universidad Autónoma de San Luis Potosí, LANCYTT, Sierra Leona 550, San Luis Potosí, SLP 78210, Mexico

(Received 14 July 2016; accepted 29 September 2016; published online 10 October 2016)

Detectors, photo-emitter, and other high order radiation devices work under the principle of directionality to enhance the power of emission/transmission in a particular direction. In order to understand such directionality, it is important to study their coupling mechanism of their active elements. In this work, we present a crystalline orientation analysis of ZnO nanorods grown epitaxially on the pentagonal faces of silver nanowires. The analysis of the crystalline orientation at the metal-semiconductor interface (ZnO/Ag) is performed with precession electron diffraction under assisted scanning mode. In addition, high resolution X-ray diffraction on a Bragg-Brentano configuration has been used to identify the crystalline phases of the arrangement between ZnO rods and silver nanowires. The work presented herein provides a fundamental knowledge to understand the metal-semiconductor behavior related to the receiving/transmitting mechanisms of ZnO/Ag nanoantennas. Published by AIP Publishing. [<http://dx.doi.org/10.1063/1.4964719>]

Metal-semiconductor materials with highly ordered matched interfaces have become more attractive in optoelectronic applications because of the unique directionality that exhibit when used as an active element.^{1,2} Crystalline phases matching at the interface junction is a key feature that both metal and semiconductor should exhibit for a controlled epitaxial growth. Most of the metal-semiconductors junctions are designed with the aim of growing the semiconductor material epitaxially from the substrate, which acts as both nucleation center and metal-linked support for electrical applications.^{3,4} Although epitaxial growth normally requires sophisticated pieces of equipment, chemical methods using microwaves can be employed with a high precise control at the nanoscale level. This is done by controlling parameters such as the deposition rate, temperature, and concentration of the species.^{5,6} Furthermore, perfectly aligned nanostructures can be monitored in real time within a transmission electron microscope as demonstrated in a previous work.⁵ Recently, microwave irradiation processes (MIPs) have been employed as an alternative in the chemical synthesis of metallic nanoparticles, quantum dots, and assembled nanostructures.^{7–9} The chemical synthesis using MIP reduces the reaction time and can produce a controlled growth with a good alignment of the crystalline nanostructures.¹⁰ In the present work, the crystalline orientation analysis at the ZnO/Ag interface is reported. ZnO rods grown on lateral faces of the pentagonal cross sectional area of silver nanowires (Ag NWs) are assembled in a hierarchical nanoantenna. The characterization at the interface has been described by precession electron diffraction (PED) through the assisted crystal orientation phase determination system (ASTAR) using transmission electron microscopy (TEM).¹¹ The PED-ASTAR analysis provides crystal phase orientation maps locally at

individual ZnO nanorods (ZnO NRs) and Ag NWs assembled epitaxially at the interface. In addition, X-ray diffraction under grazing angle mode has been performed by analyzing the peaks related to the hexagonal ZnO nanorods (ZnO NRs) and cubic Ag NWs.

Ag NWs have been synthesized using the polyol method as described by Sun *et al.*¹² However, in the present study, the time reaction has been modified in order to control the length and distribution of Ag NWs ranging from few minutes to approximately one hour. The nanowires dimensions were monitored at different times and studied by scanning electron microscopy (SEM). Subsequently, for the self-assembled process to synthesize ZnO NRs on the Ag NWs, 5–25 mM of zinc acetate dihydrate (Zn(Ac)₂, 98% reagent Sigma-Aldrich) and 5–25 mM of Hexamethylenetetramine (HMT) are mixed in a solution. Finally, a multi-mode cavity ETHOS EZ microwave digestion system has been employed to obtain the hierarchical structure of ZnO/Ag nanoantennas. The density of ZnO NRs distributed along the Ag NWs as well as their length has been controlled by changing the three main variables in the chemical process: temperature, power, and reaction time as we reported in detail previously.⁵

In order to understand the mechanism through which the ZnO NRs are coupled to the active faces planes (001) of the Ag NWs, a series of different reaction times were monitored by SEM. Figure 1 shows that the distribution of the ZnO NRs increases as a function of the reaction time. By analyzing the SEM micrographs, we observed that the initial ZnO nanorods are distributed randomly at different locations along the (001) planes of the Ag NWs until they reach the saturation, in which no more empty spaces are available to insert any additional ZnO NRs on the Ag NWs.

The well-defined 3D penta-arrangement shows that the ZnO NRs are similar to an aerial antenna configuration,

^{a)}Electronic mail: arturo.ponce@utsa.edu

Search

Published between: and

[Search syntax help](#)

Theoretical and clinical aspects of the use of thermography in non-invasive medical diagnosis

Article type: Research Article

Authors: [González, Francisco J.](#)

Affiliations: Terahertz Science and Technology Center (C2T2) and Science and Technology National Lab (LANCyTT), Universidad Autónoma de San Luis Potosí, Sierra Leona 550, Lomas 2da Sección, San Luis Potosí 78210, México. E-mail: javier.gonzalez@uaslp.mx

Abstract: Thermography is a clinical imaging technique that has been applied to diverse pathologies in very diverse clinical areas such as dermatology, rheumatology, oncology and emergency medicine to name a few. Even though there are plenty of reports that indicate thermography could be used in a clinical setting it has yet to fulfill its promise of becoming a commonly used diagnostic technique. One of the main reasons is the lack of standard procedures to obtain and analyze thermograms, standardization has proven difficult due to the lack of collaboration between physicists and physicians that could allow the integration of thermal models to clinical findings. In this general overview of the field several thermography applications are presented along with theory and modeling of thermal processes in biological tissue in an attempt to promote the formation of interdisciplinary teams that could develop medical standards for clinical thermography.

Keywords: Thermography, non-invasive clinical diagnosis, biological thermal modeling, heat transfer in biological tissue

DOI: 10.3233/BSI-160152

Journal: [Biomedical Spectroscopy and Imaging](#), vol. 5, no. 4, pp. 347-358, 2016

Published: 5 January 2017

Share this: [Twitter](#) [Facebook](#) [LinkedIn](#) [Google+](#)

+ Volume 6

- Volume 5

Issue 4

Issue 3

Issue 2

Issue 1

Issue s1

+ Volume 4

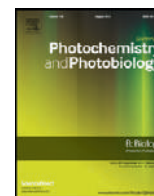
+ Volume 3

+ Volume 2

+ Volume 1

Show less

Register for enhanced features



Use of *Agave tequilana*-lignin and zinc oxide nanoparticles for skin photoprotection



José Manuel Gutiérrez-Hernández^a, Alfredo Escalante^b, Raquel Nalleli Murillo-Vázquez^b, Ezequiel Delgado^b, Francisco Javier González^a, Guillermo Toriz^{b,*}

^a Coordination for the Innovation and Application of Science and Technology, Autonomous University of San Luis Potosí, 78000 San Luis Potosí, SLP, Mexico

^b Department of Wood, Cellulose and Paper Research, University of Guadalajara, 45110 Guadalajara, Jal, Mexico

ARTICLE INFO

Article history:

Received 21 February 2016

Received in revised form 6 July 2016

Accepted 21 August 2016

Available online 24 August 2016

Keywords:

Suncare/UV protection

Nanoparticles

UV/VIS spectroscopy

Sunscreens

ABSTRACT

The use of sunscreens is essential for preventing skin damage and the potential appearance of skin cancer in humans. Inorganic active components such as zinc oxide (ZnO) have been used commonly in sunscreens due to their ability to block UVA radiation. This ultraviolet (UV) protection might be enhanced to cover the UVB and UVC bands when combined with other components such as titanium dioxide (TiO₂). In this work we evaluate the photoprotection properties of organic nanoparticles made from lignin in combination with ZnO nanoparticles as active ingredients for sunscreens. Lignin nanoparticles were synthesized from *Agave tequilana* lignin. Two different pulping methods were used for dissolving lignin from agave bagasse. ZnO nanoparticles were synthesized by the precipitation method. All nanoparticles were characterized by SEM, UV-Vis and FT-IR spectroscopy. Nanoparticles were mixed with a neutral vehicle in different concentrations and in-vitro sun protection factor (SPF) values were calculated. Different sizes of spherical lignin nanoparticles were obtained from the spent liquors of two different pulping methods. ZnO nanoparticles resulted with a flake shape. The mixture of all components gave SPF values in a range between 4 and 13. Lignin nanoparticles showed absorption in the UVB and UVC regions which can enhance the SPF value of sunscreens composed only of zinc oxide nanoparticles. Lignin nanoparticles have the added advantage of being of organic nature and its brown color can be used to match the skin tone of the person using it.

© 2016 Elsevier B.V. All rights reserved.

1. Introduction

Daily exposure to sunlight makes the use of a UV radiation screen essential. UV rays can damage the skin by sunburn [1], premature aging [2], photo-allergies [3], and can ultimately produce skin cancer [4]. UV radiation ranges from 200–400 nm and is classified into UVC (100–280 nm), UVB (280–315 nm) and UVA (315–400 nm). UVA has been subdivided into UVAI and UVAIL (315–340 nm and 340–400 nm, respectively) [5]. The whole range of UV radiation is, up to some extent, harmful to the skin. However, UVC radiation may be neglected because it is absorbed by the ozone layer. On the other hand, over 95% of the UV radiation reaching the Earth's surface is UVA and only 5% is UVB radiation, the latter being the main cause of damage to the skin due to its greater amount of energy. This is why sunscreens are usually limited to the care and protection against UVB.

There are two types of active ingredients in sunscreens that provide protection against UV radiation. They are classified as chemical or organic, and physical or inorganic [5]. Chemical ingredients absorb UV radiation and convert it into heat; other pathways for excited state decay are radiative decay (fluorescence), isomerization (i.e. octinoxate) and

photodegradation (i.e. avobenzone) [5–6]. On the other hand, physical or inorganic active ingredients create a layer on the skin that screens solar radiation by scattering and/or reflecting UV radiation. Common physical shields are ZnO and TiO₂ (titanium dioxide) [7]. Regardless of the type of active ingredient that sunscreens contain in any case, the bottom line is to protect and help to prevent skin damage from UV radiation. The ability to avoid erythema (sunburn) by a sunscreen is indicated by the SPF, which is a measure of how much more sun exposure it takes to undergo sunburn. Erythema is mainly caused by UVB radiation; however, it is necessary to cover the UVA and visible regions because they also damage the skin [8]. This fact has spurred research on inorganic components, such as TiO₂ and ZnO, which reflect or scatter UV radiation, besides absorbing, because they also provide protection against light in the visible range.

There are natural organic substances that absorb UV radiation. A clear example of this type of substance is lignin, which is an aromatic polymer from vascularized plants, whose absorbance region is exactly in the UVC and UVB regions [9]. Lignin is a highly complex biopolymer considered the second biggest source of carbon in the planet after cellulose. It performs vital functions for the structural strength of terrestrial plants, the conduction of water and the defense against pathogens. Despite these roles, the study of lignin has been limited by its own nature. The fact that the macromolecular pattern can vary from species to

* Corresponding author.

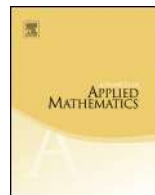
E-mail address: gtoriz@dmcyp.cucei.udg.mx (G. Toriz).



Contents lists available at ScienceDirect

Advances in Applied Mathematics

www.elsevier.com/locate/yaama



Characterizing 2-crossing-critical graphs

D. Bokal^a, B. Oporowski^b, R.B. Richter^c, G. Salazar^d^a Dept. of Math. and C. S., University of Maribor, Maribor, Slovenia^b Dept. of Math., Louisiana State University, Baton Rouge, USA^c Dept. of Comb. & Opt., University of Waterloo, Waterloo, Canada^d Instituto de Física, Universidad Autónoma de San Luis Potosí, San Luis Potosí, Mexico

ARTICLE INFO

Article history:

Received 16 February 2014

Received in revised form 14 October 2015

Accepted 16 October 2015

Available online 28 November 2015

MSC:

05C10

Keywords:

Crossing number

Crossing-critical graphs

ABSTRACT

It is very well-known that there are precisely two minimal non-planar graphs: K_5 and $K_{3,3}$ (degree 2 vertices being irrelevant in this context). In the language of crossing numbers, these are the only 1-crossing-critical graphs: they each have crossing number at least one, and every proper subgraph has crossing number less than one. In 1987, Kochol exhibited an infinite family of 3-connected, simple, 2-crossing-critical graphs. In this work, we: (i) determine all the 3-connected 2-crossing-critical graphs that contain a subdivision of the Möbius Ladder V_{10} ; (ii) show how to obtain all the not 3-connected 2-crossing-critical graphs from the 3-connected ones; (iii) show that there are only finitely many 3-connected 2-crossing-critical graphs not containing a subdivision of V_{10} ; and (iv) determine all the 3-connected 2-crossing-critical graphs that do not contain a subdivision of V_8 .

© 2015 Elsevier Inc. All rights reserved.

E-mail addresses: drago.bokal@uni-mb.si (D. Bokal), bogdan@math.lsu.edu (B. Oporowski), brichter@uwaterloo.ca (R.B. Richter), gelasio.salazar@gmail.com (G. Salazar).

<http://dx.doi.org/10.1016/j.aam.2015.10.003>

0196-8858/© 2015 Elsevier Inc. All rights reserved.

Raman Spectroscopy an Option for the Early Detection of Citrus Huanglongbing

Moisés Roberto Vallejo Pérez^{1,2}, María Guadalupe Galindo Mendoza², Miguel Ghebre Ramírez Elías³, Francisco Javier González⁴, Hugo Ricardo Navarro Contreras⁵, and Carlos Contreras Servín²

Applied Spectroscopy
0(0) 1–11
© The Author(s) 2016
Reprints and permissions:
sagepub.co.uk/journalsPermissions.nav
DOI: 10.1177/0003702816638229
asp.sagepub.com



Abstract

This research describes the application of portable field Raman spectroscopy combined with a statistical analysis of the resulting spectra, employing principal component analysis (PCA) and linear discriminant analysis (LDA), in which we determine that this method provides a high degree of reliability in the early detection of Huanglongbing (HLB) on Sweet Orange, disease caused by the bacteria *Candidatus Liberibacter asiaticus*. Symptomatic and asymptomatic plant samples of Sweet Orange (*Citrus sinensis*), Persian Lime (*C. latifolia*), and Mexican Lime (*C. aurantifolia*) trees were collected from several municipalities, three at Colima State and three at Jalisco State (HLB presence). In addition, Sweet Orange samples were taken from two other Mexican municipalities, one at San Luis Potosí and the other at Veracruz (HLB absent). All samples were analyzed by real-time PCR to determine its phytosanitary condition, and its spectral signatures were obtained with an ID-Raman mini. Spectral anomalies in orange trees HLB-positive, were identified in bands related to carbohydrates (905 cm⁻¹, 1043 cm⁻¹, 1127 cm⁻¹, 1208 cm⁻¹, 1370 cm⁻¹, 1272 cm⁻¹, 1340 cm⁻¹, and 1260–1280 cm⁻¹), amino acids, proteins (815 cm⁻¹, 830 cm⁻¹, 852 cm⁻¹, 918 cm⁻¹, 926 cm⁻¹, 970 cm⁻¹, 1002 cm⁻¹, 1053 cm⁻¹, and 1446 cm⁻¹), and lipids (1734 cm⁻¹, 1736 cm⁻¹, 1738 cm⁻¹, 1745 cm⁻¹, and 1746 cm⁻¹). Moreover, PCA–LDA showed a sensitivity of 86.9 % (percentage of positives, which are correctly identified), a specificity of 91.4 % (percentage of negatives, which are correctly identified), and a precision of 89.2 % (the proportion of all tests that are correct) in discriminating between orange plants HLB-positive and healthy plants. The Raman spectroscopy technique permitted rapid diagnoses, was low-cost, simple, and practical to administer, and produced immediate results. These are essential features for phytosanitary epidemiological surveillance activities that may conduct a targeted selection of highly suspicious trees to undergo molecular DNA analysis.

Keywords

Spectroscopy, Citrus greening disease, Chemometrics, Citrus species

Date received: 2 July 2015; accepted: 16 December 2015

Introduction

Huanglongbing (HLB) or citrus greening disease is caused by the bacteria *Candidatus Liberibacter* spp., than is classified according to the strains origin: *Candidatus Liberibacter africanus* from Africa, *Candidatus Liberibacter asiaticus* from Asia,¹ and *Candidatus Liberibacter americanus* from America.² These days, HLB is considered to be one of the most destructive diseases that threaten global citriculture.^{1,3} *Candidatus Liberibacter asiaticus* (CLAs) in Mexico is present and transmitted by the Asian citrus psyllid *Diaphorina citri* Kuwayama and currently the disease is found in orchards and backyards of 250 municipalities in 16 states, equivalent to 6.1% of

¹CONACyT Research Fellow-Universidad Autónoma de San Luis Potosí, San Luis Potosí, México

²Laboratorio Nacional de Geoprosamiento de Información Fitosanitaria (LaNGIF), CIACyT-Universidad Autónoma de San Luis Potosí, San Luis Potosí, México

³Facultad de Ciencias. Universidad Autónoma de San Luis Potosí, San Luis Potosí, México

⁴Laboratorio Nacional de Ciencia y Tecnología en Terahertz, CIACyT-Universidad Autónoma de San Luis Potosí, San Luis Potosí, México

⁵Laboratorio Nacional de la Coordinación para la Innovación y Aplicación de la Ciencia y Tecnología (CIACyT), Universidad Autónoma de San Luis Potosí, San Luis Potosí, México

Corresponding author:

Moisés Roberto Vallejo Pérez, CONACyT Research Fellow, Av. Insurgentes Sur 1582, Col. Crédito del Constructor, Del. Benito Juárez, 03940, Mexico.
Email: vallejo.pmr@gmail.com

Instrumentación de un impulsor para lámpara de LED

Instrumentation of an LED Lamp Driver

González-Ventura José Ranulfo
Universidad Autónoma de San Luis Potosí
Facultad de Ciencias, México
Correo: jose11jglz@gmail.com

Campos-Cantón Isaac
Universidad Autónoma de San Luis Potosí
Facultad de Ciencias, México
Correo: : icampos@ciencias.uaslp.mx

Camacho-Juárez Sergio
Universidad Autónoma de San Luis Potosí
Facultad de Ciencias, México
Correo: sergio_camacho@uaslp.mx

Núñez-Olvera Oscar Fernando
Universidad Autónoma de San Luis Potosí
Instituto de Investigación en Comunicación Óptica, México
Correo: oscar_n@cactus.iico.uaslp.mx

Información del artículo: recibido: abril de 2015, reevaluado: septiembre de 2015 y mayo de 2016, aceptado: julio de 2016

Resumen

En este artículo se realiza la instrumentación de un impulsor para una lámpara de LED. Se busca controlar la intensidad luminosa de la lámpara LED a través de la técnica PWM, con circuitos RC y Mosfet. Se realiza la instrumentación de la propuesta eléctrica a través del empleo del concepto de reactancia capacitiva para limitar la corriente de entrada proveniente de la línea de CA.

Abstract

This article describes the implementation of an LED lamp driver. It seeks to control the brightness of the LED lamp through PWM technique, RC and MOSFET circuits. An electrical instrumentation proposal is made by using the concept of capacitive reactance to limit the input current mains AC.

Descriptores:

- electrónica analógica
- tecnología LED
- amplificadores operacionales
- circuitos RC
- Mosfet

Keywords:

- analog electronics
- LED Technology
- operational amplifiers
- RC circuit
- Mosfet

Software based reconfiguration for the Cascaded H-Bridge multilevel converter

R. C. Martínez-Montejano*¹, R. Castillo Meraz², P. Salas-Castro³, I. Campos-Cantón⁴, M.F. Martínez-Montejano⁵.

^{1,2,4}School of Science, UASLP. Álvaro Obregón, Zona Centro S/N, 78000, San Luis Potosí, México

³Optical Communication Research Institute, UASLP, Av. Karakorum 1470, San Luis Potosí, México

⁵Research and Development Apartment, Alstom Power Switzerland, Zentralstrasse 40, 5242, Birr

Abstract— Multilevel converters have been widely accepted in medium and high power applications, their general function is to synthesize a desired AC voltage from several levels of DC voltages. For more levels, the total harmonic distortion of the output voltage, decreases, has better waveform quality, low stresses on switching devices and better performance. This paper presents the reconfiguration based software for a cascaded H-bridge multilevel converter of five levels used as active shunt filter, to obtain seven levels. The transformation of the model in terms of the sum and the difference of the square of the capacitor voltages is crucial for our developments. The reconfiguration depends on the difference of the capacitor voltages, the imbalance between each H-bridge voltage and the commutation frequency.

Keywords— adaptive law, active shunt filter, multilevel converter, pulse width modulation, total harmonic distortion, software based reconfiguration.

I. INTRODUCTION

The multilevel converters are a power electronic device that synthesizes an AC output voltage from several levels of DC voltages. They are available in wide power ratings that range from few VA to several MVA, finding application particularly on renewable energies [1]-[4]. Because distributed power sources are expected to become increasingly in the near future, the use of a multilevel converter to control the voltage output, frequency, phase angle [5], from renewable energy sources, will provide significant advantages due to its fast response and autonomous control [6]. Some advantages of multilevel technology includes, improved output waveform quality, better electromagnetic compatibility (EMC), low switching losses and capability of management high voltages [7].

There are three multilevel converter classic topologies: diode clamped, flying capacitor and series cascaded H-bridge (CHB). Diode clamped and flying capacitor needs more complex PWM controls, because more capacitors and diodes are needed for more output voltage levels. In the case of CHB each H-bridge has an independent DC source. Control and operation of this converter are simple and have robust structure than mentioned converters. The number of output levels is defined by $n = 2N + 1$, where N represents the number of DC sources which may be obtained from batteries, fuel cells or photovoltaic solar cells [8]-[9].

The asymmetric multilevel converters with unequal DC sources have been gaining attention, because they can synthesize output waveforms with a reduced harmonic content, even using a few series connected cells. The main objective is to obtain more output voltage levels without increase the power semiconductor devices or DC sources, reducing the total harmonic distortion that eliminates output filters [10]. Some authors combine different voltages, different topologies or even switch converters and linear amplifiers for hybrid asymmetric multilevel converters [11]-[13]. By properly designing and controlling the converter, it is possible to modulate the low voltage cells at inverter pulse width modulation frequency [14]. The power devices managing high voltage, switch at reduced frequency, decreasing switching losses [15].

Multilevel converters employ different modulation techniques for getting a better output voltage with the minimum harmonic distortion. The carrier based pulse width modulation, selective harmonic elimination, space vector modulation are some of the commonly use modulation for multilevel converters [16]-[17].

This paper presents the mathematical model and control process for the software reconfiguration of a CHB multilevel converter used as active shunt filter in order to obtain more output voltage levels [18]. The work is organized as follows. On section two, the system description, its mathematical model and model transform are studied. Section three develops the reconfiguration for obtaining seven levels output voltage. On section four, the results of the reconfiguration are exhibited. Finally, section five concludes the paper.

Chua's circuit from the linear system perspective

I. Campos-Cantón, M.A. Arrellanes Gómez, M. Delgadillo Vargas and F. Aguilera
*Instituto de Investigación en Comunicación Óptica, Facultad de Ciencias,
Universidad Autónoma de San Luis Potosí, Alvaro Obregón 64, 78000 San Luis Potosí, SLP, México.
email: icampos@fciencias.uaslp.mx*

Received 25 February 2016; accepted 13 April 2016

This paper analyzes the Chua's circuit, considering it linear by parts in its internal representation model. This approach allows graduate students to develop skills in matrix algebra and linear systems, using physics as a fundamental tool to model and simulate dynamic systems. Through this approach, the student will understand the importance of the knowledge of state equations to form the matrices that represent the circuit, where the main matrix dictates its values and eigenvectors, as well as its similar matrix. A physical simulation of the Chua's circuit is carried out, along with the corresponding experiments. The electric circuit is composed by resistors, capacitors, inductance, diodes and an operational amplifier.

Keywords: Nonlinear systems; phase portrait; analog circuits; differential equation; Chua's circuit.

Este trabajo analiza el circuito de Chua tomado lineal por partes en su modelo de representación interna. Este enfoque permite a los estudiantes de ciencias desarrollar sus competencias en algebra matricial y sistemas lineales, con el uso de la física como herramienta fundamental para modelar y simular sistemas dinámicos. El estudiante aprenderá que esta herramienta necesita del conocimiento de las ecuaciones de estado para formar las matrices que representan dicho circuito. Donde la matriz principal dicta sus valores y vectores propios, así como su matriz similar. Posteriormente se procederá a simular físicamente el circuito de Chua y finalmente se realizarán los experimentos correspondientes. El circuito eléctrico está constituido por resistencias, capacitores, bobina, diodos y amplificador operacional.

Descriptores: Sistemas lineales; retrato de fase; electrónica analógica; ecuaciones diferenciales ordinarias; circuito de Chua.

PACS: 02.10.Yn; 02.30.Hq; 02.10.Ab; 84.30.Sk; 84.30.Le

1. Introduction

As students pass through their education at the undergraduate and graduate level, there is a need to develop skills in various disciplines; for instance, physics and mathematics are indispensable tools to address and generate practical solutions to current problems. Therefore, students must be able not only to analyze theoretical and technical solutions, but also to observe their relation to the context and other aspects of professional fields. Within this context, a linear systems course is presented as an excellent opportunity to integrate the acquired skills in the areas of physics and mathematics in order to design, model and simulate linear systems. A topic of high importance is the concept of state space resulting from the use of matrices.

It is important to use software tools that allow us to model and simulate such systems. Also, it is well known that the use of software as an alternative in the search of a particular numerical solution from a mathematical expression, is very convenient. Once we have used the concepts of physics and mathematics, as well as the technological resources through software, it is essential to continue all the way to the experimental realization; which leaves an unforgettable impression on students.

In this paper, we take a chaotic system that has the particularity of being linear in sections. The study of chaotic phenomena using tools from linear systems, gives students great skill in handling the matrix language, and on the other hand gives them the opportunity to deal with nonlinear systems.

In the last two decades, the study of chaos theory has been of great interest in mathematics, physics and engineering areas; the erratic behavior represented by mathematical models and their implementation across physical systems are studied. Generally, these systems are modeled by a set of nonlinear ordinary differential equations. In particular, one of the most widely studied systems is the Chua's circuit [1,2], considered as the transition from practice to theory. In other words, this system was the one that first hooked the attention of many researchers because in terms of theoretical development, it is relatively easy to physically implement different types of oscillators. One example is that different authors have shown that for linear systems attractors parts can be generated with multiscroll, as is the case of Suykens and Vandewalle [3,4], where they introduced a family of n-scroll attractors. We decided to study the Chua's circuit because it gives us the ease of having a linear piecemeal approach, where each part is a linear system.

To carry out the objectives mentioned above, some definitions and explanations (grounded mathematically) are given, to understand what is happening physically and theoretically. After being in context follows the study in detail of the Chua's circuit from the equations of state, also we will show that it is easier to study this circuit with a similar matrix than with the original matrix.

Once the mathematical system is understood and solved, the next step consists in making the correspondent simulation with the help of a computer package. Later, details of the performed experiments are given, where the behavior of

Multiwall carbon nanotubes/polycaprolactone scaffolds seeded with human dental pulp stem cells for bone tissue regeneration

M. L. Flores-Cedillo¹ · K. N. Alvarado-Estrada¹ · A. J. Pozos-Guillén¹ ·
J. S. Murguía-Ibarra² · M. A. Vidal³ · J. M. Cervantes-Uc⁴ · R. Rosales-Ibáñez¹ ·
J. V. Cauich-Rodríguez⁴

Received: 13 July 2015 / Accepted: 27 November 2015
© Springer Science+Business Media New York 2015

Abstract Conventional approaches to bone regeneration rarely use multiwall carbon nanotubes (MWCNTs) but instead use polymeric matrices filled with hydroxyapatite, calcium phosphates and bioactive glasses. In this study, we prepared composites of MWCNTs/polycaprolactone (PCL) for bone regeneration as follows: (a) MWCNTs randomly dispersed on PCL, (b) MWCNTs aligned with an electrical field to determine if the orientation favors the growing of human dental pulp stem cells (HDPSCs), and (c) MWCNTs modified with β -glycerol phosphate (BGP) to analyze its osteogenic potential. Raman spectroscopy confirmed the presence of MWCNTs and BGP on PCL, whereas the increase in crystallinity by the addition of MWCNTs to PCL was confirmed by X-ray diffraction and differential scanning calorimetry. A higher elastic modulus (608 ± 4.3 MPa), maximum stress (42 ± 6.1 MPa) and electrical conductivity (1.67×10^{-7} S/m) were observed in non-aligned MWCNTs compared with the pristine PCL. Cell viability at

14 days was similar in all samples according to the live/dead assay, but the 21 day cell proliferation, measured by MTT was higher in MWCNTs aligned with BGP. Von Kossa and Alizarin red showed larger amounts of mineral deposits on MWCNTs aligned with BGP, indicating that at 21 days, this scaffold promotes osteogenic differentiation of HDPSCs.

1 Introduction

The interest in bone tissue engineering (BTE) and regeneration therapies has grown in parallel with the rise in trauma, musculoskeletal disorders and oral diseases associated with the increase in life expectancy [1, 2]. To fulfill the variety of bone defects generated under these circumstances, the current gold standard and the most successful treatment is the use of autologous bone grafts. The success of these grafts is associated with their osteoinductive properties through the presence of growth factors, vascularization and cells with osteogenic potential [3]. However, the main disadvantages of bone grafts include their limited supply and the risk of donor site morbidity and infections [4]. These limitations can be overcome by developing a proper biodegradable scaffold, seeding it with either differentiated or undifferentiated cells and providing a proper biological environment that includes mechanical stimulation and growth factors [5, 6]. In this respect, conventional bioactive polycaprolactone (PCL) scaffolds have been modified by incorporating different types of fillers, such as hydroxyapatite (HA) [7], β -tricalcium phosphate (β -TCP) [8], and tricalcium phosphate (TCP) [9] as well as bioactive glasses [10].

As an alternative to these conventional materials, it is possible to combine nanoscale structures, such as multiwall

Electronic supplementary material The online version of this article (doi:10.1007/s10856-015-5640-y) contains supplementary material, which is available to authorized users.

✉ J. V. Cauich-Rodríguez
jvcr@cicy.mx

¹ Facultad de Estomatología, Laboratorio de Ciencias Básicas, Universidad Autónoma de San Luis Potosí, San Luis Potosí, Mexico

² Facultad de Ciencias, Departamento de Electrónica, Universidad Autónoma de San Luis Potosí, San Luis Potosí, Mexico

³ Centro de Aplicación de Radiación Infrarroja, Energías Alternativas y Materiales, CIACYT, San Luis Potosí, Mexico

⁴ Centro de Investigación Científica de Yucatán, Unidad de Materiales, Mérida, Yucatán, Mexico



Perceptual security of encrypted images based on wavelet scaling analysis

C. Vargas-Olmos^a, J.S. Murguía^{b,*}, M.T. Ramírez-Torres^c, M. Mejía Carlos^a,
H.C. Rosu^d, H. González-Aguilar^b

^a Instituto de Investigación en Comunicación Óptica-Facultad de Ciencias, Universidad Autónoma de San Luis Potosí, Álvaro Obregón 64, 78000 San Luis Potosí, S.L.P., Mexico

^b Facultad de Ciencias, Universidad Autónoma de San Luis Potosí, Álvaro Obregón 64, 78000 San Luis Potosí, S.L.P., Mexico

^c Coordinación Académica Región Altiplano Oeste, Universidad Autónoma de San Luis Potosí, Álvaro Obregón 64, 78000 San Luis Potosí, S.L.P., Mexico

^d Instituto Potosino de Investigación Científica y Tecnológica, Camino a la presa San José 2055, Col. Lomas 4a Sección, 78216, San Luis Potosí, S.L.P., Mexico

HIGHLIGHTS

- DFA is applied to pixel fluctuations of encrypted images.
- The scaling exponents of the encrypted images can be used as perceptual security criteria.
- Calculations are based on a wavelet-optimized DFA method.

ARTICLE INFO

Article history:

Received 26 November 2015

Received in revised form 23 February 2016

Available online 18 March 2016

Keywords:

Encryption system

Wavelet transform

Detrended fluctuation analysis

Scaling laws

ABSTRACT

The scaling behavior of the pixel fluctuations of encrypted images is evaluated by using the detrended fluctuation analysis based on wavelets, a modern technique that has been successfully used recently for a wide range of natural phenomena and technological processes. As encryption algorithms, we use the Advanced Encryption System (AES) in RBT mode and two versions of a cryptosystem based on cellular automata, with the encryption process applied both fully and partially by selecting different bitplanes. In all cases, the results show that the encrypted images in which no understandable information can be visually appreciated and whose pixels look totally random present a persistent scaling behavior with the scaling exponent α close to 0.5, implying no correlation between pixels when the DFA with wavelets is applied. This suggests that the scaling exponents of the encrypted images can be used as a perceptual security criterion in the sense that when their values are close to 0.5 (the white noise value) the encrypted images are more secure also from the perceptual point of view.

© 2016 Elsevier B.V. All rights reserved.

1. Introduction

Data multimedia has become in recent years an important part of our daily lives. Either personal information such as a mobile phone call, an online payment, an electronic transaction or classified information as military strategies, require

* Corresponding author. Tel.: +52 4448262491.

E-mail address: ondeleto@uaslp.mx (J.S. Murguía).

**Scaling analysis of heart beat fluctuations data
and its relationship with cyclic alternating pattern
data during sleep**

R. De León-Lomeli*

Facultad de Ingeniería

*Universidad Autónoma de San Luis Potosí (UASLP)
Álvaro Obregón 64, 78000 San Luis Potosí, S.L.P., Mexico
roxyl_dl@hotmail.com*

J. S. Murguía

Facultad de Ciencias

*Universidad Autónoma de San Luis Potosí (UASLP)
Álvaro Obregón 64, 78000 San Luis Potosí, S.L.P., Mexico
ondeleto@uaslp.mx*

I. Chouvarda

Laboratory of Medical Informatics

*Aristotle University of Thessaloniki, Greece
iochou@gmail.com*

M. O. Méndez

Facultad de Ciencias

*Universidad Autónoma de San Luis Potosí (UASLP)
Álvaro Obregón 64, 78000 San Luis Potosí, S.L.P., Mexico
martin.mendez28@gmail.com*

E. González-galván

Facultad de Ingeniería

*Universidad Autónoma de San Luis Potosí (UASLP)
Álvaro Obregón 64, 78000 San Luis Potosí, S.L.P., Mexico
egonzale@uaslp.mx*

A. Alba

Facultad de Ciencias

*Universidad Autónoma de San Luis Potosí (UASLP)
Álvaro Obregón 64
78000 San Luis Potosí, S.L.P., Mexico
fac@fc.uaslp.mx*

*Corresponding author.



Effect of the oxidation of aluminum bottom electrode in a functionalized-carbon nanotube based organic rewritable memory device



I.A. Rosales-Gallegos^a, J.A. Avila-Niño^{b,c}, M. Reyes-Reyes^a, O. Núñez-Olvera^a, R. López-Sandoval^{c,*}

^a Instituto de Investigación en Comunicación Óptica, Universidad Autónoma de San Luis Potosí, Álvaro Obregón 64, San Luis Potosí 78000, Mexico

^b Instituto Tecnológico de San Luis Potosí, Av. Tecnológico, S/N Col UPA, Soledad de Graciano Sánchez 78437, Mexico

^c Advanced Materials Department, IPICYT, Camino a la Presa San José 2055, Col. Lomas 4a sección, San Luis Potosí 78216, Mexico

ARTICLE INFO

Article history:

Received 9 May 2016

Received in revised form 20 September 2016

Accepted 23 October 2016

Available online 25 October 2016

Keywords:

Al oxidation

Resistive memory

Nonvolatile memory

Carbon nanotubes

ABSTRACT

In this work, a bistable switching between ON and OFF states in current–voltage (I–V) measurements in the Al/AlO_x/functionalized-multiwalled carbon nanotubes (f-MWCNTs) embedded in a PEDOT:PSS layer/Al devices is shown. It is found that oxidizing the surface aluminum bottom electrode using UV ozone treatment enhances the performance and stability in room conditions of these memory devices. A well-defined threshold voltage is obtained, which allows the implementation of many write-read-erase-read cycles after the UV ozone treatment for 1 min. The improvement of the rewritable memory characteristics due to the UV ozone treatment is related with the increase of the thickness (and stabilization) of an aluminum oxide (AlO_x) layer, with the change in the hydrophilicity of the aluminum oxide surface as well as the creation of traps in the aluminum oxide layer.

© 2016 Published by Elsevier B.V.

1. Introduction

In recent years, there has been a huge interest in the development of new non-volatile resistive memories based on organic materials [1–4]. In general, these memories consist of semiconductor or insulating organic layer, which may contain metal nanoparticles or carbon nanostructures, between two metal electrodes (MIM devices). The interest in fabricating these non-volatile resistive memories using organic materials, also called resistive random access memory, is that they are very easy to process, lightweight, flexible and low cost [1–2]. In addition, there is interest in developing new types of nonvolatile organic resistive memories, which may have the advantages of memories of dynamic random access memory (DRAM), flash memories and hard-disk drives [3]. Among the non-volatile organic resistive memories, one of the most interesting is that in which the responsible mechanism of the electrical current bistability comes from the formation of filaments. In these kind of memories have been reported that is necessary the application of a voltage pulse to the pristine devices in order to modify permanently the electrical response of the device. This process has been called electrical forming or ‘electroforming’ [5–7]. After the forming process, the resistance of the devices can be switched between a high-resistance OFF state and a low-resistance ON state by a voltage pulse power supply. The electroforming of the device is related with the breakdown voltage of the Al₂O₃ film. Verbakel et al. [8] found this phenomenon applying a

pulse of +5 V at Al/Al₂O₃/Au devices. Moreover, they reported that the breakdown voltage of Al₂O₃ film is directly related to the thickness of the oxide film. The electroforming mechanism has been widely studied: Chen et al. [9] showed the existence of traps in the metal-organic interface in Al/Al₂O₃/polymer/Ba/Al memory devices due the electroforming by electro-optical methods. Yang et al. [10] proposed that the electroforming is due an oxygen vacancy creation via electro-reduction in a TiO₂ film in inorganic memory devices. Hensch et al. [11] proposed that the electroforming step changes the Schottky barrier contact resistance due to a drift of charged oxygen vacancies toward the bottom electrode, which narrows the depletion layer at the oxide-polymer interface. At narrow depletion widths, electron tunneling occurs reducing the contact resistance. In contrast, several organic materials whose electrical resistivity can change by the application of voltage pulses have been used as active materials in these memory devices [12–15]. In many of these memories, it has been proposed that an interfacial oxide is the responsible mechanism of the conductive switching [6–8] and great efforts have been conducted to use this effect in a controlled way [8,16–17].

Poly(3,4-ethylenedioxythiophene):poly(styrenesulfonate) (PEDOT:PSS) is a very attractive polymer because shows high conductance and stability [18–20]. It has been used as active material in several resistive memory devices [21–25], which present irreversible [21–22] or reversible resistance switching characteristics [23–25]. In addition, PEDOT:PSS has been used in combination with carbon nanostructures for the fabrication of write-once-read-many times organics memories [26] or rewritable memories [27]. On the other hand, the presence of

* Corresponding author.

E-mail address: sandov@ipicyt.edu.mx (R. López-Sandoval).

Thermal stability of magnetite hexagonal nanoflakes coated with carbon layers

M Reyes-Reyes¹, J A Ávila-Niño^{1,2}, R López-Sandoval²
and H G Silva-Pereyra²

¹ Instituto de Investigación en Comunicación Óptica, Universidad Autónoma de San Luis Potosí, Álvaro Obregón 64, San Luis Potosí 78000, Mexico

² Advanced Materials Department, IPICYT, Camino a la Presa San José 2055, Col. Lomas 4a sección, San Luis Potosí 78216, Mexico

E-mail: reyesm@iico.uaslp.mx

Received 16 October 2015, revised 12 January 2016

Accepted for publication 25 January 2016

Published 26 February 2016



CrossMark

Abstract

Magnetite nanostructures coated with carbon layers have been synthesized using spray pyrolysis of ferrocene dissolved in mixtures of alcohol and de-ionized (DI) water. It was found that the type of alcohol (methanol, ethanol or 2-propanol) used in the synthesis process is an important parameter of the thickness and type of carbon (graphitic or amorphous carbon) layers surrounding the iron oxide nanoflakes. The magnetite hexagonal nanocomposites synthesized using methanol showed lower thermal stability than those obtained by using 2-propanol or ethanol, in which the quantity of carbon layers surrounding the magnetite nanostructures is large. The magnetic properties at room temperature of the three types of samples were very similar and the differences between them can be attributed to different carbon fractions and the type of carbon layer covering the magnetite nanostructures.

Keywords: magnetite nanostructures, carbon coating, nanocomposites, thermal stability

(Some figures may appear in colour only in the online journal)

1. Introduction

Extensive studies have demonstrated that magnetite (Fe_3O_4) and maghemite ($\gamma\text{-Fe}_2\text{O}_3$) nanostructures are very promising candidates for their use in environmental and biomedical applications or as an electrode in lithium ion batteries due to their low cost, environmental benignity, biocompatibility, high density energy and long cycling performance [1–16]. Despite the existence of several methods to synthesize magnetic nanoparticles, the spray chemical vapor deposition (CVD) is very attractive because this is a one-step method that has important advantages over other methods with respect to factors such as cost, speed and adaptability [17, 18]. Using this method, magnetic nanoparticles of small size can be synthesized through thermal decomposition of organometallic compounds in organic solvents [19]. In particular, pyrolysis using ferrocene as a carbon source has been used to obtain carbon-encapsulated iron nanoparticles [20–22]. In the CVD method, the precursors turn into mist that is carried out by a gas into a furnace, then the solvent is evaporated and the precursors

cause a decomposition reaction to generate nanocrystals [17, 18]. It is well established that the magnetic iron nanostructures without any surface modification tend to agglomerate, due to the magnetic interactions between them. In addition, they present a hydrophobic surface [1–3] and cannot maintain their integrity as electrodes during several discharge/charge cycles [12–14]. For specific applications, then, the surface of these magnetic nanostructures must be tailored. This has been carried out using covalent bonding or physical coating [23, 24] which also gives them thermal stabilization [25, 26] and can be used to compensate for their shortages without reduction of their magnetic, physical and chemical properties. Furthermore, covering iron nanostructures with inert materials such as carbon nanostructures is very important in applications as a data storage system, for inks for xerography, for corrosion prevention [27], and for cellular delivery [28]. In the case of the magnetite nanostructures, carbon coatings protect them from being oxidized in external atmospheres while the magnetic properties remain unchanged [29]. Carbon-coated magnetic nanoparticles are receiving more attention at present

Experimental investigation of pedestal suppression in a figure-eight fiber laser by including a polarization asymmetrical NOLM

E. Hernández-Escobar^a, M. Bello-Jiménez^a, E. A. Kuzin^b, B. Ibarra-Escamilla^b, M. Duran-Sánchez^b, A. Díez^c, J. L. Cruz^c, M. V. Andrés^c.

^a Instituto de Investigación en Comunicación Óptica (IICO), Universidad Autónoma de San Luis Potosí, Av. Karakorum N. 1470 Lomas 4a Secc., 78210 San Luis Potosí, México;

^b Instituto Nacional de Astrofísica, Óptica y Electrónica (INAOE), Luis Enrique Erro N. 1, Departamento de Óptica, 72000 Puebla, México;

^c Departamento de Física Aplicada y Electromagnetismo, ICMUV, Universidad de Valencia, c/Dr. Moliner 50, Burjassot, 46100 Valencia, España.

ABSTRACT

A polarization asymmetrical nonlinear optical loop mirror (NOLM) is investigated to perform pedestal-free optical pulses in a figure-eight laser (F8L). The results demonstrate that in the low-power regime the NOLM operates as a half-wave plate and the output polarization is orthogonal to the input one. However, at higher power level the polarization component parallel to the input appears, with a transmission that always begins from zero at low power, allowing the rejection of low-intensity components. Experimental results demonstrate that by employing this configuration we can obtain a contrast between the peak and continuous background higher than 40 dB.

Keywords: Mode-locked fiber lasers, Passive modelocking, Nonlinear Optical Loop Mirror.

1. INTRODUCTION

The main characteristic of all-fiber lasers is the use of core-doped fibers with elements of rare-earths as gain medium. The Erbium-doped fibers are the most used, making possible to work in the region of the lowest attenuation for optical fibers¹. Among its benefits we found high concentration of power at the output beam, high stability, and low-cost, among others. Based on these properties, various configurations and methods have been investigated for the production of ultrashort optical pulses in all-fiber lasers².

The passive mode-locking is a technique that exploits nonlinear effect as a saturable absorber to avoid the use of external modulators³. The mode-locked lasers have been very attractive for industrial applications as well in optics communications, nonlinear optics and biomedicine⁴⁻⁶. Typical configurations for mode-locked fiber lasers include rings cavities or figure-eight laser (F8L) configurations, which is the focus of this work.

In a F8L the nonlinear effects play the most important role for ultrashort pulse generation³. The conventional scheme for a F8L is illustrated in the Fig. 1. The left loop is constituted by a ring cavity composed by an optical isolator and a polarization controller to ensure unidirectional operation. This loop is connected by a coupler with ratio $\alpha/(\alpha-1)$ to a nonlinear amplifying loop mirror (NALM)⁷. The NALM is formed by a four port coupler, where the two out ports P_3 and P_4 are joined to form a loop of optical fiber⁸. In this configuration and an Erbium-doped fiber (EDF) is used to provide amplification. If the EDF is not placed into the NALM loop, it will be referred to as nonlinear optical loop mirror (NOLM). The polarization is a critical issue in the NALM, which is preserved by the use of polarization controllers (PC) within the cavity. Finally the light pulse generated in the F8L is taken through a fiber coupler.

Letter

A temporal insight into the rich dynamics of a figure-eight fibre laser in the noise-like pulsing regime

E Garcia-Sanchez^{1,6}, O Pottiez¹, Y Bracamontes-Rodriguez¹,
J P Lauterio-Cruz¹, H E Ibarra-Villalon¹, J C Hernandez-Garcia^{2,3},
M Bello-Jimenez⁴ and E A Kuzin⁵

¹ Centro de Investigaciones en Óptica (CIO), Loma del Bosque 115, Col. Lomas del Campestre, León, Gto. 37150, Mexico

² Departamento de Electrónica, División de Ingenierías CIS, Universidad de Guanajuato, Carretera Salamanca-Valle de Santiago Km 3.5 + 1.8 Km, Comunidad de Palo Blanco, Salamanca, Gto. 36885, Mexico

³ Consejo Nacional de Ciencia y Tecnología, Av. Insurgentes Sur No. 1582, Col. Crédito Constructor, Del. Benito Juárez, C.P. 039040, Mexico

⁴ Instituto de Investigación en Comunicación Óptica, Universidad Autónoma de San Luis Potosí, Av. Karakorum 1470, Lomas 4ta Secc., San Luis Potosí, S.L.P. 78210, Mexico

⁵ Instituto Nacional de Astrofísica, Óptica y Electrónica (INAOE), L. E. Erro 1, Sta. Ma. Tonantzintla, Pue. 72824, Mexico

E-mail: pottiez@cio.mx

Received 14 July 2016, revised 20 August 2016

Accepted for publication 23 August 2016

Published 2 September 2016



Abstract

We report on the dynamics of noise-like pulses at the ns scale in a passively mode-locked fibre laser, which grow in complexity as wave retarder adjustments are performed. We can observe that the laser operating in the fundamental mode can be tuned to get different shapes of the noise-like pulse. Following a regime of a very stable waveform, regimes characterized by a much more variable (but still compact) waveform are observed. Then we can get the fragmentation of the main bunch and expulsion of sub-packets and, finally, a variety of puzzling dynamics with increasing complexity are evidenced. Although the collective behaviour of the multiple waveforms is at first sight random we can observe some well-defined patterns in the kinematics of light bunches at the global cavity scale. These results may be useful to unravel the subtle mechanisms at play in complex dissipative nonlinear systems such as passively mode-locked fibre lasers.

Keywords: fibre lasers, passive mode locking, noise-like pulses, laser dynamics

(Some figures may appear in colour only in the online journal)

1. Introduction

The great flexibility of fibre lasers has promoted their use in a broad range of applications that go from material processing,

sensing, optical communications, to fundamental research [1]. Although fibre lasers usually are used to generate stable pulses, they can be designed and tuned to operate in a regime known as noise-like pulsing. This regime has been attracting the attention of researchers for the potential applications in which this type of pulses can be used, such as sensing [2],

⁶ Author to whom any correspondence should be addressed.

Acousto-optic interaction in biconical tapered fibers: shaping of the stopbands

Gustavo Ramírez-Meléndez,^a Miguel Ángel Bello-Jiménez,^{a,*} Christian Cuadrado-Laborde,^{b,c} Antonio Díez,^c José Luis Cruz,^c Amparo Rodríguez-Cobos,^a Raúl Balderas-Navarro,^a and Miguel Vicente Andrés Bou^c

^aUniversidad Autónoma de San Luis Potosí, Instituto de Investigación en Comunicación Óptica, Av. Karakorum 1470 Lomas 4a Secc., 78210 San Luis Potosí, S.L.P., México

^bInstituto de Física Rosario (CONICET-UNR), Optical Metrology Lab, Ocampo y Esmeralda, S2000EYP Rosario, Argentina

^cUniversidad de Valencia, Departamento de Física Aplicada y Electromagnetismo, ICMUV, C/Dr. Moliner 50, Burjassot, 46100 Valencia, Spain

Abstract. The effect of a gradual reduction of the fiber diameter on the acousto-optic (AO) interaction is reported. The experimental and theoretical study of the intermodal coupling induced by a flexural acoustic wave in a biconical tapered fiber shows that it is possible to shape the transmission spectrum, for example, substantially broadening the bandwidth of the resonant couplings. The geometry of the taper transitions can be regarded as an extra degree of freedom to design the AO devices. Optical bandwidths above 45 nm are reported in a tapered fiber with a gradual reduction of the fiber down to 70 μm diameter. The effect of including long taper transition is also reported in a double-tapered structure. A flat attenuation response is reported with 3-dB stopband bandwidth of 34 nm. © 2016 Society of Photo-Optical Instrumentation Engineers (SPIE) [DOI: 10.1117/1.OE.55.3.036105]

Keywords: acousto-optic interaction; biconical tapered fiber; acousto-optic filter.

Paper 151598 received Nov. 13, 2015; accepted for publication Feb. 16, 2016; published online Mar. 8, 2016.

1 Introduction

In-fiber acousto-optic (AO) devices based on flexural acoustic waves have been investigated for years because of their applications as frequency shifters,¹ tunable filters,² and modulators.³ Recently, the AO has been investigated as a powerful tool for measuring axial inhomogeneities along optical fibers.⁴ When the fundamental flexural acoustic mode propagates along an uncoated single-mode optical fiber (SMF), the acoustic fields produce a periodical perturbation of the fiber, both refractive index changes and geometrical effects, which leads to an intermodal resonant coupling between the fundamental core mode and some specific cladding modes of the SMF.¹⁻³ This AO interaction can be seen as the dynamic counterpart of a conventional asymmetric long period fiber grating (LPG), whose transmission characteristics can be controlled dynamically by the amplitude and frequency of the acoustic wave. At the output fiber, only the light that remains guided by the core is transmitted, showing a transmittance spectrum with one or several attenuation notches at the wavelengths of the resonant couplings.

The effect of including tapered fibers to improve the AO response has been reported in previous works.³⁻⁸ However, these works paid attention first to the enhancement of the acoustic intensity by reducing the cross section of the fiber and second to the shift of the resonant wavelength in uniform tapered fibers. Thus, the use of a thin optical fiber produces a more efficient intermodal coupling that enables shorter and faster devices, as well as a reduction of the required acoustic power. This fiber tapering can be carried out either by chemical etching or by a fusion and pulling technique.

It is possible to adjust the wavelength of the resonant coupling between two specific modes by changing the frequency of the acoustic wave. However, the spectral bandwidth of a

given resonance is determined by the dispersion curves of the involved modes and it is not straightforward how to develop techniques to control such a bandwidth. Kim et al.⁹ explored the simultaneous excitation of the acoustic wave generator with two frequencies, while Jung et al.¹⁰ concatenated different fibers. Fedec et al.⁶ concatenated three fibers with different sections to demonstrate a gain flattening filter and pointed out the interest of exploiting the taper radius as a new degree of freedom in the design of AO filters. Jin et al.¹¹ demonstrated an enhancement of the bandwidth of the AO notches by using uniform fibers with a reduced diameter prepared with chemical etching. Complimentarily, Li et al.¹² investigated fibers with different dispersion curves in order to narrow the optical notches.

Here, we investigate how tapering can be exploited to control the spectral bandwidth of the transmission notches. It is known that the dispersion curves of both the acoustic and optical modes change with the radius of the fiber.³ Thus, smooth and long tapered fibers can effectively control the bandwidth of a given coupling by slightly shifting the resonance wavelength, enabling a geometrical design technique, since the shape of fiber tapers can be controlled accurately using a fusion and pulling technique.¹³ In Sec. 2, we start with the numerical modeling of acoustically induced LPG formed in a tapered structure. Then, in Sec. 3, we describe the experimental results and the comparison with the theory, in order to demonstrate the effects of the taper transitions on the spectral response of the AO device. Finally, our conclusions are summarized in Sec. 4.

2 Numerical Modeling of the Acousto-Optic Interaction in a Tapered Fiber

In this section, we present the numerical technique that we have implemented to simulate the spectral response of the

*Address all correspondence to: Miguel Ángel Bello-Jiménez, E-mail: m.bello@cactus.iico.uaslp.mx

Complex dynamics of a fiber laser at the edge of mode locking

E. Garcia-Sanchez,¹ O. Pottiez,^{1,*} Y. Bracamontes-Rodriguez,¹ J. P. Lauterio-Cruz,¹ H. E. Ibarra-Villalon,¹ J. C. Hernandez-Garcia,^{2,3} M. Bello-Jimenez,⁴ and E. A. Kuzin⁵

¹ Centro de Investigaciones en Óptica, Loma del Bosque 115, Col. Lomas del Campestre, León, Gto. 37150, Mexico

² Departamento de Electrónica, División de Ingenierías CIS, Universidad de Guanajuato, Carretera Salamanca-Valle de Santiago Km 3.5 + 1.8 Km, Comunidad de Palo Blanco, Salamanca, Gto. 36885, Mexico

³ Consejo Nacional de Ciencia y Tecnología, Av. Insurgentes Sur No. 1582, Col. Crédito Constructor, Del. Benito Juárez, C.P. 039040, Mexico

⁴ Instituto de Investigación en Comunicación Óptica, Universidad Autónoma de San Luis Potosí, Av. Karakorum 1470, Lomas 4ta Secc., San Luis Potosí, S.L.P. 78210, Mexico

⁵ Instituto Nacional de Astrofísica, Óptica y Electrónica, L. E. Erro 1, Sta. Ma. Tonantzintla, Pue. 72824, Mexico

*pottiez@cio.mx

Abstract: Conventional mode locking is characterized by the generation of a stable train of optical pulses. Even in the noise-like pulsing regime, corresponding to partial mode locking of fiber lasers, a periodic train of waveforms is still generated. In this work we study the dynamics of a figure-eight fiber laser away from the stable noise-like pulsing regime. By analyzing sequences of time-domain measurements performed with ns resolution, we reveal a wide range of puzzling dynamics, in which sub-structures emerge and drift away from the main bunch, decay or grow in a step-like manner, before vanishing abruptly. In some cases, sub-packets also concentrate in the central part of the period, forming one or multiple wide clouds that merge or split over time scales of seconds or minutes. Spontaneous transitions between these multiple states occur in a non-periodic manner, so that no quasi-stationary behavior is found over long time scales. These results provide a dramatic illustration of the extremely rich dynamics taking place in fiber lasers at the frontier of mode locking.

©2016 Optical Society of America

OCIS codes: (000.0000) General; (000.2700) General science.

References and links

1. P. Grelu, N. Akhmediev, "Dissipative solitons for mode-locked lasers," *Nature Photon.* **6**, 84–92 (2012).
2. F. Ö. İday, J. R. Buckley, W. G. Clark, and F. W. Wise, "Self-similar evolution of parabolic pulses in a laser," *Phys. Rev. Lett.* **92**, 213902 (2004).
3. A. Chong, J. Buckley, W. Renninger, and F. Wise, "All-normal-dispersion femtosecond fiber laser," *Opt. Express* **14**(21), 10095–10100 (2006).
4. N. Akhmediev, J. M. Soto-Crespo, and P. Grelu, "Roadmap to ultra-short record high-energy pulses out of laser oscillators," *Phys. Lett. A* **372**(17), 3124–3128 (2008).
5. A. F. J. Runge, C. Agüeray, N. G. R. Broderick, and M. Erkintalo, "Coherence and shot-to-shot spectral fluctuations in noise-like ultrafast fiber lasers," *Opt. Lett.* **38**, 4327–4330 (2013).
6. C. Lecaplain, Ph. Grelu, J. M. Soto-Crespo, and N. Akhmediev, "Dissipative rogue waves generated by chaotic pulse bunching in a mode-locked laser," *Phys. Rev. Lett.* **108**, 233901 (2012).
7. D. V. Churkin, S. Sugavanam, N. Tarasov, S. Khorev, S. V. Smirnov, S. M. Kobtsev, and S. K. Turitsyn, "Stochasticity, periodicity and localized light structures in partially mode-locked fibre lasers," *Nat. Commun.* **6**, 7004 (2015).
8. N. Akhmediev, J. M. Soto-Crespo, and G. Town, Pulsating solitons, chaotic solitons, period doubling, and pulse coexistence in mode-locked lasers: Complex Ginzburg-Landau equation approach, *Phys. Rev. E* **63**, 56602 (2001).
9. F. Amrani, A. Haboucha, M. Salhi, H. Leblond, A. Komarov, and F. Sanchez, "Dissipative solitons compounds in a fiber laser. Analogy with the states of the matter," *Appl. Phys. B* **99**(1–2), 107–114 (2010).

Experimental Investigation of Fused Biconical Fiber Couplers for Measuring Refractive Index Changes in Aqueous Solutions

Marco V. Hernández-Arriaga, Miguel A. Bello-Jiménez, A. Rodríguez-Cobos,
and Miguel V. Andrés, *Member, IEEE*

Abstract—A detailed experimental study of a simple and compact fiber optic sensor based on a fused biconical fiber coupler is presented, in which the sensitivity is improved by operating the coupler beyond the first coupling cycle. The sensor is demonstrated to perform high sensitivity measurements of refractive index changes by means of variation of sugar concentration in water. The device is operated to achieve a linear transmission response, allowing a linear relation between the sugar concentration and the output signal. The initial sensitivity was measured as 0.03 units of normalized transmission per unit of sugar concentration (g/100 mL), with a noise detection limit of a sugar concentration of 0.06 wt% of sugar concentration. Improvements in sensitivity were studied by operating the coupler beyond their first coupling cycles; achieving an improved sensitivity of 0.15 units of normalized transmission per unit of sugar concentration, and a minimum detection limit of 0.012 wt% of sugar concentration. From this result, the minimum detectable refractive index change is estimated as 2×10^{-5} refractive index unit.

Index Terms—Fiber optic sensor, fused biconical fiber coupler, refractive index sensor.

I. INTRODUCTION

FIBER-OPTIC couplers have attracted considerable attention in recent years for their ability to detect small changes in the refractive index (RI) of liquid solutions. A fiber coupler is a four-port device with a transmission spectrum that is strongly affected by the refractive index of the surrounding medium due to the evanescent field that is generated along the coupling region [1]. This effect has proven to be useful for sensing applications [2]. Recent approaches of fiber-coupler based RI sensors include fused biconical fiber couplers [3]–[7], optical microfibers [8]–[12], photonic crystal fibers [13], [14], and specially designed

two-core optical fibers [15], [16], all of them offering the advantages of high sensitivity, *in situ* measurements, compact size, and immunity to external electromagnetic interference. Most of these sensors are codified in wavelength and the achieved sensitivities are in the range of 1,125 to 30,100 nanometer (nm) per refractive index unit (RIU), with a minimum detection limit of 4×10^{-4} to 4×10^{-7} RIU, respectively.

From the point of view of implementation, the necessity of expensive equipment, such as optical spectrum analyzers, for measuring the shift in wavelength heavily affects the use of fiber-coupler based RI sensors. Thus, it is worthwhile to consider an alternative scheme based on the dependence of the power coupling on the surrounding medium. The two complementary outputs of a fiber coupler enable a straightforward normalization, i.e. the ratio between the difference and the addition, which automatically compensates for power fluctuations. In earlier works the dependence of the power coupling of traditional fused biconical tapered couplers on the external RI has been presented and it has been proposed that it is possible to use such a structure to develop a fiber based refractometer [1], [17]. Tazawa et al. [2] have implemented this power measurement approach to demonstrate a biosensor with estimated 4×10^{-6} RIU detection limit. Recently, it has been demonstrated that modal interferometers based on integrated waveguides provide one of the best resolutions ever reported (2.5×10^{-7} RIU) [18]. A fused biconical couplers is, in fact, a modal interferometer in which the phase difference between the symmetric and antisymmetric supermodes determine the power distribution at the output fibers. Small changes of the external RI do not modify substantially the coupling coefficient, but they generate a significant phase difference between supermodes. In terms of fiber-coupler based RI sensors, this last point deserves particular attention for the detection of slight changes in the refractive index of aqueous solutions. Although several schemes have reported this effect [1], [2], [17], they did not study the conditions for an optimal performance of the reported device. Here our purpose is the experimental analysis of a fused biconical fiber coupler, operated beyond the first coupling cycle, with a power transmission that depends on the surrounding medium.

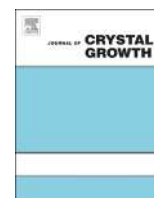
The objective is not only to gain insights into the dynamics of this kind of device, but also looking forwards an improvement of its performance. Based on this motivation, the

Manuscript received July 10, 2015; revised August 26, 2015; accepted August 27, 2015. Date of publication September 16, 2015; date of current version December 10, 2015. This work was supported in part by Promep under Grant DSA/103.5/14/10476 and in part by the Consejo Nacional de Ciencia y Tecnología under Grant 206425 and Grant 222476. The associate editor coordinating the review of this paper and approving it for publication was Dr. Anna G. Mignani.

M. V. Hernández-Arriaga, M. A. Bello-Jiménez, and A. Rodríguez-Cobos are with the Instituto de Investigación en Comunicación Óptica, Universidad Autónoma de San Luis Potosí, San Luis Potosí 78210, Mexico (e-mail: dmxsol@hotmail.com; m.bello@cactus.iico.uaslp.mx; roca@cactus.iico.uaslp.mx).

M. V. Andrés is with the Departamento de Física Aplicada y Electromagnetismo, Institute of Materials Science, Universidad de Valencia, Valencia 46100, Spain (e-mail: miguel.andres@uv.es).

Digital Object Identifier 10.1109/JSEN.2015.2475320



Tuning emission in violet, blue, green and red in cubic GaN/InGaN/GaN quantum wells



I.E. Orozco Hinostroza^a, M. Avalos-Borja^{a,b}, V.D. Compeán García^c, C. Cuellar Zamora^c,
A.G. Rodríguez^c, E. López Luna^c, M.A. Vidal^{c,*}

^a Instituto Potosino de Investigación Científica y Tecnológica, Camino a la Presa San José 2055, Col. Lomas 4a Sección, 78216 San Luis Potosí, México

^b Centro de Nanociencias y Nanotecnología, Universidad Nacional Autónoma de México, A. Postal 2681, Ensenada, Baja California, México

^c Coordinación para la Innovación y Aplicación de la Ciencia y Tecnología (CIACyT), Universidad Autónoma de San Luis Potosí (UASLP), Álvaro Obregón 64, 78000 San Luis Potosí, México

ARTICLE INFO

Article history:

Received 9 October 2015

Received in revised form

18 November 2015

Accepted 25 November 2015

Communicated by H. Asahi

Available online 2 December 2015

Keywords:

A3. Quantum wells

A3. Molecular beam epitaxy

B2. Semiconducting III–V materials

B3. Heterojunction semiconductor devices

ABSTRACT

Light emission in the three primary colors was achieved in cubic GaN/InGaN/GaN heterostructures grown by molecular beam epitaxy on MgO substrates in a single growth process. A heterostructure with four quantum wells with a width of 10 nm was grown; this quantum wells width decrease the segregation effect of In. Photoluminescence emission produced four different emission signals: violet, blue, green-yellow and red. Thus, we were able to tune energy transitions in the visible spectrum modifying the In concentration in cubic $\text{In}_x\text{Ga}_{1-x}\text{N}$ ternary alloy.

© 2015 Elsevier B.V. All rights reserved.

1. Introduction

In the past decades, nitride semiconductors have been used to fabricate electronic and optoelectronic devices [1–17]. Among the most important applications is solid-state lighting. Using α -GaN and α -InGaN it was possible to build a blue light-emitting diode (LED) [1]. Since this major breakthrough, the development of methods to improve growing conditions has brought remarkable results in light emitting devices [2–6]. Theoretically, due to band gap energy values of α -GaN (3.4 eV) and α -InN (0.7 eV), the ternary InGaN alloy can be used to cover the electromagnetic spectrum from UV to near infrared. Growing conditions that result in more than a 30% concentration of In may lead to high defect density because of the large lattice mismatch between GaN and InN (11%). Furthermore, high indium content leads to a strong quantum confinement stark effect, which reduces the radiative recombination efficiency of carriers and hinders the long wavelength range transitions. Recent reports have studied the optimization of green-yellow emission in hexagonal InGaN-based devices [3–5]. Nonetheless, red wavelength transitions with planar

InGaN heterostructures remain difficult to obtain. Thus, to produce white light emitting diodes, a blue or UV LED is covered with a phosphor, which absorbs the light and reemits it with a longer wavelength. However, using phosphors such as $\text{Ce}^{3+}:\text{Y}_3\text{Al}_5\text{O}_{12}$ (one of the most common phosphors) reduces the long-term reliability and lifetime of the device [6]. Different approaches have been made to overcome this issue. One of them is to synthesize quantum wells by varying the In mole fraction in the active layer to obtain the long wavelength emission without phosphors [7]. Another approach to produce white light is to use the structures such as quantum dots in wells [8], dots in wires [9], nanorods [10], nanopillars [11] and other nanostructures [12]. Typically, these nitride semiconductors crystallize into a hexagonal phase. Therefore, most of the previous work is based on the InGaN wurtzite phase. Nevertheless, the cubic phase has some advantages over the hexagonal phase, such as the lack of spontaneous and piezoelectric polarization [9]. Moreover, β -GaN has a lower band gap energy (3.28 eV) than α -GaN. Thus, low energy emissions in the ternary β -InGaN alloy can be obtained with a smaller In concentration than in α -InGaN.

Although it is more difficult to synthesize InGaN and GaN cubic films, it has been possible to grow them using the Metal-Organic Chemical Vapor Deposition (MOCVD), Metal-Organic Vapor Phase Epitaxy and Molecular Beam Epitaxy (MBE) techniques on the 3C-

* Corresponding author.

E-mail addresses: ignacio.orozco@ipicyt.edu.mx (I.E. Orozco Hinostroza), mavidalborbolla@yahoo.com.mx (M.A. Vidal).

Acousto-optic interaction in biconical tapered fibers: shaping of the stopbands

Gustavo Ramírez-Meléndez,^a Miguel Ángel Bello-Jiménez,^{a,*} Christian Cuadrado-Laborde,^{b,c} Antonio Díez,^c José Luis Cruz,^c Amparo Rodríguez-Cobos,^a Raúl Balderas-Navarro,^a and Miguel Vicente Andrés Bou^c

^aUniversidad Autónoma de San Luis Potosí, Instituto de Investigación en Comunicación Óptica, Av. Karakorum 1470 Lomas 4a Secc., 78210 San Luis Potosí, S.L.P., México

^bInstituto de Física Rosario (CONICET-UNR), Optical Metrology Lab, Ocampo y Esmeralda, S2000EYP Rosario, Argentina

^cUniversidad de Valencia, Departamento de Física Aplicada y Electromagnetismo, ICMUV, C/Dr. Moliner 50, Burjassot, 46100 Valencia, Spain

Abstract. The effect of a gradual reduction of the fiber diameter on the acousto-optic (AO) interaction is reported. The experimental and theoretical study of the intermodal coupling induced by a flexural acoustic wave in a biconical tapered fiber shows that it is possible to shape the transmission spectrum, for example, substantially broadening the bandwidth of the resonant couplings. The geometry of the taper transitions can be regarded as an extra degree of freedom to design the AO devices. Optical bandwidths above 45 nm are reported in a tapered fiber with a gradual reduction of the fiber down to 70 μm diameter. The effect of including long taper transition is also reported in a double-tapered structure. A flat attenuation response is reported with 3-dB stopband bandwidth of 34 nm. © 2016 Society of Photo-Optical Instrumentation Engineers (SPIE) [DOI: 10.1117/1.OE.55.3.036105]

Keywords: acousto-optic interaction; biconical tapered fiber; acousto-optic filter.

Paper 151598 received Nov. 13, 2015; accepted for publication Feb. 16, 2016; published online Mar. 8, 2016.

1 Introduction

In-fiber acousto-optic (AO) devices based on flexural acoustic waves have been investigated for years because of their applications as frequency shifters,¹ tunable filters,² and modulators.³ Recently, the AO has been investigated as a powerful tool for measuring axial inhomogeneities along optical fibers.⁴ When the fundamental flexural acoustic mode propagates along an uncoated single-mode optical fiber (SMF), the acoustic fields produce a periodical perturbation of the fiber, both refractive index changes and geometrical effects, which leads to an intermodal resonant coupling between the fundamental core mode and some specific cladding modes of the SMF.¹⁻³ This AO interaction can be seen as the dynamic counterpart of a conventional asymmetric long period fiber grating (LPG), whose transmission characteristics can be controlled dynamically by the amplitude and frequency of the acoustic wave. At the output fiber, only the light that remains guided by the core is transmitted, showing a transmittance spectrum with one or several attenuation notches at the wavelengths of the resonant couplings.

The effect of including tapered fibers to improve the AO response has been reported in previous works.³⁻⁸ However, these works paid attention first to the enhancement of the acoustic intensity by reducing the cross section of the fiber and second to the shift of the resonant wavelength in uniform tapered fibers. Thus, the use of a thin optical fiber produces a more efficient intermodal coupling that enables shorter and faster devices, as well as a reduction of the required acoustic power. This fiber tapering can be carried out either by chemical etching or by a fusion and pulling technique.

It is possible to adjust the wavelength of the resonant coupling between two specific modes by changing the frequency of the acoustic wave. However, the spectral bandwidth of a

given resonance is determined by the dispersion curves of the involved modes and it is not straightforward how to develop techniques to control such a bandwidth. Kim et al.⁹ explored the simultaneous excitation of the acoustic wave generator with two frequencies, while Jung et al.¹⁰ concatenated different fibers. Feced et al.⁶ concatenated three fibers with different sections to demonstrate a gain flattening filter and pointed out the interest of exploiting the taper radius as a new degree of freedom in the design of AO filters. Jin et al.¹¹ demonstrated an enhancement of the bandwidth of the AO notches by using uniform fibers with a reduced diameter prepared with chemical etching. Complimentarily, Li et al.¹² investigated fibers with different dispersion curves in order to narrow the optical notches.

Here, we investigate how tapering can be exploited to control the spectral bandwidth of the transmission notches. It is known that the dispersion curves of both the acoustic and optical modes change with the radius of the fiber.³ Thus, smooth and long tapered fibers can effectively control the bandwidth of a given coupling by slightly shifting the resonance wavelength, enabling a geometrical design technique, since the shape of fiber tapers can be controlled accurately using a fusion and pulling technique.¹³ In Sec. 2, we start with the numerical modeling of acoustically induced LPG formed in a tapered structure. Then, in Sec. 3, we describe the experimental results and the comparison with the theory, in order to demonstrate the effects of the taper transitions on the spectral response of the AO device. Finally, our conclusions are summarized in Sec. 4.

2 Numerical Modeling of the Acousto-Optic Interaction in a Tapered Fiber

In this section, we present the numerical technique that we have implemented to simulate the spectral response of the

*Address all correspondence to: Miguel Ángel Bello-Jiménez, E-mail: m.bello@cactus.iico.uaslp.mx

Dynamical and Tuneable Modulation of the Tamm Plasmon/Exciton–Polariton Hybrid States Using Surface Acoustic Waves

J.V.T. BULLER^{a,*}, E.A. CERDA-MÉNDEZ^a, R.E. BALDERAS-NAVARRO^b AND P.V. SANTOS^a

^aPaul-Drude-Institut für Festkörperelektronik, 10117 Berlin, Germany

^bInstituto de Investigación en Comunicación Óptica-UASLP, 78000 San Luis, Mexico

In this work, we discuss theoretically the formation of the Tamm plasmon/exciton–polariton hybrid states in an (Al,Ga)As microcavity and their modulation by surface acoustic waves. The modulation of the Tamm plasmon/exciton–polariton states origins in the change of the excitonic band gap energy and the thickness change of the sample structure layers due to the induced strain fields by surface acoustic waves. The frequency f_{SAW} of the acoustic modulation of the Tamm plasmon/exciton–polariton states is limited by the thickness of the upper distributed Bragg reflector. For the Tamm plasmon/exciton–polariton states in $\text{Al}_x\text{Ga}_{1-x}\text{As}/\text{GaAs}$ structures f_{SAW} is in the range of 370 MHz while f_{SAW} in GHz range is possible for the parametric Tamm plasmon/exciton–polariton states. In both cases, the acoustic modulation is several meV for typical acoustic power levels.

DOI: [10.12693/APhysPolA.129.A-26](https://doi.org/10.12693/APhysPolA.129.A-26)

PACS: 71.36.+c, 42.55.Sa, 85.50.-n

1. Introduction

The development of new optoelectronic devices operating at low threshold powers and at high switching frequencies is a complex and challenging task, which can only be overcome by exploiting new physical phenomena [1–4] and applying them to device implementations [5, 6]. One of such new promising physical phenomenon are exciton–polaritons in semiconductor microcavities (MCs). Exciton–polaritons are unique bosonic half-light half-matter quasiparticles that result from the strong coupling between the photonic mode of a MC and quantum well (QW) excitons embedded in the active MC region (*cf.* Fig. 1a, [7]). The inter-excitonic interactions between polaritons give rise to optical nonlinearities several orders of magnitude higher than in purely photonic systems. Due to the photonic component polaritons have a very low effective mass (10^{-5} – 10^{-4} mass of a free electron) leading to a de Broglie wavelength λ_{dB} of a few μm and thus to the possibility to form macroscopic coherent quantum phases at low densities and at elevated temperatures (on the order of a few K) as well as to be manipulated by micro-scale potentials [8, 9]. Various polariton-based device concepts, like polariton-based transistors and logic gates, as well as their implementation in quantum information processing have been proposed [10, 11].

The fabrication of polaritonic devices requires reliable and practical potentials for controlling, confining and guiding exciton–polaritons in MC structure. One interesting option is provided by dynamic strain

potentials [12] induced by a surface acoustic wave (SAW) [13, 14]. SAWs are mechanical vibrations propagating along a surface (*cf.* Fig. 1c): the strain field of a SAW with wavelength λ_{SAW} smaller than λ_{dB} creates a tuneable acoustic lattice for the control of the polariton properties. Since the SAW penetration depth is comparable to λ_{SAW} , an efficient acoustic modulation requires that λ_{SAW} is larger than the thickness of the upper MC distributed Bragg reflector (DBR). In this contribution, we demonstrate that this limitation can be overcome by exploiting plasmonic resonances induced by thin metallic stripes deposited on the top of the MC structure. In this case, new quasiparticles called the Tamm plasmon/exciton–polaritons (TPEP) form by the superposition of the Tamm plasmons (TPs) at the metal–semiconductor interface and the exciton–polaritons in the MC [10]. The aim of this work is to explore the dynamical and tuneable modulation of TPEP modes by SAW at frequencies close to and in the gigahertz range.

2. Sample design

The proposed sample structure supporting TPEP states consists of a gold layer on top of a DBR consisting of $\text{Al}_x\text{Ga}_{1-x}\text{As}$ layers with a thickness $\lambda/(4n_i)$ ($i = \text{Al}_{15}\text{Ga}_{85}\text{As}$, $\text{Al}_{80}\text{Ga}_{20}\text{As}$), where n_i is the refractive index and λ the MC resonance wavelength (*cf.* Fig. 1a). The structure supports TP modes at the metal–semiconductor interface only when the DBR layer adjacent to the metal has a higher refractive index than its following DBR layer [16]. The energy E_{T} of the TP mode can be tuned by changing the thickness of the metal and/or of the adjacent DBR layer. When E_{T} is in resonance with the MC mode and the QW exciton energy, the resulting coupled system can be described using the three level coupled oscillator model given by

*corresponding author; e-mail: buller@pdi-berlin.de

Exciton-polariton gap soliton dynamics in moving acoustic square latticesJ. V. T. Buller,^{1,*} R. E. Balderas-Navarro,^{1,2} K. Biermann,¹ E. A. Cerda-Méndez,^{1,2,3} and P. V. Santos¹¹*Paul-Drude-Institut für Festkörperelektronik, 10117 Berlin, Germany*²*Instituto de Investigación en Comunicación Óptica, Universidad Autónoma de San Luis Potosí, Avenida Karakorum 1470, Lomas 4^a Secc, 78216, San Luis Potosí, México*³*Instituto de Física Universidad Autónoma de San Luis Potosí, Avenida Manuel Nava #6, Zona Universitaria, Código Postal 78290 San Luis Potosí, México*

(Received 18 May 2016; revised manuscript received 22 August 2016; published 22 September 2016)

The modulation by a surface acoustic wave (SAW) provides a powerful tool for the formation of tunable lattices of exciton-polariton macroscopic quantum states (MQSs) in semiconductor microcavities. The MQSs were resonantly excited in an optical parametric oscillator configuration. We investigate the temporal dynamics of these lattices using time and spatially resolved photoluminescence (PL). Photoluminescence images of the MQSs clearly show the motion of the lattice at the acoustic velocity. Interestingly, the PL intensity emitted by the MQSs as well as their coherence length oscillate with the position of the lattice sites relative to the exciting laser beam. The coherence length and the PL intensity are correlated. The PL oscillation amplitude depends on both the intensity and the size of the exciting laser spot and increases considerably for excitation intensities close to the optical threshold power for the formation of the MQS. The oscillations are explained by a model that takes into account the combined effects of SAW reflections, which dynamically distort the amplitude of the potential, and the spatial phase of the acoustic lattice within the exciting laser spot. This paper could pave the way to tailor polariton-based light-emitting sources with intensity variations controlled by the SAWs.

DOI: [10.1103/PhysRevB.94.125432](https://doi.org/10.1103/PhysRevB.94.125432)**I. INTRODUCTION**

Exciton-polaritons result from the strong coupling between photons confined in a microcavity (MC) and excitons in quantum wells (QWs) inserted in it. They are half-light, half-matter quasiparticles with bosonic character. The excitonic component gives rise to strong nonlinear interactions between exciton-polaritons, while the photonic component leads to a very low effective mass m_{eff} (10^{-4} – 10^{-5} mass of the electron) and, consequently, de Broglie wavelengths λ_{dB} of a few microns [1,2]. The latter enables the formation of macroscopic quantum states (MQSs) of exciton-polaritons at particle densities considerably lower and at temperatures considerably higher than in atomic systems [3,4]. These remarkable properties of exciton-polaritons in semiconductor optical MCs have opened the way for several device functionalities such as polariton-based lasers [5,6], transistors [7,8], and logic gates [9,10].

In analogy to optical lattices of cold atoms [11], tunable lattices for exciton-polariton MQSs can be formed via the periodic spatial modulation introduced by a surface acoustic wave (SAW). Surface acoustic waves are mechanical vibrations that can be electrically excited using interdigital transducers (IDTs) deposited on the MC surface [12] [cf. Fig. 1(a)]. The moving strain field of the SAW creates regions of tension and compression in the MC, thus spatially modulating the MC optical resonance energy as well as the band gap energy of the embedded QWs [13]. By superimposing two orthogonal SAW beams, one can create the two-dimensional square lattice potential illustrated in Fig. 1(a). For small SAW amplitudes Φ_{SAW} , λ_{dB} can become comparable to or even longer than the SAW wavelength λ_{SAW} . Under this condition, the acoustic

modulation creates a folded band structure for exciton-polariton MQSs with dispersion and energy gaps controlled by Φ_{SAW} . The mini-Brillouin zones (MBZs) formed by the lattice, which are illustrated in the inset of Fig. 1(b), have dimensions $k_{\text{SAW}} = 2\pi/\lambda_{\text{SAW}}$ determined by the SAW periodicity.

As for the polariton dispersion, the symmetry and spatial coherence of MQSs in an acoustic lattice also depend on the lattice amplitude Φ_{SAW} . Large Φ_{SAW} flattens the lowest dispersion branch and inhibits the tunneling of exciton-polaritons between lattice sites, thus fragmenting the extended phase via the formation of independent MQSs localized at the minima of the SAW potential [14]. Phases with extended coherence appear, in contrast, for moderate Φ_{SAW} , where the lowest dispersion branch exhibits considerable energy dispersion [15]. Interestingly, the most robust MQS under a moderate Φ_{SAW} does not form at the Γ point of the lowest dispersion branch but rather at the M points, where the effective mass of exciton-polaritons is negative [cf. Fig. 1(b)]. Recently, we have demonstrated that these phases are gap-soliton-like condensates (GSs) [16]. Gap-soliton-like condensates are metastable self-localized excitations originating from the compensation of the repulsive interparticle interactions by their negative kinetic energy. Gap-soliton-like condensates have also been observed in other physical systems [17] and may prove to be of relevance for quantum information processing [18,19].

Previous investigations on exciton-polaritons and GSs in acoustic lattices have been carried out using optical spectroscopy in the continuous wave (cw) domain and were, therefore, unable to capture the GS temporal dynamics in the moving acoustic lattice. In this paper, we address this issue via photoluminescence (PL) studies carried out with time and spatial resolutions which are much shorter than the temporal and spatial SAW periods, respectively. We start by describing the experimental techniques employed to prepare the MC sample and to map the time-dependent GS wave

*buller@pdi-berlin.de

Real-time measurement of the average temperature profiles in liquid cooling using digital holographic interferometry

Carlos Guerrero-Mendez,^{a,b,*} Tonatiuh Saucedo Anaya,^b M. Araiza-Esquivel,^a Raúl E. Balderas-Navarro,^c Said Aranda-Espinoza,^d Alfonso López-Martínez,^a and Carlos Olvera-Olvera^a

^aUniversidad Autónoma de Zacatecas, Unidad Académica de Ingeniería Eléctrica, Av. Ramón López Velarde 801, Zacatecas C.P. 98000, México

^bUniversidad Autónoma de Zacatecas, Unidad Académica de Física, Calzada Solidaridad Esq. Con Paseo La Bufa S/N, Zacatecas C.P. 98060, México

^cInstituto de Investigación en Comunicación Óptica (IICO-UASLP), Avenue Karakorum 1470, Lomas 4ta. Sección, San Luis Potosí C.P. 78210, México

^dUniversidad Autónoma de San Luis Potosí, Instituto de Física, Avenue Salvador Nava 6, Zona Universitaria, San Luis Potosí C.P. 78290, México

Abstract. We present an alternative optical method to estimate the temperature during the cooling process of a liquid using digital holographic interferometry (DHI). We make use of phase variations that are linked to variations in the refractive index and the temperature property of a liquid. In DHI, a hologram is first recorded using an object beam scattered from a rectangular container with a liquid at a certain reference temperature. A second hologram is then recorded when the temperature is decreased slightly. A phase difference between the two holograms indicates a temperature variation, and it is possible to obtain the temperature value at each small point of the sensed optical field. The relative phase map between the two object states is obtained simply and quickly through Fourier-transform method. Our experimental results reveal that the temperature values measured using this method and those obtained with a thermometer are consistent. We additionally show that it is possible to analyze the heat-loss process of a liquid sample in dynamic events using DHI. © 2016 Society of Photo-Optical Instrumentation Engineers (SPIE) [DOI: [10.1117/1.OE.55.12.121730](https://doi.org/10.1117/1.OE.55.12.121730)]

Keywords: digital holographic interferometry; refractive index difference; liquids temperature; phase difference.

Paper 160626SS received Apr. 26, 2016; accepted for publication Oct. 6, 2016; published online Oct. 27, 2016.

1 Introduction

The thermal conditions of liquid samples are of interest in many areas of science, and determining the temperature of liquid substances is very important in engineering applications, such as the design of air-conditioning units, heat transfer equipment, machines and industrial processes, and thermal energy storage systems.¹ The temperature values of substances are commonly determined using devices that must be in contact with the specimen. However, these devices often affect the dynamic evolution or the mechanical properties of the fields of temperature in a substance. In contrast, common optical techniques are noninvasive, noncontact, and nondestructive, and they have been developed for this purpose using the thermo-optical effect,² which is thermal modulation of the refractive index n of a material.³ However, they only obtain temperature data over a small region of the sample.^{4,5}

New advanced optical techniques are more precise and higher resolution, and yield stable full-field measurements between optical fields; these techniques are generally preferred for monitoring the dynamic evolution of entire optical fields. Some of these methods include the Schlieren, shadowgraph, and interferometry techniques.⁶ Digital holographic interferometry (DHI) is an optical metrology technique based on holography that records and reconstructs wavefronts to interferometrically compare two or more wavefronts

obtained at different moments or states of an object using a computer. Furthermore, DHI is a fast, simple, high-precision, nondestructive, full-field optical technique for measuring variations of physical properties of phase objects in dynamic processes.⁷⁻⁹

Some new studies based on DHI have obtained measurements of phase differences and used these data to visualize and determine how flow fields change constantly in both time and space. Several authors have established a physical model to determine a relationship between the phase and the parameter to be analyzed.¹⁰ These investigators have obtained measurements of the temperature variation in fluids,¹¹ flames,¹²⁻¹⁶ and liquids.^{11,17-23} However, these methods use the entire wrapped phase map difference or a part of this phase map, and also necessitate a robust algorithm to unwrap the phase map to obtain a physical parameter. Other DHI methods obtain measurements of a phase variation linked with a punctual value of concentration in the crystallization evolution process,^{10,24,25} but they neglect the temperature values in their mathematical expressions.

We present an alternative method to measure the temperature of transparent, nonscattering liquid samples. Using a physical model to determine the relation between the phase difference and the temperature variation between a certain time of sample and a reference temperature, we can calculate the temperature value at each point of the liquid sample. The wrapped phase difference map between a

*Address all correspondence to: Carlos Guerrero-Mendez, E-mail: capacti@gmail.com



Contents lists available at ScienceDirect

Applied Surface Science

journal homepage: www.elsevier.com/locate/apsusc



Real-time reflectance-difference spectroscopy during the epitaxial growth of InAs/GaAs/(001)

A. Armenta-Franco, A. Lastras-Martínez*, J. Ortega-Gallegos, D. Ariza-Flores, L.E. Guevara-Macías, R.E. Balderas-Navarro, L.F. Lastras-Martínez

Instituto de Investigación en Comunicación Óptica, Universidad Autónoma de San Luis Potosí, San Luis Potosí, C.P. 78000, México

ARTICLE INFO

Article history:

Received 31 July 2016
Received in revised form 28 August 2016
Accepted 30 August 2016
Available online xxx

Keywords:

Quantum dots
Molecular beam epitaxy
Real time monitoring

ABSTRACT

We report on real-time Reflectance-difference spectroscopy measurements carried out during the growth of InGaAs quantum dots (QDs) on GaAs (001) substrates. Measurements were performed with a recently developed rapid RD spectrometer, at a rate of 10 spectra per second. Our results demonstrate the potential for RD spectroscopy as an optical probe for the real-time monitoring of the epitaxial growth of InAs/GaAs QDs. We show that RD provides information on the kinetics of formation of QDs, including the rate of InAs coverage of the GaAs substrate and the rate of growth of InGaAs QDs. Results further suggest that the formation of QDs is mediated by the formation of InAs-rich islands that eventually disappear as QDs mature.

© 2016 Elsevier B.V. All rights reserved.

1. Introduction

Self-assembled quantum dots (QDs) integrated into semiconductor heterostructures are highly attractive for device application because of their discrete energy levels and optical properties. QDs find application in devices such as quantum dot computers, quantum dots lasers and infrared photodetectors [1]. It is accepted that the nucleation of InAs QDs on GaAs (001) substrates follows a two-step process. In a first step, InAs growth proceeds through a two-dimensional (2D), layer by layer, mode until a critical thickness of about 1.5 monolayer is reached. Afterwards, additional In and As species arriving at the surface incorporates into the growing film in a three-dimensional (3D) mode as a result of accumulated surface strain, resulting in the growth of InGaAs quantum dots on top of the 2D InAs wetting layer [2].

While InAs QDs grow spontaneously on GaAs once the critical thickness is reached, to take advantage of the unique quantum dot physical properties, the kinetics of the QDs growth process should be understood and controlled. Optical techniques, being remote, non-invasive and instrumentally simple, are well suited as probes for the real-time monitoring and study of the epitaxial growth process of zincblende semiconductors. Among optical techniques, Reflectance-difference (RD) spectroscopy results

particularly attractive for this application due to its high surface specificity. RD measures the difference in reflectance for two mutually orthogonal polarizations and thus provides information on the surface anisotropies associated to the breakdown of the cubic symmetry at or near the sample surface [3].

Surface anisotropies in zincblende semiconductors have been reported to be associated to a number of physical phenomena, including α and β dislocations [4], surface electric fields [5], local field effects [6], surface reconstruction [7,8], surface dimmers [9,10] and surface roughness [3]. While the multiple sources of optical anisotropies make the physical interpretation of RD spectra challenging, they do as well indicate the high potential for RD as a surface probe. In the particular case of InAs Quantum dots, several mechanisms may lead to an optical anisotropic surface, including the elastic interaction of anisotropic QD's with the GaAs surface [11] and the anisotropic relaxation of the interface strain by preferential generation of α -type mismatch dislocations [12]. In this paper we report on in situ, real-time RD spectroscopy during the Molecular Beam Epitaxy (MBE) growth of InAs QDs on GaAs (001) substrates that shows RD spectroscopy to be a powerful tool for the real-time monitoring of the heteroepitaxial growth of zincblende semiconductors.

2. Experimental

Epitaxial growth was carried out on semi insulating GaAs (001) substrates at a temperature of 480 °C in a solid source MBE chamber. A valved As cell allowed for the control of As flux which was

* Corresponding author.
E-mail addresses: alastras@gmail.com, alm@cactus.iico.uaslp.mx (A. Lastras-Martínez).

Residual electric fields of InGaAs/AlAs/AlAsSb (001) coupled double quantum wells structures assessed by photorefectance anisotropy

J. V. González-Fernández*, R. Herrera-Jasso, N. A. Ulloa-Castillo,
J. Ortega-Gallegos, R. Castro-García, L. F. Lastras-Martínez,
A. Lastras-Martínez and R. E. Balderas-Navarro†

*Instituto de Investigación en Comunicación Óptica,
Universidad Autónoma de San Luis Potosí,
Av. Karakorum 1470, Lomas 4a sección,
San Luis Potosí CP 78210, México*

*janogf@gmail.com

†rnb@cactus.iico.uaslp.mx

T. Mozume and S. Gozu

*National Institute of Advanced Industrial Science and Technologies,
2-1 Tsukuba Central, 1-1-1 Umezono, Tsukuba, Ibaraki 305-8568, Japan*

Received 9 June 2015

Revised 23 September 2015

Accepted 12 October 2015

Published 9 December 2015

We report on photorefectance anisotropy (PRA) spectroscopy of InGaAs/AlAs/AlAsSb coupled double quantum wells (CDQWs) with extremely thin coupling AlAs barriers grown by molecular beam epitaxy (MBE), with no intentional doping. By probing the *in-plane* interfacial optical anisotropies (OAs), it is shown that PRA spectroscopy has the ability to detect and distinguish semiconductor layers with quantum dimensions, as the anisotropic photorefectance (PR) signal stems entirely from buried quantum wells (QWs). In order to account for the experimental PRA spectra, a theoretical model at $k = 0$, based on a linear electro-optic effect through a piezoelectric shear strain, has been employed to quantify the internal electric fields across the QWs. The dimensionalities of the PR lineshapes were tested by using reciprocal (Fourier) space analysis. Such a complementary test is used in order to correctly employ the PRA model developed here.

Keywords: Photorefectance spectroscopy; polarized photorefectance; coupled double quantum wells; electric fields; zincblende semiconductors.

PACS numbers: 78.66.Fd, 77.55.dj, 73.20.-r, 78.40.-q

*†Corresponding authors.



PAPER

Spatial self-organization of macroscopic quantum states of exciton-polaritons in acoustic lattices

OPEN ACCESS

RECEIVED

8 December 2015

REVISED

27 May 2016

ACCEPTED FOR PUBLICATION

6 June 2016

PUBLISHED

1 July 2016

Original content from this work may be used under the terms of the [Creative Commons Attribution 3.0 licence](#).

Any further distribution of this work must maintain attribution to the author(s) and the title of the work, journal citation and DOI.

J V T Buller¹, E A Cerda-Méndez^{2,4}, R E Balderas-Navarro², K Biermann¹ and P V Santos¹¹ Paul-Drude-Institut für Festkörperelektronik, Hausvogteiplatz 05-7, D-10117 Berlin, Germany² Instituto de Investigación en Comunicación Óptica, Universidad Autónoma de San Luis Potosí, Av. Karakorum 1470, Lomas 4ª Secc, 78210, San Luis Potosí, México³ Instituto de Física Universidad Autónoma de San Luis Potosí, Av. Manuel Nava #6, Zona Universitaria, C.P. 78290 San Luis Potosí, México⁴ Author to whom any correspondence should be addressed.E-mail: ecerda@cactus.iico.uaslp.mx**Keywords:** semiconductor microcavities, surface acoustic waves, exciton-polaritons, solitonsSupplementary material for this article is available [online](#)**Abstract**

Exciton-polariton systems can sustain macroscopic quantum states (MQSs) under a periodic potential modulation. In this paper, we investigate the structure of these states in acoustic square lattices by probing their wave functions in real and momentum spaces using spectral tomography. We show that the polariton MQSs, when excited by a Gaussian laser beam, self-organize in a concentric structure, consisting of a single, two-dimensional gap-soliton (GS) state surrounded by one dimensional (1D) MQSs with lower energy. The latter form at hyperbolic points of the modulated polariton dispersion. While the size of the GS tends to saturate with increasing particle density, the emission region of the surrounding 1D states increases. The existence of these MQSs in acoustic lattices is quantitatively supported by a theoretical model based on the variational solution of the Gross-Pitaevskii equation. The formation of the 1D states in a ring around the central GS is attributed to the energy gradient in this region, which reduces the overall symmetry of the lattice. The results broaden the experimental understanding of self-localized polariton states, which may prove relevant for functionalities exploiting solitonic objects.

1. Introduction

The manipulation of macroscopic quantum states (MQS), systems where a collection of particles share a single macroscopic wave function, is a fascinating topic that has been investigated in diverse research fields [1, 2]. The possibility to engineer artificial periodic potentials to shape the properties of a MQS has allowed the simulation of solid-state quantum phase-transitions [3], the implementation of quantum computation protocols [4] and the exploration of the cross-over of MQS physics with nonlinear optics concepts [5]. Notable examples of MQS systems are atomic Bose-Einstein condensates (BECs) in optical and/or magnetic traps and supercurrents in superconducting circuits. Another type of MQS exists in semiconductor planar microcavities (MC) [6, 7], where, in contrast to atoms in BECs or Cooper pairs in superconductors, the components are photonic states dressed by excitons called exciton-polaritons. Exciton-polaritons are bosonic light-matter quasi-particles that form when photons couple strongly with quantum-well (QW) excitons in a semiconductor MC. While the inter-excitonic interactions provide an optical nonlinearity which is several orders of magnitude stronger than in purely photonic systems, the small mass arising from the photonic component gives polaritons a de Broglie wavelength of a few micrometres. The latter enables them to generate MQSs at lower densities and higher temperatures (on the order of a few kelvin) than in atomic systems as well as to be coherently manipulated by micrometric potentials [8–15]. Of particular interest are tuneable modulation schemes, which can produce potentials for polaritons analogue to optical lattices for cold atoms. Such potentials may be provided by the

Structural Characterization of a Capillary Microfluidic Chip Using Microreflectance

Luis F. Lastras-Martínez¹, Raul E. Balderas-Navarro¹,
Ricardo Castro-García², Karen Hernández-Vidales¹,
Juan Almendarez-Rodríguez¹, Rafael Herrera-Jasso¹,
Adrian Prinz³, and Iris Bergmair³

Applied Spectroscopy
0(0) 1–6
© The Author(s) 2016
Reprints and permissions:
sagepub.co.uk/journalsPermissions.nav
DOI: 10.1177/0003702816671961
asp.sagepub.com



Abstract

The structural characterization of capillary microfluidic chips is important for reliable applications. In particular, nondestructive diagnostic tools to assess geometrical dimensions and their correlations with control processes are of much importance, preferably if they are implemented in situ. Several techniques to accomplish this task have been reported; namely, optical coherence tomography (OCT) jointly with confocal fluorescence microscopy (CFM) to investigate internal features of lab-on-a-chip technologies. In this paper, we report on the use of a simple optical technique, based on near-normal incidence microreflectance, which allows mapping internal features of a microfluidic chip in a straightforward way. Our setup is based on a charge-coupled device camera that allows a lateral resolution of $\sim 2.5 \mu\text{m}$ and allows us to measure in the wavelength range of 640–750 nm. The technique takes advantage of the Fabry–Perot interferences features in the reflectance spectra, which are further analyzed by a discrete Fourier transform. In this way, the amplitude of the Fourier coefficients is modulated by the presence of a microfluidic channel.

Keywords

Capillary microfluidic chip, dimensional metrology, microreflectance, microscopy, tomography

Date received: 20 June 2016; accepted: 23 August 2016

Introduction

There is a growing interest for the integration of microelectronic circuits to carry out signal processing stemming from biosensing. In particular, lab-on-a-chip systems are good candidates for biomedical applications,¹ wherein an important component is capillary microfluidic chips (CMC).² Such CMC are designed for a wide range of applications including mixing fluids,³ micro-reactions,⁴ and stem cell biology⁵ among others.⁶ Besides, microelectronics components have been implemented in CMC to monitor transport and chemical properties in microfluid systems.^{7,8}

Typically, the capillaries forming CMC rely on the formation of a buried channel when bonding, for instance, two similar materials with one of them containing the capillary. Upon bonding, a direct assessment of the channel topography can be a difficult task. In this regard, the characterization of the buried channels in CMC is essential to assure fluid dynamics uniformity. Optical techniques to characterize the surface topography along the channel are very attractive as they are noninvasive and can be applied online during the manufacture process. Both, optical

coherence tomography (OCT) and confocal fluorescence microscopy (CFM) have been reported for critical parameters including channel width, height, and cross-sectional area.⁹ Although having high sensitivity, they can be expensive and require interferometry-based setups. Additionally, digital holographic microscopy (DHM) has been used to develop a three-dimensional (3D) phase-imaging microscope to study fluid dynamics, interaction of biomolecules, and cell activities.¹⁰

Considering that the optical techniques are quite convenient to study not only the structure of the CMC but also

¹Universidad Autónoma de San Luis Potosí, Instituto de Investigación en Comunicación Óptica, San Luis Potosí SLP, México

²CONACyT-Universidad Autónoma de San Luis Potosí, Instituto de Investigación en Comunicación Óptica, San Luis Potosí SLP, México

³STRATEC Consumables GmbH, Anif, Austria

Corresponding author:

Luis F. Lastras-Martínez, Universidad Autónoma de San Luis Potosí, Instituto de Investigación en Comunicación Óptica, Alvaro Obregón 64, CP 78000, San Luis Potosí SLP, México.
Email: lflm@cactus.iico.uaslp.mx

Two-dimensional heteroclinic attractor in the generalized Lotka–Volterra system

Valentin S Afraimovich¹, Gregory Moses² and Todd Young²

¹ Universidad Autonoma de San Luis Potosi, IICO, Mexico

² Department of Mathematics, Ohio University, OH, USA

E-mail: gm192206@ohio.edu

Received 21 November 2014, revised 15 September 2015

Accepted for publication 3 March 2016

Published 5 April 2016



CrossMark

Recommended by Dr Dmitry Turaev

Abstract

We study a simple dynamical model exhibiting sequential dynamics. We show that in this model there exist sets of parameter values for which a cyclic chain of saddle equilibria, O_k , $k = 1, \dots, p$, have two-dimensional unstable manifolds that contain orbits connecting each O_k to the next two equilibrium points O_{k+1} and O_{k+2} in the chain ($O_{p+1} = O_1$). We show that the union of these equilibria and their unstable manifolds form a two-dimensional surface with a boundary that is homeomorphic to a cylinder if p is even and a Möbius strip if p is odd. If, further, each equilibrium in the chain satisfies a condition called ‘dissipativity’, then this surface is asymptotically stable.

Keywords: heteroclinic orbits, Lotka–Volterra equations, unstable manifolds
Mathematics Subject Classification numbers: 34A34

(Some figures may appear in colour only in the online journal)

1. Background

In the last decade it has become clear that typical processes in many neural and cognitive networks are realized in the form of sequential dynamics (see [5, 23, 14, 24, 26, 25, 2] and references therein). The dynamics are exhibited as sequential switching among metastable states, each of which represents a collection of simultaneously activated nodes in the network, so that at most instants of time a single state is activated. Such dynamics are consistent with the winner-less competition principle [2, 26]. In the phase space of a mathematical model of such a system each state corresponds to an invariant saddle set and the switchings are determined by trajectories joining these invariant sets. In the simplest case these invariant sets may be saddle equilibrium points coupled by heteroclinic trajectories, and they form a heteroclinic



Ag-N dual acceptor doped p-type ZnO thin films by DC reactive magnetron co-sputtering



J.J. Ortega ^{a,*}, A.A. Ortiz-Hernández ^b, J. Berumen-Torres ^c, R. Escobar-Galindo ^d,
V.H. Méndez-García ^e, J.J. Araiza ^a

^a Unidad Académica de Física, Universidad Autónoma de Zacatecas, Calzada Solidaridad esq. Paseo de la Bufa, Fracc. Progreso, C.P. 98060, Zacatecas, México

^b Doctorado Institucional de Ingeniería y Ciencia de Materiales, Universidad Autónoma de San Luis Potosí, Av. Salvador Nava, Zona Universitaria, C.P. 78270, San Luis Potosí, México

^c Centro de Investigación y de Estudios Avanzados del IPN Unidad Querétaro, Libramiento Norponiente 2000, Col. Real de Juriquilla, C.P. 76230, Querétaro, México

^d Instituto de Ciencia de Materiales de Madrid, Sor Juana Inés de la Cruz, 3, Canto blanco, C.P. 28049, Madrid, España

^e Laboratorio Nacional-CIACyT, Universidad Autónoma de San Luis Potosí, Av. Sierra Leona 550, Col. Lomas 2a. Sección, C.P. 78210, San Luis Potosí, México

ARTICLE INFO

Article history:

Received 5 February 2016

Received in revised form

25 May 2016

Accepted 1 June 2016

Available online 2 June 2016

Keywords:

P-type zno

Ag-n doping zno

High hole concentration

Co-sputtering

ABSTRACT

ZnO p-type thin films were deposited by dual acceptor co-doping using nitrogen and silver via DC reactive magnetron co-sputtering. As precursor material were used a Zn and an Ag metallic targets with a purity of 99.99%. X-ray energy dispersive spectroscopy (EDX) confirmed the presence of Ag and N in ZnO:Ag,N films. The electrical properties were explored by Hall Effect measurement and showed a low hole concentration for the as-deposited ZnO:Ag,N film. However, after annealing treatment, the films remained p-type and the electrical properties were improved significantly. The best electrical properties showed a low resistivity of $8.56 \times 10^{-3} \Omega\text{cm}$, Hall mobility of $23 \text{ cm}^2/\text{Vs}$ and a very high hole concentration of $3.17 \times 10^{19} \text{ cm}^{-3}$.

© 2016 Elsevier B.V. All rights reserved.

1. Introduction

II-VI semiconductor materials have been of great interest due to their properties for optoelectronic devices. In this group, ZnO is widely used in electronic and photonic materials, and it has a great potential for applications in information technology, biotechnology, short wavelength semiconductors and nanoscale science and engineering [1–4]. However, to develop the ZnO based on optical devices, the principal difficulty has been the fabrication of high quality and electrical stability p-type ZnO thin films due to the low solubility of the acceptor dopants, deep acceptor level, and the compensation effect between the acceptor dopants and the native donors in ZnO [5–7].

Recently, a dual-doping method using two acceptor agents namely Li-N [8–10] or As-N [11] was proposed to prepare p-type ZnO. In this line, the dual-doping method has demonstrated to be the best channel to overcome the difficulties in achieving p-type ZnO thin films and theoretical researches have suggested that Ag and N are the better candidates for producing p-type ZnO considering the strain effects and energy levels of substitutional Ag-Zn

and N-O acceptors [12,13]. In the experimental context, publications focused to the fabrication of p-type ZnO:Ag,N thin films with good electrical properties have been reported using ultrasonic spray pyrolysis technique [14–18], ion beam assisted deposition [19] and sol-gel method [20]. However, until this moment, there are not reported studies on ZnO:Ag,N thin films by co-sputtering process in the literature.

In the present paper, the deposition of p-type ZnO:Ag,N by DC reactive magnetron co-sputtering method is reported. Additionally, the influence of dual doping on the structural and electrical properties of samples are presented.

2. Experimental details

Ag-N dual acceptor doping ZnO thin films were deposited on GaAs (100) substrates by DC reactive magnetron co-sputtering using zinc (99.99%) and silver (99.99%) metallic targets as precursors. For this purpose, the deposition chamber was evacuated to a base pressure of 3.5×10^{-6} Torr and the room temperature depositions were performed at a pressure of 6×10^{-3} Torr, employing a power densities of 4 and 1.5 W/cm^2 on zinc and silver targets respectively, in presence of a reactive atmosphere of argon (99.995%), oxygen (99.999%) and nitrogen (99.999%). The gas flux

* Corresponding author.

E-mail address: jjosila@hotmail.com (J.J. Ortega).



[SUBMIT YOUR ARTICLE](#)

[SIGN UP FOR ALERTS](#)

[Home](#) > [Journal of Vacuum Science & Technology B, Nanotechnology and Microelectronics: Materials, Processing, Measurement, and Phenomena](#) > [Volume](#) ← →

[Check for updates](#)

[34, Issue 2](#) > [10.1116/1.4942898](#)

Published Online: March 2016 Accepted: February 2016

Determination of the depletion layer width and effects on the formation of double-2DEG in AlGaAs/GaAs heterostructures

Irving Eduardo Cortes-Mestizo^{a)}, Leticia Ithsmel Espinosa-Vega, Jose Angel Espinoza-Figueroa, Alejandro Cisneros-de-la-Rosa, Eric Eugenio-Lopez, and Victor Hugo Mendez-Garcia

less

[View Affiliations](#)

• Center for the Innovation and Application of Science and Technology, Universidad Autonoma de San Luis Potosi, Sierra Leona 550, Lomas 4a Secc., San Luis Potosi, San Luis Potosi 78210, Mexico

Edgar Briones and Joel Briones

• Departamento de Física y Matemáticas, Instituto Tecnológico y de Estudios Superiores de Occidente, Periférico Sur Manuel Gómez Morín 8585, Tlaquepaque, Jalisco 45604, Mexico

Luis Zamora-Peredo

• Centro de Investigación en Micro y Nanotecnología, Universidad Veracruzana, Calzada Ruiz Cortines 455, Boca del Río, Veracruz 94294, Mexico

Ravindranath Droopad

• Ingram School of Engineering, Texas State University, San Marcos, Texas 78666

Cristo Yee-Rendon



[SUBMIT YOUR ARTICLE](#)

[SIGN UP FOR ALERTS](#)

[Home](#) > [Journal of Vacuum Science & Technology B, Nanotechnology and Microelectronics: Materials, Processing, Measurement, and Phenomena](#) > [Volume](#) ← →

[Check for updates](#)

[34, Issue 2](#) > [10.1116/1.4942900](#)

Published Online: March 2016 Accepted: February 2016

Effects of growth temperature on the incorporation of nitrogen in GaNAs layers

José Ángel Espinoza-Figueroa, Víctor Hugo Méndez-García, Miguel Ángel Vidal, and Esteban Cruz-Hernández^{a)}

less

[View Affiliations](#)

• Coordinación para la Innovación y Aplicación de la Ciencia y la Tecnología, Av. Sierra Leona #550, Col. Lomas 2a Sección, CP 78210 UASLP, San Luis Potosí, México

Máximo López-López and Salvador Gallardo-Hernández

• Physics Department, Centro de Investigación y Estudios Avanzados del IPN (CINVESTAV), Av. IPN #2508, San Pedro Zacatenco, 07360 México, D.F., México

Journal of Vacuum Science & Technology B, Nanotechnology and Microelectronics: Materials, Processing, Measurement, and Phenomena **34**, 02L111 (2016); doi: <http://dx.doi.org/10.1116/1.4942900>

New orientations in the stereographic triangle for self-assembled faceting

R. Méndez-Camacho,¹ V. H. Méndez-García,¹ M. López-López,²
and E. Cruz-Hernández^{1,a}

¹*Coordination for the Innovation and Application of Science and Technology, Universidad Autónoma de San Luis Potosí, S.L.P. 78210, México*

²*Physics Department, CINVESTAV-IPN, Apartado Postal 14-740, México D.F. 07000, México*

(Received 11 March 2016; accepted 17 June 2016; published online 24 June 2016)

Energetically unstable crystalline surfaces, among their uses, can be templates for the growth of periodic arrays of one-dimensional (1D) nanoscale structures. However, few studies have explored self-assembled faceting on high-index (HI) planes inside the stereographic triangle, and extant studies have not produced any criteria for encouraging the formation of one-dimensional periodic arrays. In this Letter, by analyzing the MBE growth of homoepitaxial facets on (631)A GaAs, a HI plane inside the triangle, we present a criteria to produce highly uniform 1D periodic arrays on unexplored surfaces. These families of planes are those belonging to the lines connecting the energetically stable HI GaAs (11 5 2) plane with any of the (100), (110), and (111) planes at the corners of the stereographic triangle. This novel strategy can lead to new possibilities in self-assembling 1D structures and manipulating physical properties, which in turn may result in new HI- and 1D-based experiments and devices. © 2016 Author(s). All article content, except where otherwise noted, is licensed under a Creative Commons Attribution (CC BY) license (<http://creativecommons.org/licenses/by/4.0/>). [<http://dx.doi.org/10.1063/1.4954998>]

INTRODUCTION

Energetically unstable crystalline surfaces, which tend to break up into facets of low free energy, can be used as templates for growing nanoscale one-dimensional periodic arrays (1DPAs) such as quantum wires.¹⁻⁴ Ultra-high-vacuum techniques such as molecular beam epitaxy (MBE) and metalorganic vapor phase epitaxy have been used to grow periodic corrugated structures with remarkable uniformity on surfaces with an unstable high Miller index (HI) or vicinal GaAs substrates (VSs).⁵⁻⁸ In addition to its potential for promoting self-assembled structures, epitaxial growth on HI substrates has exhibited many interesting features. For example, HI planes have many characteristics that make them important in basic and applied research, such as the amphoteric nature of Si impurities,^{9,10} atypical piezoelectric effects,¹¹ high degree of light polarization in arrays of quantum wires,⁴ observation of anisotropic topological surface states,^{12,13} and the enhancement of (In,Ga,Al)P-GaP light-emitting diodes.¹⁴

By convention, the HI and VSs are chosen to be oriented along the edges of the stereographic triangle (ST), whose corners are the (100), (110), and (111) low-index (LI) planes (which are energetically stable), as shown in Fig. 1. Such surfaces on the sides of the ST are chosen because only the LI corners can form low-energy reconstructions, and because any given HI or VS on it should decay into facets composed of combinations of two of the corner planes. By contrast, the HI planes in the ST likely have a very complex structure because it should comprise combinations of the three LI planes. For these reasons, there have been very few studies on HI planes inside the ST, and they are chosen without following specific criteria for 1DPA formation.

^aElectronic mail: esteban.cruz@uaslp.mx

Research Article

Photoluminescence and Raman Spectroscopy Studies of Carbon Nitride Films

J. Hernández-Torres,¹ A. Gutierrez-Franco,¹ P. G. González,²
L. García-González,¹ T. Hernandez-Quiroz,¹ L. Zamora-Peredo,¹
V. H. Méndez-García,³ and A. Cisneros-de la Rosa³

¹Centro de Investigación en Micro y Nanotecnología, Universidad Veracruzana, 94292 Boca del Río, VER, Mexico

²CONACYT Research Fellow-Centro de Ingeniería y Desarrollo Industrial, 76125 Querétaro, QRO, Mexico

³Coordinación para la Innovación y Aplicación de la Ciencia y Tecnología, Universidad Autónoma de San Luis Potosí, 78210 San Luis Potosí, SLP, Mexico

Correspondence should be addressed to J. Hernández-Torres; julihernandez@uv.mx
and P. G. González; pedro.gonzalez@cidesi.edu.mx

Received 9 November 2015; Accepted 27 January 2016

Academic Editor: Jau-Wern Chiou

Copyright © 2016 J. Hernández-Torres et al. This is an open access article distributed under the Creative Commons Attribution License, which permits unrestricted use, distribution, and reproduction in any medium, provided the original work is properly cited.

Amorphous carbon nitride films with N/C ratios ranging from 2.24 to 3.26 were deposited by reactive sputtering at room temperature on corning glass, silicon, and quartz as substrates. The average chemical composition of the films was obtained from the semiquantitative energy dispersive spectroscopy analysis. Photoluminescence measurements were performed to determine the optical band gap of the films. The photoluminescence spectra displayed two peaks: one associated with the substrate and the other associated with CN_x films located at $\approx 2.13 \pm 0.02$ eV. Results show an increase in the optical band gap from 2.11 to 2.15 eV associated with the increase in the N/C ratio. Raman spectroscopy measurements showed a dominant *D* band. I_D/I_G ratio reaches a maximum value for N/C ≈ 3.03 when the optical band gap is 2.12 eV. Features observed by the photoluminescence and Raman studies have been associated with the increase in the carbon sp^2/sp^3 ratio due to presence of high nitrogen content.

1. Introduction

Light elements based materials which associate 2p and 3p elements, mainly from columns III to V of the periodic system, are of great interest due to their physicochemical properties. In this sense, the elevate hardness, chemical inertia, good thermal conductivity, optical transparency (on a wide wave number range), highly refractory character, electric insulator behavior, and high band gap values are the most representative [1].

Concerning their production, two main routes of synthesis have been developed to obtain carbon nitrides as thin films or as bulk materials. Many publications devoted to the synthesis of CN_x thin films have jointly concluded that the existence of the crystalline stoichiometric C_3N_4 phase has not been clearly evidenced yet. To date, the so-obtained deposits are generally amorphous and can eventually contain some

nanometric CN_x crystallites [2]. However, these amorphous thin films seem to present interesting electrical, mechanical, tribological, and optical properties [3–6].

In recent years, study of the optical properties of amorphous carbon nitrides ($\alpha-CN_x$) films became an interesting field. The reported characteristics have provided evidence for a possible utilization in optoelectronic devices, such as electroluminescence devices [7] or photovoltaic solar cells. In this sense, the optical properties of $\alpha-CN_x$ have been extensively studied via diverse techniques such as Raman, photoluminescence (PL), or absorption spectroscopy. Typically, the Raman spectra of carbon nitrides, measured at any excitation energy, have a similar form to those of N-free amorphous carbons, that is, showing the *D* and *G* bands. The existence of a *D* band indicates the presence of aromatic rings. The *G* band for carbon materials arises from vibration of all sp^2 sites and in both chain and ring configurations.



Structural characterization of AlGaAs:Si/GaAs (631) heterostructures as a function of As pressure

Leticia Ithsmel Espinosa-Vega, Miguel Ángel Vidal-Borbolla, Ángel Gabriel Rodríguez-Vázquez, Irving Eduardo Cortes-Mestizo, Esteban Cruz-Hernández more...

[View Affiliations](#)

Journal of Vacuum Science & Technology B, Nanotechnology and Microelectronics: Materials, Processing, Measurement, and Phenomena **34**, 02L119 (2016); doi: <http://dx.doi.org/10.1116/1.4944452>

PDF ABSTRACT FULL TEXT FIGURES CITED BY TOOLS SHARE METRICS

III-V semiconductors Thin film growth Epitaxy Semiconductor growth Phonons

ABSTRACT

AlGaAs:Si/GaAs heterostructures were grown on (631) and (100) GaAs substrates and studied as a function of the As cell beam equivalent pressure. High-resolution x-ray diffraction patterns showed that the highest quality AlGaAs epitaxial layers were grown at $P_{As} = 1.9 \times 10^{-5}$ for (100)- and $P_{As} = 4 \times 10^{-5}$ mbar for (631)-oriented substrates. Raman spectroscopy revealed higher crystalline quality for films grown on (631) oriented substrates. The GaAs- and AlAs-like modes of the AlGaAs(631) films exhibited increased intensity ratios between the transverse optical phonons and longitudinal optical phonons with increasing P_{As} , whereas the ratios were decreased for the (100) plane. This is in agreement with the selection rules for (631) and high-resolution x-ray diffraction observations. Anisotropy and surface corrugation of the AlGaAs(631) films also were characterized using atomic force microscopy and Raman spectroscopy.



Study of InAlAs/InGaAs self-switching diodes for energy harvesting applications

Irving Eduardo Cortes-Mestizo¹, Edgar Briones^{1,2}, Joel Briones², Ravindranath Droopad³, Manuel Perez-Caro³, Stefan McMurtry⁴, Michel Hehn⁴, François Montaigne⁴, and Victor Hugo Mendez-Garcia^{1*}

¹CIACyT, Universidad Autónoma de San Luis Potosí, San Luis Potosí, 78210 SLP, Mexico

²Department of Mathematics and Physics, ITESO, Jesuit University of Guadalajara, 45604 Tlaquepaque, Mexico

³Ingram School of Engineering, Texas State University, San Marcos, TX 78666, U.S.A.

⁴Institut Jean Lamour, CNRS, Université de Lorraine, F-54506 Vandoeuvre Les Nancy, France

*E-mail: victor.mendez@uaslp.mx

Received August 14, 2015; revised November 4, 2015; accepted November 4, 2015; published online December 21, 2015

In order to improve the rectification efficiency and current–voltage characteristics of self-switching diodes (SSD) the DC response is analyzed using technology computer aided design (TCAD). It is demonstrated that by varying geometrical parameters of L- and V-shaped SSDs or changing the dielectric permittivity of the trenches, a near zero threshold voltage can be obtained, which is essential for energy harvesting applications. The carrier distribution inside the nanochannel is successfully simulated in two-dimensional mode for zero-, reverse-, and forward-bias conditions. This process allows for the evaluation of the effect of the lateral surface-charge on the formation and spatial distribution of the depletion region, in addition to, obtaining information on the physics of the SSD through the proposed optimized geometries that were designed for tailoring and matching the desired frequencies of operation. The numerical results showed some insights for the improvement of the rectification efficiency and integration density using parallel SSD arrays. © 2016 The Japan Society of Applied Physics

1. Introduction

Surface physics plays an important role for the functioning and performance of semiconductor nano-devices since surface atoms make up a considerable part of the devices at nanoscale dimensions. When the translational symmetry of an ideal crystalline solid is interrupted at the surface, the properties of the topmost atoms affect the optical and electrical properties of the devices.¹⁾ Thus, it is imperative to understand and predict how surface states, surface charge and depletion regions can be manipulated in order to engineer nanoscale devices. A good example of surface states engineering as applied to III–V semiconductor devices is the so-called self-switching diode (SSD), developed by Song,²⁾ which consists of a nanochannel between two L-shaped insulating grooves that is fabricated by electron beam lithography. The depletion region caused by surface states in the walls of the groove allows the current to flow across the channel in one direction only, similar to a standard p–n diode. The simplicity of the fabrication process^{3,4)} and the novel functionalities of this surface-state device, such as the ability to detect weak signals (by a rectifying square-law mechanism), the high sensitivity without applied bias and the potential to operate in the terahertz regime,⁵⁾ make the SSD concept ideal for a broad range of applications. The THz frequency, for example, is useful for the detection of millimeter and sub-millimeter waves avoiding the use of X-rays. Conventional THz imaging currently is an expensive alternative because it is limited by the scarcity of available detectors and the slow operation speed.⁶⁾ The SSD concept has been explored using two-dimensional electron gas (2DEG) systems in InAlAs/InGaAs⁷⁾ and AlGaAs/GaAs⁸⁾ heterostructures even though the working principle is not entirely dependent on the 2DEG properties. For instance, SSDs have been fabricated in bulk materials like silicon,⁹⁾ transparent semiconductors like ZnO¹⁰⁾ and indium tin oxide (ITO),¹¹⁾ and more recently a graphene-based SSD has been also demonstrated.¹²⁾

It is worth to comment that electrical rectification at optical frequencies for energy harvesting systems has been

the most explored method to recover free-propagating radiation, for wavelengths in the visible, infrared and THz range.^{13,14)} This task has been commonly achieved by antenna coupled ultra-fast metal–insulator–metal (MIM), metal–insulator–insulator–metal (MIIM) tunnel barriers or p–n semiconductor junctions (reverse Esaki tunnel diodes).^{14–16)} In spite of the high-speed performance of these rectifiers, they exhibit low rectification due to their poor diode-like behavior. Conversely, SSD rectification has shown current–voltage (I – V) curves with nearly zero slope in the reverse bias condition. Since this type of devices combine geometrical effects with electronic transport properties, an analysis of the effects of size and shape is necessary in order to find the optimum geometry that may improve the SSD I – V response, which is the aim of this work, developed by using a numerical simulation approach by Silvaco Atlas.

2. Geometry parameters and simulation method

We perform a systematic geometrical analysis and comparison of two different types of self-switching structures, the L- and V-shaped channels. The schematic top view of the L- and V-shaped SSDs showing the geometrical parameters used in the simulation is presented in Figs. 1(a) and 1(b), respectively. In the SSD the surface charge density, n_s , which exists on the trench walls, induces a depletion region along the nanochannel. The working principle of the SSD relies on the modulation of this depletion region by an applied bias.²⁾ The reduction (augmentation) in the volume of the depletion region decreases (increases) the electrical resistance in the nanochannel under direct (reverse) bias originating in a diode-like effect. With the aim of determining the SSD I – V characteristics, we employed a physically-based device simulator in two-dimensional mode, similar to that reported for 2DEG-based InGaAs SSD and silicon-on-insulator structures.^{3,9,17)} The electrical properties of 2DEG samples utilized in the simulation were: background doping $n = 1 \times 10^{17} \text{ cm}^{-3}$, electron mobility $\mu = 12,000 \text{ cm}^2 \text{ V}^{-1} \text{ s}^{-1}$, with no impurity scattering. Unless otherwise stated, the dielectric in grooves was considered to be air ($\epsilon_r = 1$) thus inducing a surface charge density of $n_s = 0.4 \times 10^{12} \text{ cm}^{-2}$. The contact